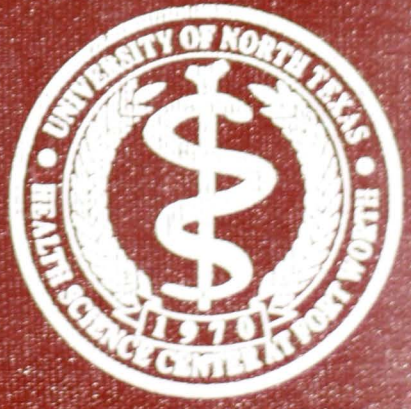
UNIVERSITY OF NORTH TEXAS
HEALTH SCIENCE CENTER AT FORT WORTH
1970

Kern, Jami RaDel, Molecular Regulation of Wound Contraction and Scar Formation Using a Three-Dimensional Connective Tissue Model. Doctor of Philosophy (Biomedical Sciences, Biochemistry and Molecular Biology), December 2002, 156 pp., 1 table, 27 illustrations, references, 112 titles.

The focus of these studies was to characterize a novel connective tissue model for use in experiments examining possible contraction initiators in the wound healing process, i.e. endothelin-1 (ET-1). Through these studies, it has been shown that use of a telomerized dermal fibroblast cell line addresses the concerns relating to variations due to heterogeneity of normal human cells cultured *in vitro*, without creating a cancerous cell line or interfering with normal phenotypic changes. In addition, the incorporation of telomerized cells into our TE, which does not spontaneously contract (US Patent #6471958), provides a unique model to study the contraction and scar formation process. Using the TE populated with hTERT fibroblasts, an innovative technique was developed to identify the initiation of tissue contraction using an optical fiber interferometry system. The process allows observation of contraction within five minutes of stimulus addition and also enables continuous data capture over a period of several hours. The greatest strength of this system is its sensitivity, since the optic interferometer allows measurement of displacement (contraction) to the tens of nanometers.

Along those lines, the current studies have identified ET-1 as a potential early initiator in wound healing and suggest a novel pathway through which it functions. This proposed mechanism includes both direct effects of ET-1 through the Rho-associated kinase pathway and indirect effects potentiated by TGF-β. Future studies addressing whether TGF-β converges on the Rho-associated kinase pathway or acts independently through other signaling mechanisms should be initiated. The discovery of early initiators of tissue contraction is essential in the identification of potential therapeutic targets in the quest to reduce prolonged and severe tissue contracture and scaring.

MOLECULAR REGULATION OF WOUND CONTRACTION AND SCAR FORMATION USING A THREE-DIMENSIONAL CONNECTIVE TISSUE MODEL

Jami RaDel Kern, B.A.

APPROVED:

Major Professor

Committee Member

Committee Member

Committee Member

Committee Member

University Member

Chair, Department of Molecular Biology and Immunology

Dean, Graduate School of Biomedical Sciences

MOLECULAR REGULATION OF WOUND CONTRACTION AND SCAR FORMATION USING A THREE-DIMENSIONAL CONNECTIVE TISSUE MODEL

DISSERTATION

Presented to the Graduate Council of the

Graduate School of Biomedical Sciences

University of North Texas

Health Science Center at Fort Worth

In Partial Fulfillment of the Requirements

For the Degree of

Doctor of Philosophy

By

Jami RaDel Kern, B.A.

Fort Worth, Texas

December 2002

ACKNOWLEDGEMENTS

I would like to take this opportunity to acknowledge the support and assistance I have received throughout my graduate career. First, thanks to my dissertation committee, Thomas Yorio, Ph.D., Robert W. Gracy, Ph.D., Peter B. Raven, Ph.D., Julian Borejdo, Ph.D., and Patricia Gwirtz, Ph.D., and especially to my advisor, S. Dan Dimitrijevich, Ph.D and our entire lab group. Special thanks are in order for Dr. Raven, who gave me my first exposure to the world of research and the opportunity to participate in his research, and in a collaborative effort with Dr. Dimitrijevich which culminated in the work discussed here. Dr. Yorio's entire laboratory group was particularly supportive and helpful, above all Ganesh Prasanna, Ph.D.

In addition to those associated with UNTHSC, I received immeasurable instruction and educational opportunities through collaborations with Tristan J. Tayag, Ph.D. (Texas Christian University) and Daniel McMillan, Ph.D. (University of Texas Southwestern) and would like to express my gratitude for their willingness to participate in my graduate training.

Lastly, to my family, friends, and my exceptionally supportive husband, I extend my appreciation for continual encouragement throughout this experience.

TABLE OF CONTENTS

LIST OF TABLES

CHAPTER II

LIST OF ILLUSTRATIONS

CHAPTER I

CHAPTER II

CHAPTER III

CHAPTER IV

CHAPTER V

Chapter I

Statement of Problems

There are a number of gaps in our understanding of scar formation and the mechanisms that regulate it. Because of the deleterious effects of excessive scarring, it is desirable not only to understand but also to be able to intervene in this process. The present work focused on the characterization of an *in vitro* connective tissue equivalent model proposed to study the processes of tissue contraction and scar formation in three dimensions. Furthermore, the model is used to examine the role of endothelin – 1 as an early initiator of tissue contraction and scar development.

Lack of a dimensionally stable *in vitro* tissue model and of a near normal fibroblast cell line produce confusing results when studies of tissue contraction *in vitro* are performed. Thus, the characterization of telomerized fibroblasts as a standard cellular component of a stable three-dimensional connective tissue equivalent addresses major deficiencies of *in vitro* models.

Specific Aim 1: To demonstrate that fibroblasts transfected with the catalytic subunit of human telomerase are a good cellular model for studies of fibroblasts activated to a wound healing phenotype. Specifically, to demonstrate that telomerized fibroblasts are able to function normally in response to various wound healing scenarios both in monolayer and as cellular components of tissue equivalents.

Hypothesis 1: Fibroblasts transfected with the catalytic subunit of human telomerase behave in a manner similar to normal human fibroblasts in response to wound healing stimuli.

Hypothesis 2: Telomerized fibroblasts as cellular components of tissue equivalents are a valid model to study normal wound healing, and particularly tissue contraction.

Telomerized fibroblasts were characterized in monolayer culture and as cellular components of the three-dimensional connective tissue equivalent by evaluating their ability to function in various wound-healing scenarios. For example, the ability of normal and telomerized cells to proliferate in response to basic fibroblast growth factor (FGF2), synthesize and secrete collagen in response to ascorbate, migrate within a collagen matrix, and contract that matrix was examined and compared. In addition, the cytoskeletal protein expression and localization in both cell types was studied via immunofluorescence and western analysis. Finally, reservations with respect to the constitutive ectopic expression of telomerase were addressed by a series of experiments designed to show that the telomerized fibroblasts are in a quiescent state in the connective tissue equivalent.

The inability to accurately measure the extent of *in vitro* tissue contraction, particularly in the initial phases of the process, makes it difficult to establish a complete list of significant contractile ligands and delineate their synergy. Development of a novel system for quantifying matrix contraction establishes a

basis for understanding some early initiators of the contractile process *in vitro*, including endothelin – 1.

Specific Aim 2: To develop a method to measure the early stages of contraction.

Hypothesis 3: It is possible to measure the initial stages of tissue equivalent contraction utilizing an optical fiber interferometer system.

An optical fiber interferometer system originally described to measure the out-of-plane displacement of microelectromechanical structures was modified and used to measure initial contraction of a connective tissue equivalent following stimulation with 20% fetal bovine serum or 10ng/ml transforming growth factor-beta (TGF-β).

Furthermore, while endothelin has been extensively studied as a contractile factor in several physiological systems, its role in wound healing had not yet been examined. Utilizing the newly characterized connective tissue equivalent model based on the telomerized fibroblast cell line established endothelin as an initiator of wound contraction and proposed some of the signaling involved in that process.

Specific Aim 3: To determine the role endothelin–1 plays during the wound healing process.

Hypothesis 4: Endothelin–1 is an initiator of alpha-smooth muscle actin (α-SMA) expression in human fibroblasts and thus a mediator of tissue

contraction, either directly or via stimulation of transforming growth factor-beta (TGF-β) release.

These experiments utilized monolayer cultures and telomerized fibroblasts as the cellular components of connective tissue equivalents to examine the role of endothelin as an early initiator of tissue contraction. Through immunofluorescence and western analysis, cytoskeletal changes following endothelin treatment were examined and the presence of the endothelin receptor A (ET_A) was identified in both normal and telomerized fibroblasts. Also, tissue equivalent contraction was measured following stimulation with endothelin. In addition, collagen synthesis and proliferation in response to endothelin was measured. Endothelin stimulated calcium influx was examined using fura-2 calcium imaging. Finally, endothelin-1 stimulated transforming growth factor-beta 1 (TGF-β1) secretion was analyzed using ELISA.

Together, these experiments focused on delineating the contribution of endothelin-1 in the early stages of tissue contraction and were based on a working schematic of endothelin-1 signaling in non-muscle cells (**Fig. 1**).

Introduction to the Studies

Tissue Structure and Function

Living organisms function through the coordinated performance of a number of organs. These complex tissues are composed of a variety of cells, extracellular matrix macromolecules, and water. Tissue components are arranged to confer a three-dimensional architecture that assists with the necessary physiological functions and provides mechanical stability. Therefore, tissue may be soft (connective tissue) or hard (bone), and cell-rich (epithelia, muscle) or matrix-rich (dermis, cartilage). During embryonic development cells and matrix compose a dynamic state of complexity as the organism prepares for self-supporting functions. In the post-natal period, tissues continue to change in order to support life through the full range of physiological and mechanical tasks. This sophistication can only be maintained by an intricate balance of the functions of tissue components working in concert. This orchestration depends on numerous cell-cell and cell-matrix interactions, the consequences of which are just beginning to be studied and appreciated. As important as these intricate structure-function relationships are in homeostasis (quiescent tissue), the complexity and maintenance of dynamics become even more critical when the equilibrium is disrupted by injury or disease. When the continuum of tissue architecture is interrupted, its normal function is disrupted. Rather than maintenance, the primary objective then becomes that of structural repair so that proper function may resume as quickly as possible. It is the regulation of these

processes at molecular and cellular levels that governs the rate, the extent, and the quality of tissue repair and the restoration of its function.

Tissue Components

A large component of tissue is the extracellular matrix (ECM). ECM is composed of a number of biologically active polymers synthesized, extruded and deposited into the extracellular space by the appropriate cells. These biopolymers include three different families of macromolecules: collagens, elastin, and glucosaminoglycans. While elastin enables tissue to be flexible and retain its shape following displacement by external forces, collagens are essential for mechanical strength [1-3]. Glucosaminoglycans maintain the tissue's water homeostasis, facilitate the passage of small molecules (nutrients, essential ions), and maintain the appropriate spatial relationships between collagen and elastin [4]. These macromolecules continue to adopt higher levels of organization until they can fulfill the appropriate requirements of mature, fully functional tissue architecture. By definition these macromolecules are insoluble in their aqueous physiological environment and are resistant to the general proteolytic enzymes present. They are, however, subject to damage and turnover during injury and tissue repair and their proteolysis or excessive synthesis may become a problem during certain disease processes [4].

The most abundant extracellular matrix (ECM) component in the human body is collagen, a member of the super-family of rigid insoluble proteins,

particularly prominent in connective tissue [1, 5]. The collagen type and organization is dictated by the structural role it plays in each tissue or organ. For example, in the vitreous humor of the eye and in the extracellular matrix, collagen confers firmness and reinforces strength of the gel-like structure [6]. Alternatively, in tendons collagen is bundled into tight fibers and, in cooperation with elastin, provides strength and stretching stability [7]. In the cornea, collagen is arranged in sheets of fibers with a specific diameter so that the matrix can transmit light without scattering [6].

The basic rope-like structure of collagen is formed by three polypeptide α-chains, composed of a repeated tripeptide (Gly – X – Y, where X is often proline and Y is often hydroxyproline or hydroxylysine), which coil around each other in a triple helix [1]. The type of collagen that results depends on the sequence of amino acids that compose each of the three chains and the combination of those α-chains. For example, in collagen type I, the triple helix is formed from two α1 chains and one α2 chain. The polypeptide precursors (α-chains) are synthesized in fibroblasts (**Fig. 2**) and secreted into the extracellular matrix where enzymatic modification by lysyl oxidase primes the triple helical molecules for further organization into fibrils [1]. Fibrilogenesis and higher levels of collagen organization (aggregation) occur by cross-linking of the collagen monomers.

Normal collagens are hydrophobic and highly stable, with half-lives as long as several months. Collagen is extracted from tissue with minimal denaturation using aqueous acid (hydrochloric or acetic) or salt solutions [8, 9].

An acidic solution of collagen is typically stored at 4°C to maintain its original composition (i.e., resist hydrolysis). When neutralized and allowed to attain 37°C, aqueous collagen solution begins to undergo fibrilogenesis (polymerization), to form a stable gel [9]. Because collagen is not soluble in aqueous environments and is denatured when extracted from tissue, it has been difficult to study its structure by conventional methods and little is known about its three-dimensional organization into fibrils, fibers, and bundles. However, predictions have been made using modeling programs [10]. For example, Silver et al [10] modeled the flexibility of the alpha1-chains found in types I-III collagen molecules and microfibrils in order to understand the molecular basis of elastic energy storage in collagen fibers by analyzing the areas under conformational plots for dipeptide sequences. Their results of stereochemical modeling suggested that the collagen triple helix is made up of rigid and flexible domains that alternate with periods that are multiples of three amino acid residues [10]. Although a number of genes involved in collagen synthesis have been cloned [11-14], the intracellular processes of collagen translation, its post–translational modifications, and the fact that there are extracellular processes involved in its organization, make collagen synthesis an extremely complex process to study. Consequently, recombinant methods for the production of human collagen have yet to be developed. Most researchers in the tissue construct arena utilize commercially available bovine collagen or in-house purified rat-tail collagen [5, 8, 9]. Impurities in collagen solutions affect the interactions between collagen fibrils and interfere

with the three-dimensional collagen gel structure. Therefore, collagen free of denatured fragments is required for proper fibrilar organization. While the conditions promoting collagen polymerization have been established, they remain imprecise. For example, detailed relationships between the time of initiation or rate of polymerization and concentration of collagen have not been studied. There is also little or no information about the effect of temperature on the initiation or the rate of collagen polymerization.

While collagen is extremely stable, connective tissue, like all other tissues, is dynamic and is continuously being remodeled. This largely occurs during growth or repair in response to injury. Extracellular matrix degradation is accomplished by a family of matrix degrading enzymes, metalloproteinases [15]. Collagenases are a group of metalloproteinases that specifically cleave collagen into small fragments that may then be phagocytosed by cells to be further degraded into component amino acids and recycled [15]. Collagenase activity is controlled by a number of factors, including parathyroid hormone, adrenocorticoid steroids, and colchicines [16]. A strict balance between collagen deposition and degradation is vital to extracellular matrix maintenance and becomes particularly important during wound healing. While chronic wounds and inflammatory diseases are often characterized by excessive collagen degradation, overproduction of collagen (fibrotic diseases) is equally undesirable and can lead to excessive scar formation and loss of function [17, 18]. In addition to the obvious structural obstacles that overabundance of extracellular matrix proteins

can present, especially when it is densely concentrated, the interactions of the cells with their tissue environment are also compromised.

Cell – Matrix Interaction

The extracellular matrix exerts profound control over cellular functions. The effects of the matrix are primarily mediated by integrins, a family of cell surface receptors that are used to form attachments to the matrix, and which are now known to mediate mechanical and chemical signaling [19]. Integrins are composed of two transmembrane subunits, α and β, with each $\alpha\beta$ heterodimer having its own binding specificity and signaling properties. They participate in bi-directional signal transduction (**Fig. 3**). Thus, the attachment of cells to the extracellular matrix involves signaling activities and utilization of integrins and originates from within the cell (inside-out signaling) [20]. These actions occur both by inducing the conformational change in and altering the affinity of integrin heterodimers, and also by clustering integrins [19]. As with signal transmission to other parts of the cell, plasma membrane receptors presumably regulate integrins by triggering post-translational changes that affect the activity and/or subcellular localization of key enzymes and substrates in integrin-regulated pathways [20]. The signaling activity in the opposite direction (outside-in signaling) occurs when a cell responds to changes in the extracellular matrix domains and signals are transmitted into the cell [21]. This type of signaling can affect cell migration, contraction, and ultimately cell survival. For example, when

$\alpha_2\beta_1$ integrin interactions with the extracellular matrix are blocked, migration is halted and the cells adopt a spherical morphology by distributing integrins evenly around the cell periphery [22]. For attachment dependent cells, change in or loss of an anchorage to ECM components can trigger the process of apoptosis [23]. Integrin signaling is intimately linked with the assembly and functions of the cytoskeleton. When cells come into contact with the extracellular matrix, they extend filopodia. Outside the cell, integrin subunits at the filopodia tip associate with each other and bind to specific recognition sites (domains) on the ECM macromolecules [22]. This assembly initiates the formation of focal adhesion complexes (plaques) at the cytoplasmic ends of the integrin [21]. These focal adhesion plaques are aggregates of the cytoplasmic integrin subunits and linker proteins (paxilin, vinculin, talin, etc.), and through cytoskeletal proteins link the extracellular matrix to the nucleus [20]. The advanced establishment of focal adhesion complexes relies on phosphorylation events, mainly by focal adhesion kinase (FAK) [24]. The organization of actin filaments into stress fibers causes further clustering of integrins and facilitates focal adhesion assembly. Specialized control of these events (attachment to the matrix, integrin clustering, focal adhesion formation) finally affects changes in cell shape and function. During cell-mediated tissue contraction the cell pulls on the matrix, whereas in cell migration, cyclic pull and release of the matrix takes place [19]. In addition, physical forces exerted on the nucleus by integrin-induced changes in the cytoskeleton may regulate nuclear events without evoking classical second

messenger mechanisms, but remain dependent upon protein phosphorylation or dephosphorylation [22]. Thus, the coordinated control of cell shape, survival, division, and movement by integrins is important in the establishment and maintenance of tissue architecture.

Fibroblast Phenotype

The principal cell type that has frequently been used to model cell-matrix interactions is the fibroblast, the most abundant cell type in the body [25]. Quiescent fibroblasts that are cellular components of a normal three-dimensional tissue undergo phenotypic changes ("differentiation") to the activated myofibroblast phenotype (MyoFbs) when an injury to surrounding tissue occurs [26]. Therefore, it is believed that the myofibroblasts are the wound healing cells that proliferate, migrate into the wound [22], synthesize and deposit new collagen and other matrix macromolecules, and through tissue contraction close the wound [27]. Although *in vitro* experiments have shown that fibroblasts carry out individual tissue repair functions [25], it has not been demonstrated in real time that the myofibroblast phenotype is responsible for these functions. In order to carry out migratory and contractile tasks, the fibroblasts alter their profile of cytoskeletal proteins. For example, in order to contract the matrix and close the wound the fibroblasts adopt smooth muscle cell characteristics, specifically the complete contractile cytoskeleton and become myofibroblasts (**Fig. 4**) [28]. The accepted marker for this transition is the transient expression of alpha-smooth

muscle actin (α-SMA) and its involvement in stress fiber formation [29]. However, the mechanisms leading to these cytoskeletal changes remain poorly understood [30]. Furthermore, the fate of the myofibroblast once it has performed its necessary function(s) is not clear. One hypothesis is that the cells undergo phenotypic "dedifferentiation" to quiescent fibroblasts [25]. This view is based on the fact that cells within the matrix are required to continue the remodeling phase long after acute wound healing has ceased, and also the fact that scars are not always acellular. On the other hand, some dense scar tissue does not contain cells, and thus the opposing view that the myofibroblasts undergo apoptosis following wound contraction has been advanced. According to the latter hypothesis, the condensed extracellular matrix is a source of a crisis signal for the myofibroblast, leading to cell death via apoptosis [25]. The extracellular matrix therefore, functions not only as a scaffolding for the fibroblasts, but also is intimately involved in the signaling cascades leading to the changes in fibroblast phenotype. Several research groups have developed three-dimensional connective tissue models in order to study in a more *in vivo* like fashion these interactions and other tissue related phenomena in homeostasis and tissue repair.

Connective Tissue Models

Since the dermis has relatively simple composition and skin is a readily available human tissue, skin models (skin equivalents) have been the first tissue

developed by a number of laboratories [31]. A variety of dermal models (dermal equivalents, DEs) have been proposed, ranging from a simple monolayer of fibroblasts cultured on a collagen coated plastic surface or collagen gels to fibroblasts dispersed into a three-dimensional matrix composed of multiple extracellular matrix macromolecules [3, 5, 8, 9, 23, 32, 33]. The applications of these "tissue equivalents" are as numerous as the models themselves. Dermal and skin equivalents have been used to address issues ranging from the basic problems in skin biology, to the mechanisms of the wound healing process [5, 23]. In the clinical setting they have been proposed as tissue substitutes (grafts) for treatment of burns and other skin injuries [8, 9, 33].

Unfortunately, every dermal equivalent constructed and utilized to date contracts spontaneously. This contraction occurs within the first few hours following completion of the assembly process and results in a dense, opaque tissue [5, 8]. When used as grafts, severe contraction due to loss of water decreases the surface area and volume of the graft, leading to undesirable outcomes. For example, this process forms a scar, and interferes with the invasion of cells required for the remodeling phase of wound healing [5, 33]. While a certain amount of tissue contraction is acceptable and desirable so that wound closure may occur in an appropriate time frame, excessive contraction produces contractures (very dense scars) that are impenetrable to vascularization and innervation [34]. Heavy scars may also be acellular which is another undesirable outcome since the remodeling phase of wound healing is

reliant upon resident cells. A number of spontaneously contracting models have been frequently used as research tools in studies examining the mechanisms of contraction and scar formation [31, 35-38]. Such an unfortunate choice of model leads to conclusions that do not clarify our understanding of the tissue contraction process. Since the model is already in a state of contraction and the fibroblasts have been activated to the contractile phenotype, the signaling cascade initiated by additional ligands is superimposed on an already activated pathway. These may act in an additive, synergistic, or opposing manner. Furthermore, once the model is dense and opaque, it is impossible to monitor the morphological status of the cells by simple non-intrusive methods (e.g. light, fluorescent, or scanning laser confocal microscopy).

The transient or stable expression of green fluorescent protein (GFP) by fibroblasts is beginning to be used to address the difficulties in the real time monitoring of cells in three-dimensional models. GFP is a biological marker protein cloned from jellyfish and facilitates, amongst other applications, the observation of cell morphology in three-dimensions by scanning laser confocal microscopy [39].

Measurement of contraction has also been a difficult task in research that utilizes various models in studies of the contraction process. The most common and perhaps most primitive method involves determining the wet weight of the contracted equivalent and reporting the change as a percentage weight loss of the control (untreated) collagen gel [9]. Weight loss remains an obvious indicator

of contraction, because as the resident cells contract the matrix, they force water out of the equivalent, thus reducing its wet weight. Along the same lines, measuring the diameter or thickness of the contracted model has been frequently used as the easiest measurement of the extent of contraction [17, 35, 38, 40-45]. However, since the cells are randomly arranged throughout the collagen gel, contraction occurs non-uniformly. Therefore, while measurement of the diameter approximates the range of contraction, it does not take into consideration the total contraction process. Other methods have been proposed for assessing tissue contraction including: the counting of wrinkles created by cell contraction on a silicone film [46], the use of fluorescently labeled latex beads dispersed into the collagen matrix to visualize local distortions of the matrix in two-dimensions [47], and complex measuring devices coupling strain gauges to gel contraction [36]. Short of elaborate equipment and complex computer assisted mathematical modeling systems, there have been no simple methods established for measurement of collagen gel contraction, particularly in the early stages when contraction is not detectable by optical microscopy.

Another drawback of the existing connective tissue models is the use of primary fibroblasts as the principle cellular component. *In vitro* behavior of primary fibroblasts (and other cells) varies significantly from donor to donor, with respect to donor age and gender, and from passage to passage [48]. Such variability produces data that is difficult to interpret and makes it formidable to demonstrate statistical significance of changes over several experiments. It

seems that the most effective way to address this problem is to develop a human dermal fibroblast cell line with extended *in vitro* life span. A minimally altered cell line should result from the introduction of constitutive expression of the recently cloned catalytic subunit of human telomerase in primary human dermal fibroblasts.

Telomerase and Cell Cycle Control

All normal human cells, even fibroblasts, undergo a finite number of cell divisions when cultured *in vitro,* and ultimately enter a state of replicative senescence or terminal differentiation [49]. It has been proposed that telomere shortening is the molecular mechanism that leads to senescence [50]. Telomeres are single stranded DNA fragments that cap the ends of eukaryotic chromosomes. They maintain chromosomal stability by protecting the ends from exonuclease digestion or illegitimate recombination and also ensure complete chromosome replication [51]. Human telomeric DNA is composed of the hexanucleotide repeat TTAGGG [51]. During *in vitro* mitosis, telomeres shorten with each successive cell division due to the incomplete replication of the lagging strand by DNA polymerase, thus supporting the contention that telomeres serve as a cellular mitotic clock. In each cell type critically shortened telomeres can no longer perform their protective function, and trigger replicative senescence or crisis leading to cell death [52]. In developing organisms that require continuous

cell division, and most cancer cells, the telomere length is maintained by telomerase activity.

Telomerase is a ribonucleoprotein complex that synthesizes and maintains telomeric DNA by adding the repeat units onto the 3' ends of single-stranded telomeric DNA [53]. Telomerases contain several protein components and an RNA subunit [53]. The catalytic subunit has recently been cloned from a variety of species, including human [50, 51]. It is a specialized reverse transcriptase that uses its RNA subunit as a template for the synthesis of telomeric DNA repeats. The human telomerase catalytic subunit is designated hTERT (human telomerase reverse transcriptase), and when stably expressed, has been shown to extend the life span of normal human cells [54]. While telomerase is not expressed in most human somatic tissues, increased telomerase activity through ectopic expression of hTERT has enabled normal human fibroblasts to bypass senescence [51]. Introduction of viral oncogenes such as the SV40 large T antigen, E6/E7 genes of the human papillomavirus, and adenoviral ET-1 have also been used to extend the life span of various cell types. However, these immortalizing strategies not only circumvent senescence, but also alter the differentiation programs of the cells. In contrast, ectopic expression of telomerase is believed to confer replicative immortality on cells without affecting other regulatory systems, such as those that control differentiation [52]. As telomerase expression is also detected in the majority of neoplastic cells, reservations concerning the use of cells engineered to express

telomerase constituitively are being addressed [55]. To date no evidence has emerged to suggest that telomerized cells implanted into animal models give rise to tumors. There is no evidence of an increased growth rate as found in many cancer cell lines, and telomerized cells remained contact inhibited [55]. Also, the ectopic expression of telomerase did not affect the integrity of the pRb checkpoint or the p53-mediated cell cycle checkpoint and thus did not bypass cell cycle induced checkpoint controls [55]. Finally, cytogenetic analysis showed that hTERT fibroblasts were of a predominently normal karyotype with a low frequency of chromosomal aberrations [55]. Therefore, it has been proposed that use of a telomerized dermal fibroblasts cell line addresses the concerns relating to variations due to heterogeneity of normal human cells cultured *in vitro*, without creating a cancerous cell line or interfering with normal phenotypic changes. This is a particularly important cell line since the wound healing process involves fibroblasts at various stages of phenotypic differentiation.

Normal Wound Healing Process

Wound healing involves a highly regulated and coordinated sequence of biochemical and cellular events that initiate the restoration of the structural and functional integrity of the tissue [2]. This is a complex and dynamic process, requiring an intricate collaboration of different components of the surrounding healthy tissue and systemic links throughout the multiple overlapping phases [56]. In skin, these phases include formation of the fibrin clot and the consequent

inflammatory response, reepithelialization, fibroplasia, neovascularization, matrix deposition, wound contraction, and extracellular matrix reorganization/matrix remodeling [2].

In addition to hemostasis following blood vessel rupture, the formation of a fibrin clot creates a temporary barrier to protect the wound bed and leads to the establishment of a provisional matrix over and into which cells may migrate [57]. The provisional matrix also serves as a reservoir of cytokines and growth factors, which provides chemotactic cues to recruit inflammatory cells to the wound site [56]. Neutrophils and monocytes invade the wound site from the circulating blood. In addition to their role of clearing bacterial contamination early in the inflammatory process, neutrophils are also a source of cytokines that may serve as early signals to activate and recruit fibroblasts and epithelial cells to the wound [56]. Under normal conditions, neutrophils populate the wound within minutes of injury and remain there for a few days [58]. Macrophages continue to accumulate at the wound site as a result of the differentiation of the recruited monocytes [2]. Their tasks include phagocytosis of any pathogenic organisms and cell and matrix debris resulting from the injury [59]. Activated macrophages also release various cytokines (Tumor Necrosis Factor (TNF), Interleukin-8 (IL-8)) and growth factors (e.g. Platelet Derived Growth Factor (PDGF), Epithelial Growth Factor (EGF), basic Fibroblast Growth Factor (FGF2), and Transforming Growth Factor beta (TGF-β)), thus amplifying the signals initiated earlier in the process by the neutrophils [56, 59].

Wound healing of dermal tissue has been most extensively studied because skin is exposed to a wide variety of insults. More importantly, due to its accessibility, it is relatively easy to observe progression of the tissue repair process. Despite some tissue specific differences, the repair process generally follows a similar course. In dermal wound healing, several hours after injury, keratinocytes (epidermal epithelial cells) begin to migrate from the wound edges onto the provisional matrix to reepithelialize the wound [60]. Since this stratified epithelium serves as a protective barrier, it is imperative that a functional epidermis be reestablished as quickly as possible. The lag in keratinocyte response is in part due to the rearrangement of the cellular cytoskeletal apparatus and changing integrin expression to facilitate motility over the unfamiliar matrix [2, 56]. Once the denuded wound surface has been covered by a monolayer of keratinocytes, migration and proliferation stop, differentiation is activated, and the new stratified epidermis is established from the wound margin inward [60]. The process of reepithelialization is aided by the contraction of the underlying connective tissue, which brings the wound edges closer together thus reducing the area to be epithelialized [56].

One of the early responses to injury is recruitment of fibroblasts (dermal) from the wound edge. Fibroblasts proliferate in response to secreted mitogens (e.g. FGF, EGF, and TGF - β) to repopulate the wound bed and synthesize and secrete collagen and glucosaminoglycans (GAGs) so that the normal composition of connective tissue matrix may be reestablished. Granulation tissue

begins to form approximately four days after injury [2]. Finally, the fibroblasts assemble a contractile cytoskeleton, similar to that found in smooth muscle cells, in order to contract the matrix and close the wound [56]. In a number of tissues where fibroblasts are not the principal cellular component, but are present, fibroblast activation appears to be a preferred event. In most cases the fibroblasts adopt the leading role in tissue repair because the principal cells lack mitotic activity and perhaps motility. This type of wound healing (fibrosis) culminates in scar formation that is both structurally and functionally inappropriate. The resulting fibrotic scars interrupt the continuum of tissue and are a serious problem in a number of organs (e.g. heart, liver, lungs, kidney) [61-64]. Activation of fibroblasts and the consequent scar formation is therefore a serious global problem, occurring more frequently than would appear upon superficial analysis.

The provisional matrix is also known as granulation tissue, a term related to its pink granular appearance, which is due to the developing vascular bed [56]. Revascularization is driven by vascular endothelial growth factor (VEGF) secreted at the wound site to promote angiogenesis [2]. As with the fibroblasts and epithelial cells previously mentioned, vascular endothelial cells must upregulate specific cell matrix interactions, $\alpha_v\beta_3$ integrins, in order to respond to the angiogenic signals [2, 65]. Vascularization is critical in order to satisfy the increasing demand for oxygen and other nutrients required by the cells invading the wound site [45, 65]. Innervation also begins to be reestablished at this time,

in response to the nerve growth factor (NGF) released by the resident cells [66]. It has been established in experimental animal models and observed in patients that sparsely innervated areas of the body tend to develop spontaneous ulcerations and heal poorly when injured [56]. This supports the hypothesis that the neural network and the neuropeptides it secretes play an important role in homeostasis and tissue repair. The mechanisms involved in the participation of the neurogenic component during tissue repair are poorly understood. It is possible that innervation plays some stimulatory role in the healing process by secreting neuropeptides and other neurotrophins at the wound site [56].

Matrix remodeling during the transition of granulation tissue to a mature scar is dependent upon the controlled synthesis/deposition and degradation of the extracellular matrix by fibroblasts. Further remodeling occurs through myofibroblast contraction of the matrix and the formation of larger collagen bundles and intricate cross-linking which serves to gradually increase the strength of the scar [2].

A strict balance between synthesis and deposition of ECM components is critical to maintain tissue structure and function. The ECM-degrading proteinases can be subdivided into three classes: 1. serine proteinases, 2. metalloproteinases (MMPs), and 3. cysteine proteinases (cathepsins) [15]. Serine proteinases and metalloproteinases play major roles in most physiological and pathological states involving tissue remodeling [15]. Plasminogen activators (PAs) are the major members of the serine proteinase class, responsible for the

conversion of plasminogen to plasmin. Plasmin has broad substrate specificity, and is therefore responsible for the degradation of fibronectins, laminin, proteoglycan cores, gelatins, and partially degraded collagens [15]. Plasmin can also activate certain prometalloproteinases by cleavage of the pro-domain to yield an active MMP. MMPs are a family of enzymes that are secreted as inactive zymogens and degrade ECM components including laminin, collagen, fibronectin, proteoglycans, gelatin and elastin [15]. Their proteolytic activity is inhibited by tissue-derived metalloproteinase inhibitors (TIMPs). TIMPs block the activity of all MMPs of mammalian origin, but have no efficacy against other proteases, including metalloenzymes [15]. In normal wound healing, the activation of proteases and their inhibitors is tightly regulated. The dysregulation often characteristic of pathogenic situations exemplifies the importance of maintaining a balance during wound repair and remodeling.

While these basic processes are generally understood, detailed knowledge about which growth factor or combination of growth factors are involved in the initiation, upregulation, and maintenance or downregulation of signaling is not known. In order to intervene and modulate scar formation, it is imperative to understand not only cell-matrix interactions, but also the role of extracellular ligands and their signaling cascades. This is particularly important for wound repair modulation, targeting a more regenerative and less scar-based outcome [56].

Tissue Contraction

In normal tissue repair processes, tissue contraction is beneficial, resulting in rapid wound closure and restoration of the tissue integrity. However, frequently excessive contraction takes place and is detrimental [17, 34, 67]. For example, the loss of large expanses of skin after chemical or thermal injury results in the formation of large areas of contracting granulation tissue. These can result in restricted blood flow, limited joint mobility, and disfiguring scars [3, 8, 18]. In some types of injuries the healing interface forming the scar can form a barrier between the two areas of healthy tissue (e.g. wound edges, grafted and host tissue) impeding integration. To date, there are no pharmacological agents available to reduce or prevent inappropriate or excessive contraction. Thus, a primary goal of wound healing research has been to develop specific strategies that allow repair of wounded tissues without excessive contraction and extensive scarring.

Excessive connective tissue contraction and scar formation are not necessarily inevitable consequences of wound healing. Significant experimental evidence indicates that during development, response to injury is fundamentally different from that in the adult organism [67]. Fetal wound healing occurs without escar formation, without the inflammation characteristically associated with adult wound healing, and in the presence of an altered ratio and generally reduced level of cytokines [34]. Since hyaluronic acid (HA) is a substantially greater component of the fetal ECM, its presence has been correlated to scarless wound

healing [68]. One possible explanation for this is that tissue contraction induced loss of water from a matrix rich in highly hydrophilic HA is reversible, whereas a significantly more hydrophobic collagen matrix cannot easily rehydrate [68]. It has also been shown that myofibroblasts are absent in fetal wounds and consequently, the process of tissue contraction is minimal or may not take place at all [29]. Although every point of difference between adult and fetal wound healing is not necessarily significant in terms of scarring, defining and understanding all the factors responsible for scarless fetal wound healing is important. It is perhaps even more important to elucidate all the effectors of adult tissue contraction and tissue regeneration and the molecular mechanisms of their action. While the list of contractile ligands is long and comprehensive (**Table 1**), the role of some peptides in scar formation has not been explored.

Endothelin – 1

One contractile ligand that has not been thoroughly studied is endothelin. Endothelins are a family of peptides originally identified as potent vasoconstrictors secreted by vascular endothelial cells. In 1988, Yanagisawa et al isolated, purified, sequenced and cloned endothelin-1 (ET-1) from the culture media of porcine aortic endothelial cells [69]. The ET-1 gene is found on the human chromosome 6 and is translated into a 203 amino acid pre-pro peptide, the cleavage of which yields a 38 amino acid pro-endothelin, Big ET. Proteolytic cleavage between Trp 21 and Val 22 by endothelin-converting enzyme (ECE)

produces the bioactive 21 amino acid peptide, ET-1 [70]. ET production appears to be mainly regulated at the level of gene expression or translation of mRNA [69].

Receptors

ETs initiate their biological effects by binding to 7-transmembrane, G-protein coupled receptors, with an extracellular amino terminus and an intracellular carboxy terminus. They are members of the rhodopsin superfamily of transmembrane receptors, the second intracellular loop of which is highly conserved. These receptors are designated ET_A and ET_B according to the primary ligand affinity (ET-1 and ET-2, respectively) and are subject to ligand-induced down regulation. ET-1 pretreatment decreased ET-1 binding sites and attenuated the ability of ET-1 to increase intracellular calcium in Swiss 3T3 fibroblasts. Exposure of Swiss 3T3 fibroblasts to ligand also increased turnover of ET_A receptors [69].

Signaling

ET-1 is known to induce the phosphorylation of numerous cytosolic and membrane-bound proteins that are part of signal transduction pathways involved in cell proliferation and differentiation [70]. Since ET-1 was first identified as a potent vasconstrictor, studies of its signaling have been historically targeted to vascular cells. In addition to its acute role in modulating vascular tone, ET-1 plays a critical role in the long-term control of cellular growth and remodeling of the vascular network. In order to produce such a diverse range of biological

responses, ET-1 is able to activate distinct effector systems including phospholipase C (PLC), phospholipase D (PLD), phospholipase A_2 (PLA_2), adenylate and guanylate cyclases, and numerous cytosolic and nuclear protein kinases [70]. The wide range of biological activities that ET-1 exerts on the vasculature includes vascular contractility, cell division, and differentiation. This wide range of actions, combined with the fact that endothelin receptors have been identified in numerous cell types, has led to studies of ET-1 in many systems.

In Swiss 3T3 fibroblasts, endothelin receptor activation leads to increased activity of PLC, increased phosphatidylinositol (PI) turnover, and ultimately an elevation of intracellular calcium [71]. Pertussis toxin fails to inhibit phosphatidylinositol turnover in rat-1 fibroblasts stimulated with ET, leading to the conclusion that multiple G proteins couple ET receptors to PLC [71]. ET also stimulates a dose-dependent increase in diacylglycerol and phosphorylation of a protein kinase C (PKC) substrate in fibroblasts [71, 72]. The focal adhesion associated protein, paxillin, was phosphorylated following ET-1 stimulation of Swiss 3T3 cells, linking endothelin to focal adhesion assembly in fibroblasts [73]. The stimulation of focal adhesion plaque formation by Rho and Rho-associated kinase (ROCK) in non-muscle cells has been well established [74-77]. However, the link between endothelin and Rho signaling in normal fibroblasts has not been clearly established. Cultured hepatic stellate cells, when stimulated with ET-1, assembled F-actin fibers and showed increased myosin light chain

phosphorylation. Contraction was also induced by endothelin. The addition of Y-27632, a specific rho-associated kinase inhibitor diminished these effects [78]. Therefore, in some cell types, but not in human dermal fibroblasts, the cytoskeletal effects of endothelin have been linked to Rho associated signaling.

The finding that ET is a potent mitogen for cultured cells demonstrates that ET regulates gene expression to produce long-term responses. One pathway activated by ET and possibly responsible for the subsequent nuclear events is signaling involving the *c- fos* proto-oncogene. *c-Fos* belongs to a group of inducible genes that convert short-term, transmembrane signals into long-term responses requiring transcriptional regulation of target genes. Therefore, *fos* genes act as switches for activating the transcription of multiple genes in response to a variety of extracellular signals including growth factors and neurotransmitters. Expression of *c-fos* in response to ET-1 stimulation has been demonstrated in glomerular mesangial cells, vascular smooth muscle cells, and 3T3 fibroblasts, but not in human dermal fibroblasts [71].

The Role of ET – 1 in Wound Healing

Although initially ET-1 was classified as a potent vasoconstrictor, recent evidence suggests that it also regulates a wide variety of non-vascular functions. It is a potent mitogen in Swiss 3T3 fibroblasts [79], normal rat kidney cells [80], and smooth muscle cells [81]. ET-1 contracted renal fibroblasts [82], caused concentration dependent granulation tissue contraction in male Wistar rats [83],

and contracted collagen lattices populated with human dermal fibroblasts [32, 84]. However, these studies were performed using spontaneously contracting collagen gels, so that the contraction reported was a percentage of the reduced controls. ET-1 was also shown to affect collagen synthesis. It stimulated normal, human dermal fibroblasts to synthesize collagen types I and III by a mechanism dependent upon both the ET_A and ET_B receptors. ET-1 also enhanced the steady state levels of collagen mRNA and activated the proα2(I) collagen promoter [84]. Both an increase in procollagen synthesis and in procollagen stabilization was shown in human fetal lung fibroblasts treated with ET-1 [81]. ET-1 and ET-3 have also been shown to regulate cytoskeletal actin organization, and restore stress fibers in rat astrocytes [85]. Endothelins increase the expression of sarcomeric myosin in kidney mesangial cells and liver stellate cells [82] and stimulate paxillin tyrosine phosphorylation in Swiss 3T3 cells [73]. All these changes in the cytoskeletal organization and the status of the focal adhesion plaque caused by endothelin stimulation may also activate normal human dermal fibroblasts and prime them for matrix contraction and/or cell migration.

As discussed above, the wound healing process involves the activated fibroblast phenotype, the myofibroblast. Normal wound healing requires that the activated fibroblasts, be they myofibroblasts or not, have the ability to (1) divide and migrate within the provisional matrix of the wound, (2) proliferate to repopulate the wound site, (3) synthesize collagen to rebuild the extracellular matrix and (4) contract the matrix to close the wound. Every one of these phases

of wound healing has been shown to be stimulated by endothelin in a variety of models.

A clear role remains to be established for endothelin as an important player in scar formation. However, evidence is beginning to accumulate to support the presence of endothelin after injury in various systems. Using experimental animal models, changes in ET-1 levels (mRNA and protein), receptor kinetics and functional reactivity (EC_{50}) have been observed, thus implicating ET-1 in the etiology of a variety of diseases [70]. ET-1 has been shown to be upregulated during renal injury [82] and elevated circulating levels of ET-1 have been reported in a variety of vascular and inflammatory diseases, and in the connective tissue disease scleroderma [84]. A role for ET-1 in the chronic inflammation associated with atherosclerosis has been demonstrated. Myofibroblasts stained positively for ET-1 immunoreactivity in human atherosclerotic coronary tissue [86]. In addition, wounded male Wistar rats showed an increase in myofibroblasts at the site of granulation tissue over time and a time dependent increase in ET-1 expression in endothelial cells at the same sites [83]. Endothelin expression can also be induced by thrombin, a factor known to be at the wound site [72] and can also be expressed by macrophages [69]. Therefore, recent studies have implicated endothelin in processes of wound healing and injury, and have suggested relevant sources of endothelin at the wound site.

The following studies are directed toward satisfying some of the deficiencies discussed. Further work should target the discovery of agents that are able to prevent deleterious scar formation.

Table 1. Effect of various components on collagen matrix contraction [35].

Treatment	Diameter (mm) Day 1	Day 6
20% FBS	21.75	13.75 +/-1
Control	53	16.5 +/-1
Dexamethasone (55ng/ml)	53	15.8 +/-3
Dihydrotestosterone (10nM)	51	17.0 +/-1
β-estradiol (10nM)	52	16.5 +/-1
Glucagon (5μg/ml)	53	20.2 +/-2
Hydrocortisone (500nM)	47.8	15.0 +/-1
Progesterone (100nM)	53	17.8 +/-1
Prostaglandin D_2 (100ng/ml)	45	13.5 +/-1
Prostaglandin E_1 (100ng/ml)	53	26.5 +/-2
Prostaglandin F_2 (100ng/ml)	49	19.5 +/-2
Somatostatin (10ng/ml)	53	17.8 +/-2
Endothelial Growth Supplement (100μg/ml)	35.5	15.75 +/-1
Epidermal Growth Factor (100ng/ml)	48.3	20.3 +/-2
Fibroblast Growth Factor (100ng/ml)	48.5	20.5 +/-3
Nerve Growth Factor (10ng/ml)	50.8	16.0 +/-1
Platelet Derived Growth Factor (2U/ml)	30.8	13.75 +/-1
Ascorbic Acid (10μg/ml)	53	24.75 +/-7
Human Transferrin (100μg/ml)	50.53	19.75 +/-1
Fibronectin (8μg/ml)	53	25.0 +/-7
Thrombin (1μg/ml)	41	16.0 +/-1
Ethanol (1%)	44	16.0 +/-1

Figure 1. Schematic representation of proposed signaling by endothelin – 1 in wound healing fibroblasts.

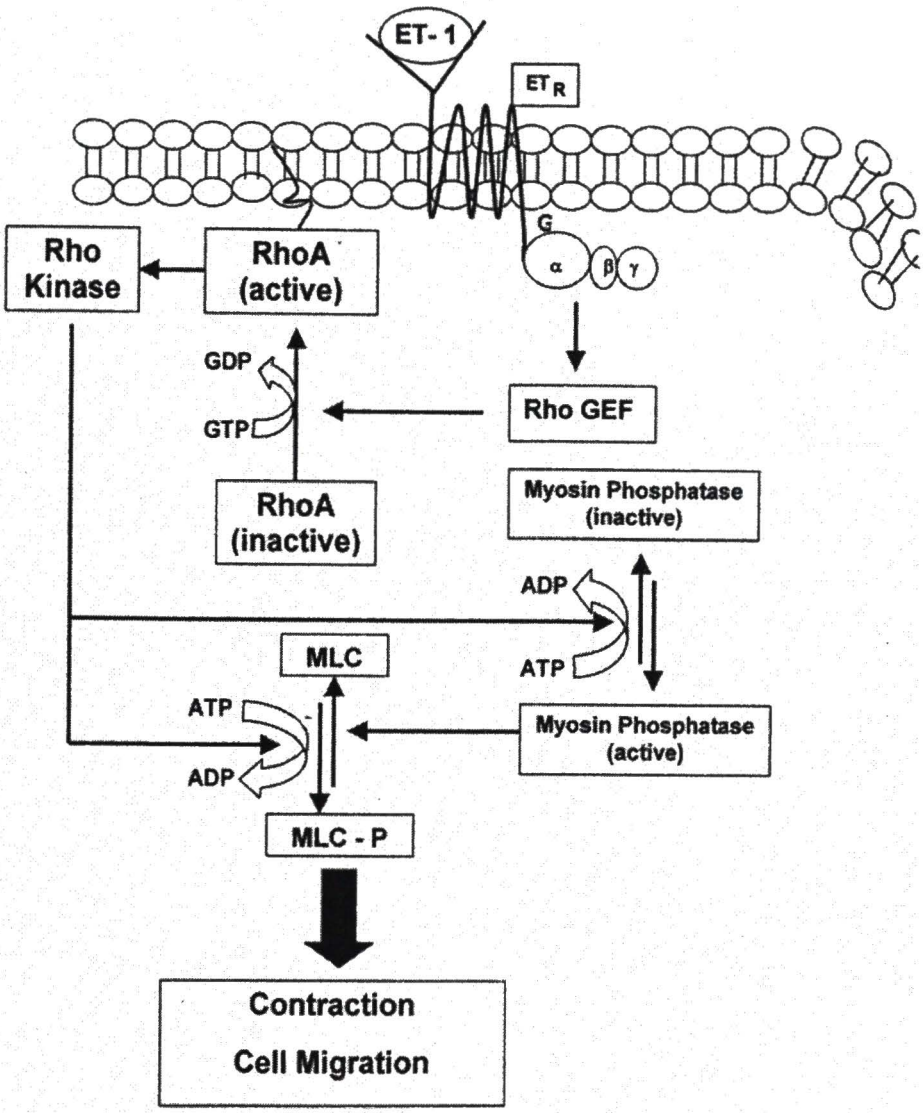
ET- 1
ET R
G
α
β
γ
Rho Kinase
RhoA (active)
GDP
GTP
Rho GEF
RhoA (inactive)
Myosin Phosphatase (inactive)
ADP
ATP
MLC
ATP
ADP
Myosin Phosphatase (active)
MLC - P
Contraction
Cell Migration

Figure 2. Collagen synthesis by wound healing fibroblasts.

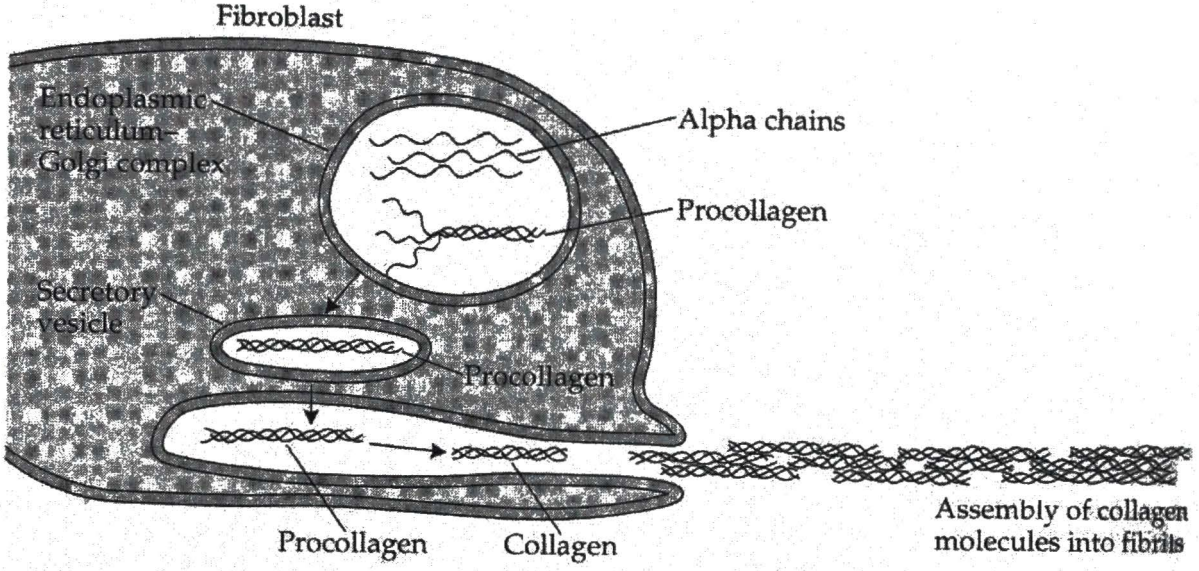
Fibroblast
Endoplasmic reticulum
Golgi complex
Alpha chains
Procollagen
Secretory vesicle
Procollagen
Procollagen
Collagen
Assembly of collagen molecules into fibrils

Figure 3. Cell-Matrix Interactions [Biocarta.com].

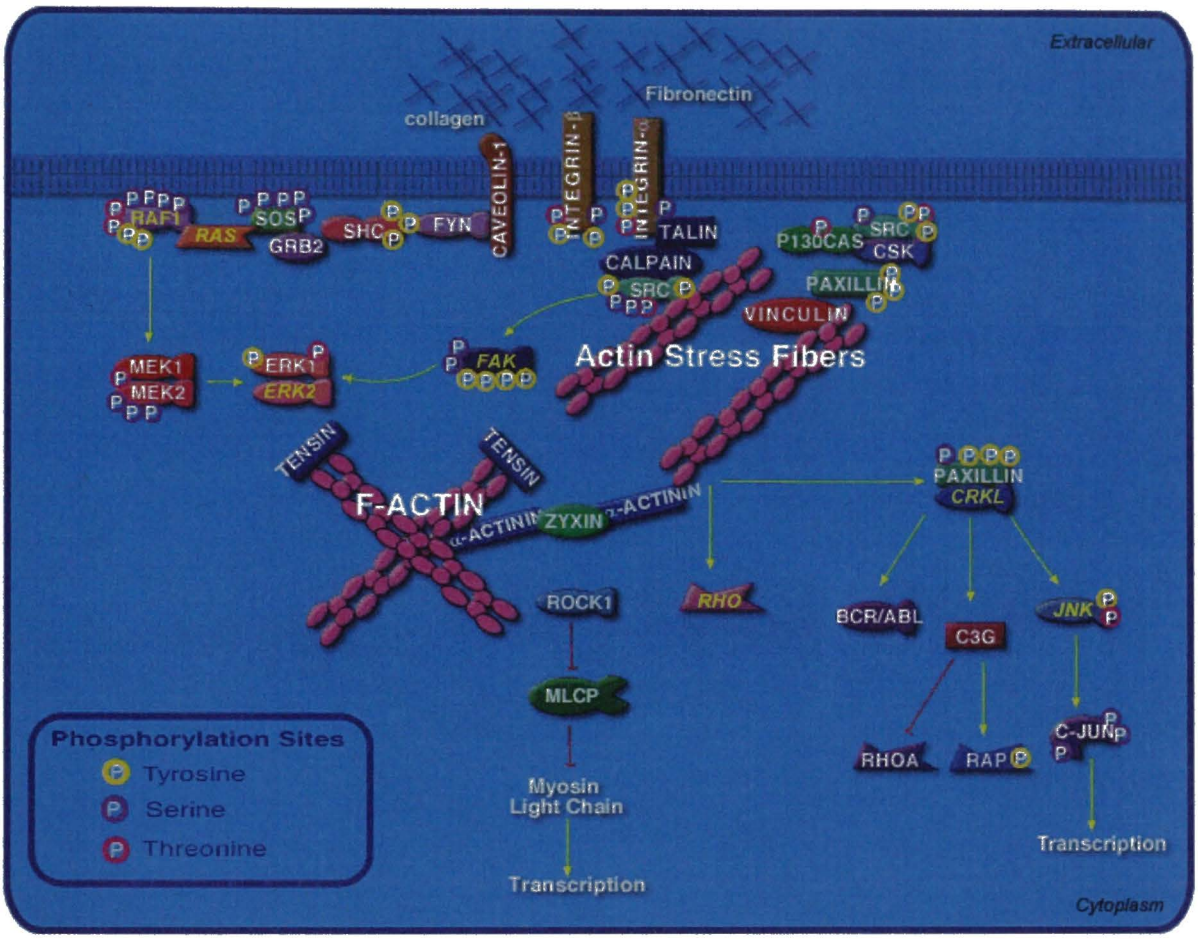
Extracellular
collagen
Fibronectin
CAVEOLIN-1
INTEGRIN-β
INTEGRIN-α
TALIN
RAF1
RAS
SOS
GRB2
SHC
FYN
CALPAIN
SRC
P130CAS
CSK
PAXILLIN
VINCULIN
Actin Stress Fibers
MEK1
MEK2
ERK1
ERK2
FAK
TENSIN
TENSIN
F-ACTIN
α-ACTININ
ZYXIN
α-ACTININ
PAXILLIN
CRKL
ROCK1
RHO
BCR/ABL
C3G
JNK
MLCP
RHOA
RAP
C-JUN
Myosin
Light Chain
Transcription
Transcription
Phosphorylation Sites
Tyrosine
Serine
Threonine
Cytoplasm

Figure 4. Schematic Representation of Myofibroblast Evolution [25].

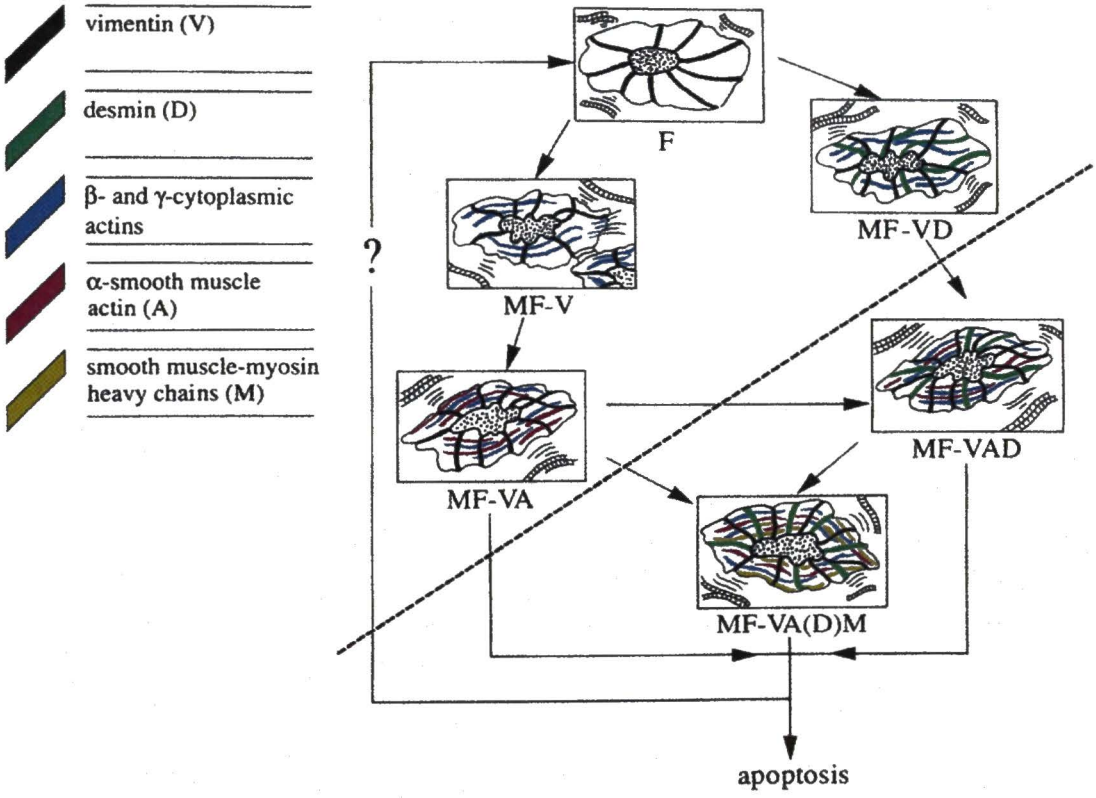
vimentin (V)
desmin (D)
β- and γ-cytoplasmic actins
α-smooth muscle actin (A)
smooth muscle-myosin heavy chains (M)
F
MF-V
MF-VD
MF-VA
MF-VAD
MF-VA(D)M
?
apoptosis

Chapter II

Telomerized Human Fibroblasts Respond Normally to a Wound Healing Environment in Monolayer Culture and as Cellular Components of a Connective Tissue Model

Introduction

When cultured *in vitro*, normal human fibroblasts undergo a finite number of cell divisions and ultimately enter a state of replicative senescence [49]. Introduction of viral oncogenes such as the SV40 large T antigen, E6/E7 genes of the human papillomavirus, and adenoviral ET-1 have been used to extend the life span of various cell types. However, these immortalizing strategies not only circumvent senescence, but also alter a number of normal cellular functions. In contrast, ectopic expression of telomerase is believed to confer replicative immortality on cells without affecting other regulatory systems, such as those that control differentiation [52].

Telomere shortening has been proposed as the principle molecular mechanism that leads to senescence [50]. Telomeres are single stranded DNA fragments that cap the ends of eukaryotic chromosomes. They maintain chromosomal stability by protecting the ends from exonuclease digestion or illegitimate recombination and also ensure complete chromosome replication [51]. The catalytic subunit of telomerase reverse transcriptase (TERT) has

recently been cloned from a variety of species, including human (hTERT) [50, 51]. When stably expressed, hTERT extended the life span of several normal human cell types [54].

While telomerase is not expressed in most human somatic tissues, increased telomerase activity through ectopic expression of hTERT enables normal human fibroblasts to bypass senescence [51]. As many human cancers have been shown to express telomerase activity, reservations concerning the use of cells engineered to express telomerase constituitively are being addressed [55]. To date no evidence has emerged to suggest that telomerized cells implanted into animal models give rise to tumors, there is no evidence of an increased growth rate as found in many cancer cell lines, and telomerized cells remain contact inhibited [55]. Furthermore, ectopic expression of telomerase did not affect the integrity of the pRB or the p53 – mediated cell cycle checkpoints, and thus did not bypass cell cycle induced controls [55]. Finally, cytogenetic analysis showed that hTERT fibroblasts were of a predominantly normal karyotype with a low frequency of chromosomal aberrations [55].

It is therefore likely that telomerized cells may combine the advantages of cell lines and primary cultures to produce cells with an extended lifespan and seemingly near normal cell functions. The utility of such cells as components of three-dimensional *in vitro* models is beginning to be studied.

The *in vivo* tissue repair process involves the activation of fibroblasts to perform a variety of functions. Quiescent fibroblasts populating normal tissue,

undergo phenotypic change upon stimulation, and produce the activated myofibroblasts [26]. It is believed that myofibroblasts are the wound healing cells that proliferate, migrate within the matrix [22], synthesize and deposit new collagen and other matrix macromolecules, and through tissue contraction close the wound [27]. Behavior of hTERT fibroblasts under these conditions has not been studied. In order to demonstrate that hTERT fibroblasts respond normally to wound healing stimuli, we compared cell proliferation, collagen synthesis, migration and contraction capabilities of normal, human fibroblasts with that of the telomerized fibroblasts both in monolayer culture and in a three–dimensional tissue equivalent (TE).

Materials and Methods

Cell Culture.

General. Cells were passaged before they reached confluency using trypsin/EDTA (Gibco-BRL) and were cultured on tissue culture flasks (Corning) in 37°C incubators with 5% CO_2. They were cultured in Dulbecco's Modified Eagle Medium (DMEM, Gibco-BRL) with 10% Fetal Bovine Serum (FBS), unless otherwise indicated.

Infant Fibroblasts. Dermal fibroblasts were obtained from infant human foreskin explants as previously described [87]. Briefly, human infant foreskins were incubated at 4°C in a solution of 20 U/ml dispase (Collaborative Research) in DMEM for 48 hours. The epidermis was separated from the dermis and

processed further for epidermal cells. Infant fibroblasts were obtained as out growths from explanted dermal tissue, following incubation at 37°C in DMEM + 10% FBS. All experiments were performed with Infant fibroblasts between passages 3 and 9, population doubling 9.13 to 27.67.

hTERT Fibroblasts. The catalytic subunit of human telomerase was retrovirally transfected into normal human infant fibroblasts [50]. This transfection was stable, and hTERT fibroblasts at population doubling 232.8 or higher were used in the experiments. Cells were a gift from Dr. Jerry Shay, University of Texas Southwestern Medical School.

hTERT + eGFP Fibroblasts. Following numerous attempts at stable transfection using more conventional methods (Superfect, Fugene, lipofectamine, calcium chloride), enhanced green fluorescent protein was lentivirally transfected into hTERT fibroblasts [88]. Cells expressing green fluorescent protein were selected using a fluorescent automated cell sorter (FACS). Because fibroblasts are attachment dependent cells, they were separated into a single cell stream by passing them through a fine mesh and sorted twice to assure a homogenous cell population. This transfection was stable and cells were used at population doubling higher than 240.

Tissue Equivalent (TE) Construction. The collagen matrix was prepared by mixing 8 parts collagen (0.3%, Vitogen-100 (Celtrix Pharmaceuticals); 0.5%, ICN (ICN Biomedicals), 1 part 10X Ham's F-12 medium, and 1 part Reconstitution Buffer (0.05N NaOH, $NaHCO_3$, Hepes). The appropriate number

of cells was suspended within the collagen mixture and the TE was allowed to polymerize at 37°C, 5% CO_2. TE were supplied with Ham's F-12 Nutrient Medium + 5% FBS (Gibco) every other day unless otherwise indicated.

***In Vitro* Quiescence.** Normal and hTERT fibroblasts (0-350,000 cells/ml collagen) were added to a collagen mixture (0.3 or 0.5% Collagen I) in 24 well plates (1ml collagen/well). The tissue equivalents (TE) were removed on days 3, 6, 9, 12, 15 and 20. Wet weight and volume (water displacement) were analyzed and the equivalents were dissolved using collagenase (Sigma) to count cell number. The combination of these parameters is designed to show that the cells are quiescent within the matrix and are not activated to their myofibroblast phenotype. A one-way ANOVA or Kruskal-Wallis one-way analysis of variance on ranks was performed on the average TE wet weights for each cell type and cell number to determine that no statistically significant difference between the two cell types exists.

Western Analysis. Infant or hTERT fibroblasts were lysed using lysis buffer (1.0M Tris, pH 7; 0.5% SDS; 5% sucrose). The amount of total protein was determined using the BCA protein assay (Pierce). Briefly, it combines the reduction of Cu^{2+} to Cu^{1+} by protein in an alkaline medium (the biuret reaction) with the highly selective and sensitive colorimetric detection of the cuprous cation using a reagent containing bicinchoninic acid (BCA). Approximately 10 □g total protein was added to each well of a 4-15% gradient Tris-Glycine gel and SDS-PAGE was completed using the BioRad vertical electrophoresis system. The gels

were transferred to a nitrocellulose membrane at 20 mAmps overnight using the BioRad transfer system. The membranes were blocked with 1% Bovine Serum Albumin (BSA, Sigma) and 5% milk in 1X PBS, and then incubated at 4° C overnight with monoclonal primary antibody diluted in 1X PBS + 0.1% Tween 20 (alpha- smooth muscle actin, 1:400; myosin light chains, 1:200; myosin heavy chain, 1:1000). Membranes were washed with 1X PBS + 0.1% Tween 20, and the appropriate secondary antibody was incubated on the membrane for 30 min. to 1 hour at RT (1:1000 dilution in 1X PBS + 1% BSA). Once the membranes were washed again, the bands were detected using the ECL chemiluminescence method (Amersham).

Indirect Immunofluorescence. Normal infant fibroblasts and hTERT fibroblasts were cultured in chamber slides or on glass coverslips. After fixing with Methanol: Acetone (1:1) at 4°C for 10 min., the cells were blocked with 1% BSA in 1X PBS overnight at 4°C. Primary monoclonal antibody diluted in 1% BSA in 1X PBS (Vimentin, 1:200; α-Smooth Muscle Actin, 1:200; Myosin Light Chain, 1:200) was incubated on the cells overnight at 4°C. Following multiple washes with 0.1% Tween 20 in 1X PBS, the cells were incubated with secondary antibody (AlexaFluor or FITC, Molecular Probes, diluted 1:1000 in 1% BSA in 1X PBS) for 1 hr. at 37°C. The slides were washed again, mounted using FluorSave (CalBiochem) and were examined by fluorescence microscopy.

Proliferative Response to a Growth Factor. Infant human dermal fibroblasts and hTERT fibroblasts were plated at 2000 cells/well and cultured in

96 well plates. They were serum starved overnight and then stimulated with basic Fibroblast Growth Factor (FGF2, 0 – 4nM) over 7 days. Cell proliferation was determined using the Sulfrhodamine B (SRB) method [89]. Briefly, the cells were fixed with 10% TCA for 10 min. at 4°C and stained with SRB in 1% acetic acid. Once dry, the dye was solubilized in 10mM Tris base. The absorbance was read at 564nm. The dye binds total protein and the cell number reported is the result of the same experiment performed on a known number of cells to create a standard curve. An unpaired t-test was performed on the averages of normal and hTERT fibroblasts at each bFGF concentration to show there is no statistically significant difference between the two cell types ($p = 0.100$).

Matrix Biosynthesis. Infant human dermal fibroblasts and hTERT fibroblasts were plated at 40,000 cells/well and cultured in 96 well plates. They were serum starved overnight and stimulated with ascorbate (50μg/ml) in phenol red free DMEM + 0.1% BSA over 48 hours. Collagen synthesis was determined using a picrosirius dye, as described by Walsh et al [90]. Briefly, the medium was removed from the wells at 8 and 48 hours and dispensed into fresh 96 well plates. The medium was allowed to evaporate. The plates were rinsed three times in distilled water and assayed immediately. Additionally, the collagen produced but still associated with the cells was measured; cells were lysed with rapid freeze thawing and were allowed to dry on the plates. Once rinsed, the wells were filled with 100μl of 0.1% Sirius Red F3BA (Direct Red, Sigma) in saturated picric acid and stained for one hour at room temperature. The plates

were washed five times with 200μl of 10mM HCl. The collagen bound stain was then eluted with 200μl of 0.1M NaOH for 5 min. The eluted stain was dispensed into a fresh 96 well plate and the absorbance read at 450nm. The dye is specific for collagen type I and the collagen concentration was derived form a standard curve of known collagen concentrations. An unpaired t-test was performed on the averages of normal and hTERT fibroblasts at each time point (8 and 48 hours) to show there is no statistically significant difference between the two cell types.

Tissue Contraction Assay. Normal and hTERT TE were constructed in BSA (2% in 1X PBS) coated wells and then stimulated with serum (10 - 20%) or TGF-β (10ng/ml) to induce contraction of the collagen gel. Contraction was quantitated by weighing and measuring the contracted TE and compared to non-contracted controls. Mean wet weight +/- standard deviation was reported, and a one-way ANOVA followed by a Tukey Test or an unpaired t-test was utilized to show statistically significant differences ($p<0.050$).

Migration Assay. Telomerized fibroblasts expressing green fluorescent protein (hTERT+eGFP fibroblasts) were plated on a 12 – well plate insert at high density. Once confluent, an acellular collagen gel was constructed in the insert. The cells were allowed to migrate into the matrix for two weeks. The equivalents were optically sectioned using scanning laser confocal microscopy (SLCM) to visualize cell fronts, extent of migration, and organization within the equivalent.

Results

Telomerized fibroblasts populating a tissue equivalent remain quiescent. Normal and hTERT fibroblasts were dispersed in a 0.5% collagen type I matrix and sustained for 20 days. Every three days tissue equivalents (TE) were weighed and dissolved with collagenase to determine wet weight and cell number. Slight variation among each TE in volume and cell number occurs due to the viscosity of the collagen solution and the resulting difficulty in evenly dispersing the cells within the matrix. The wet weight serves as a measure of contraction since as cells contract the matrix, they squeeze water from it, and thus decrease the wet weight of the TE. Wet weight over the 20 days remained constant (**Fig. 1**). Therefore, the cells have not been activated to contract the TE spontaneously. This experiment was also conducted with a 0.3% collagen matrix and the results were the same (data not shown).

It is also important to show that the telomerized fibroblasts are not hyperproliferative in the three–dimensional matrix environment, to address concerns regarding telomerase and its role as a marker for some types of cancer. Thus, the cells were counted following dissolution of each TE with collagenase, and the cell numbers over the 20-day period were consistent with the number of cells initially dispersed into the TE (**Fig. 2**).

Normal cytoskeletal expression and organization is retained by telomerized fibroblasts. Since changes in certain cytoskeletal proteins are recognized indicators during activation of fibroblasts, western analysis and

indirect immunofluorescence were performed on both hTERT and Infant fibroblasts as monolayer cultures. Using western analysis (**Fig. 3**), it was shown that the expression levels of myosin light and heavy chains were the same in both cells types. In addition, alpha smooth muscle actin (α-SMA) expression was similar between the two groups. This is particularly important since α-SMA is the accepted marker for the activated myofibroblast phenotype [28]. The cytoskeletal organization was examined by immunofluorescence (**Fig. 4**), and confirmed that the hTERT fibroblasts preserved the cytoskeletal arrangement of the normal cells.

Fibroblast growth factor stimulates hTERT fibroblasts to proliferate. A key stimulus that fibroblasts receive during wound–healing is basic fibroblast growth factor (FGF2), which causes fibroblast proliferation and wound bed repopulation. Therefore, we examined proliferation of Infant and hTERT fibroblasts in response to 0 to 4nM FGF2 (**Fig. 5**). Both cell types responded to FGF2 over a seven day time period, proliferating to over 5000 cells/well in response to the highest dose (4nM). The difference in the mean values of the two cell types at the concentrations of FGF2 used in this experiment was analyzed via t-test and is not statistically significant ($p>0.050$).

Collagen synthesis and deposition following stimulation with ascorbic acid. Another characteristic of the myofibroblast phenotype is the synthesis and deposition of matrix proteins, especially collagen type I. In both cell types, stimulation by ascorbate over 48 hours leads to the synthesis and

secretion of collagen type I (**Fig. 6**). The total collagen type I synthesized and secreted doubled within 48 hours for both Infant and hTERT fibroblasts. Again, a t-test was used to show that the mean values obtained at 8 and 48 hours were not statistically significantly different between the two groups of cells ($p>0.050$).

Contraction of the three–dimensional TE. While spontaneous contraction in TE is not desirable, the fibroblasts must be responsive to factors that activate them to contract the matrix. In wound healing, this occurs to close the wound and often leads to scar formation. The telomerized fibroblasts did contract the matrix following the addition of serum or transforming growth factor beta (**Fig. 7**), two stimuli found at the wound site and shown to be potent stimulators of wound contraction. The mean wet weights of hTERT fibroblast TE treated with 20% FBS decreased by nearly half within 18 hours of serum addition (**Fig. 7A**). The mean wet weights of treated TEs were statistically significantly different from the 5% FBS treated control TEs ($p<0.050$). Also, TE treated with 10ng/ml TGF-β showed statistically significant contraction over 20 days (unpaired t-test, $p<0.001$) (**Fig. 7B**).

Migration of the hTERT fibroblasts into an acellular collagen matrix. Migration through the matrix is another function of the activated fibroblast. Cells transfected with both the human catalytic subunit of telomerase (hTERT) and enhanced green fluorescent protein (eGFP) were used to visualize cell migration into an acellular collagen matrix (**Fig. 8**). This system allowed non-intrusive, real-time visualization of the movement of fibroblasts into the acellular matrix. Within

one week, cells had begun to migrate into the matrix. At two weeks, laser scanning confocal microscopy was used to obtain optical sections of the model and analyze it for cell migration. There appear to be surges of fibroblast cell fronts, leading the migration and perhaps showing a wave of migration occurring at regular time intervals. Optical sectioning of the collagen matrix and determination of the amount of fluorescence in each section shows the migrating cell fronts graphically. Since the cells are cultured on a membrane in monolayer and have the ability to proliferate on the surface of the collagen, there is no simple technique for quantifying the number of cells that enter the matrix.

Discussion

The purpose of this study was to characterize the hTERT fibroblast cell line for use in wound healing studies, including as part of our three-dimensional TE. Since the vast majority of tumor cells express telomerase while most normal human cells do not, it was imperative to show that cells immortalized by hTERT retain normal growth control and checkpoint mechanisms and a stable karyotype [48]. To this end, the quiescence experiments illustrate that hTERT fibroblasts are neither hyperproliferative within the three-dimensional collagen matrix, nor do they spontaneously contract the matrix. Furthermore, we wanted to demonstrate that ectopic expression of telomerase by dermal fibroblasts did not drive them irreversibly toward their proliferative phenotype, but that they are able to respond to various wound healing stimuli to perform all the other functions required of the

fibroblast during the tissue repair process. In fact, hTERT fibroblasts in TE behaved identically to normal cells and remained contact inhibited within the collagen matrix.

The expression and localization of cytoskeletal proteins including desmin, vimentin, myosin light chain, myosin heavy chain, and alpha smooth muscle actin was similar for both normal human and hTERT fibroblasts, suggesting that phenotypes requiring special cytoskeletal arrangements can be obtained.

FGF2 has been well established as a potent mitogen for several cell types, including fibroblasts [91]. At the wound site, FGF2 is thought to promote angiogenesis and facilitate the closure of lesions by accelerating granulation tissue formation [92]. Ectopic telomerase expression is thought to drive proliferation in the hTERT fibroblast cells, and it has therefore been hypothesized that they may not be as sensitive to growth factor stimulus as normal cells. Therefore, the experiments showing that hTERT fibroblasts proliferate in response to FGF2 in a manner comparable to that of infant fibroblasts were particularly important. Not only did the telomerized fibroblasts remain contact inhibited, they were also able to respond to proliferation stimulus provided by FGF2. As proliferation is an important function of the wound healing fibroblast phenotype, it was important to show that these cells have retained the ability to respond in an appropriate fashion to their environment.

For the reasons outlined above, hTERT fibroblasts also had to be evaluated for their ability to perform other wound healing functions, including

collagen synthesis and deposition, matrix contraction, and migration through the matrix. In each instance, the hTERT fibroblasts responded appropriately to the environmental factors. Hence, while they have an expanded lifespan due to the ectopic expression of telomerase, hTERT fibroblasts were able to function normally and were not solely proliferative at the expense of other wound healing functions.

Therefore, as cellular components of our three-dimensional connective tissue equivalent, telomerized fibroblasts reduce the variation due to donor gender, ethnic origin and age, and allow the performance of multiple experiments with a homogeneous "cell line". This will allow a more systematic approach to studies of the molecular mechanisms involved in wound healing and when combined with the recent advancement of our non-contracting connective tissue equivalent (US Patent #6471958), provides a novel way to study these processes in three dimensions.

In particular, studies focused on the tissue contraction and scar formation processes require a three-dimensional tissue model to appropriately examine the cell-matrix interactions that are necessary for the subsequent matrix contraction. The effects of the matrix are now known to mediate mechanical and chemical signaling [19]. Thus, collagen not only serves as scaffolding for the fibroblasts, but also promotes the appropriate signals essential to the tissue contraction process. Additionally, the utilization of a three-dimensional tissue equivalent for studies of wound closure and tissue contraction enables obvious, gross changes

in the tissue model which can be easily observed and subsequently measured. In contrast, cellular models require elastic substrates that wrinkle upon fibroblast contraction or constant microscopic observation to visualize changes in the contractile function of the fibroblast. Therefore, the connective tissue equivalent characterized in the present study remains the most advanced and suitable way to study the contraction process proposed to date.

Figure 1. Stability of Connective Tissue Equivalents. Infant (A) and hTERT (B) fibroblasts (0 to 350,000 cells/mL collagen) dispersed into 0.5% collagen type I matrices do not spontaneously contract over a 20 day period. The mean wet weights (g) +/- standard deviation of each group are reported, and are not statistically significantly different ($n = 6$, ANOVA, $p>0.050$).

A.

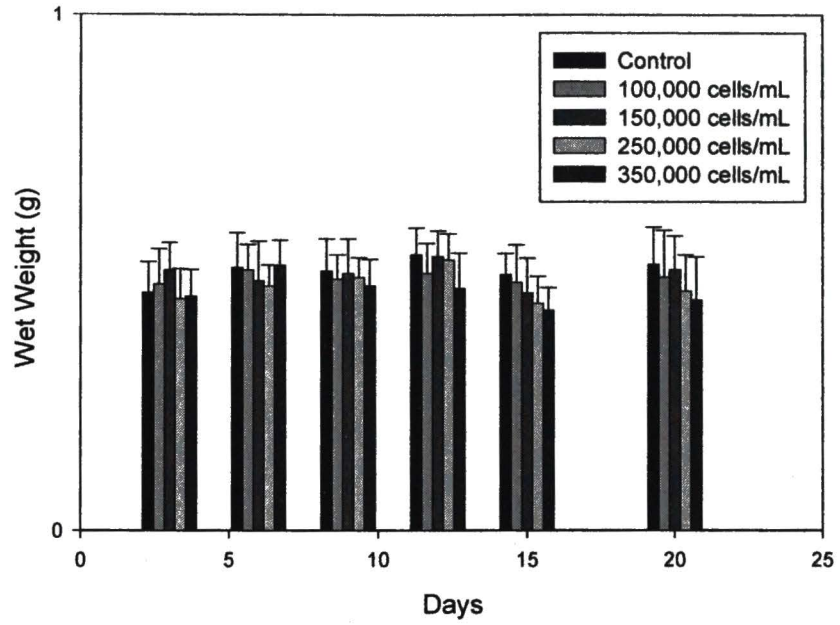
Control
100,000 cells/mL
150,000 cells/mL
250,000 cells/mL
350,000 cells/mL
Wet Weight (g)
1
0
0
5
10
15
20
25
Days

B.

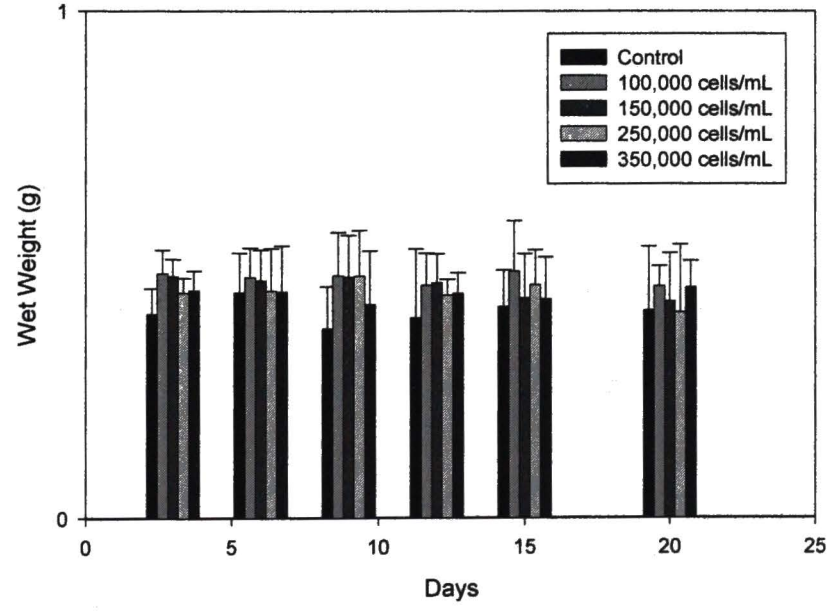
Control
100,000 cells/mL
150,000 cells/mL
250,000 cells/mL
350,000 cells/mL
Wet Weight (g)
1
0
0
5
10
15
20
25
Days

Figure 2. Fibroblasts are quiescent in three-dimensional connective tissue equivalent. The cell number of Infant (A) and hTERT (B) fibroblasts remains constant over 20 days in TE culture. The mean cell numbers are reported +/- standard deviation.

A.

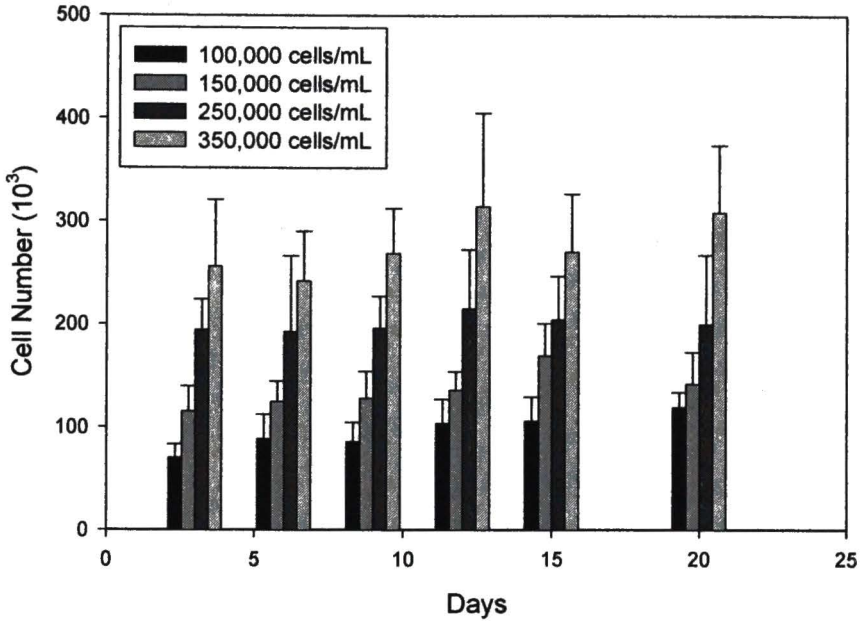
100,000 cells/mL
150,000 cells/mL
250,000 cells/mL
350,000 cells/mL
Cell Number (10^3)
Days
0
100
200
300
400
500
0
5
10
15
20
25

B.

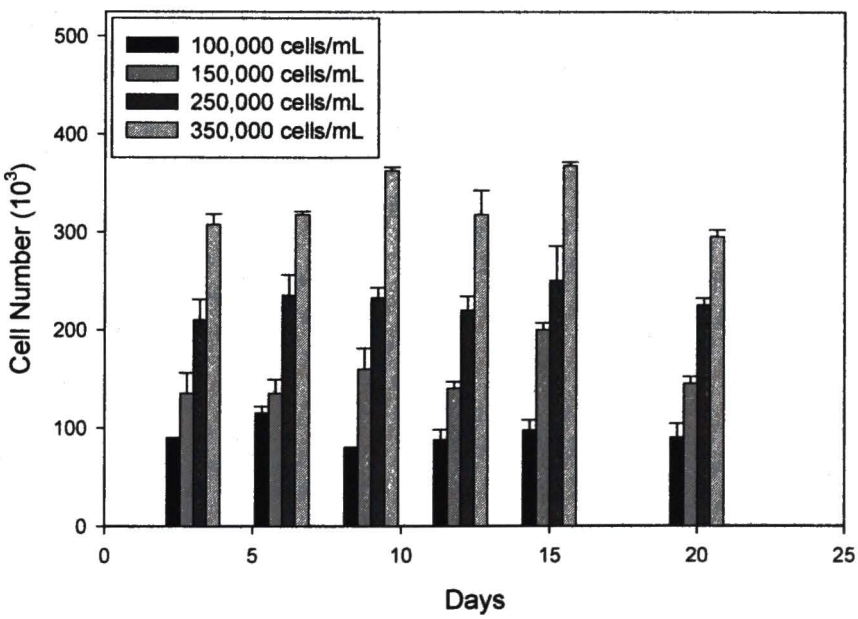
100,000 cells/mL
150,000 cells/mL
250,000 cells/mL
350,000 cells/mL
Cell Number (10^3)
Days
0
100
200
300
400
500
0
5
10
15
20
25

Figure 3. Western Analysis of Infant and hTERT fibroblasts. Expression of α-SMA (A), myosin light chains (B), and myosin heavy chain (C) in Infant and hTERT fibroblasts was examined via western analysis. In panel C, fibroblasts were cultured at high (HD) and low (LD) densities. No significant difference in expression was observed. Blots shown are representative of two separate experiments.

A.


~ 43kd
Infant
hTERT

B.

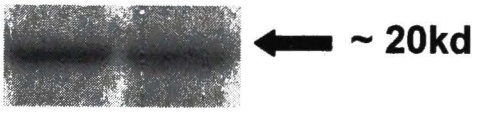
~ 20kd
Infant
hTERT

C.

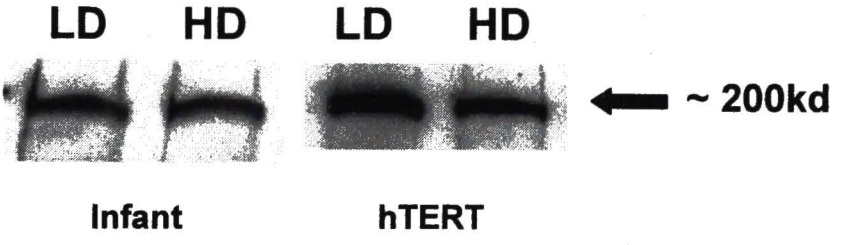
LD
HD
LD
HD
~ 200kd
Infant
hTERT

Figure 4. Localization of cytoskeletal proteins via indirect immunofluorescence. Infant and hTERT fibroblasts were cultured on glass coverslips and key cytoskeletal protein localization was examined via indirect immunofluorescence. Vimentin (A&B), α-SMA (C&D), and myosin light chain (E&F) expression was observed in both cell types. While the expression appears slightly different (due to the use of two different secondary antibodies), the localization of each protein is the same for both cell types. The total protein expression was analyzed by the more quantitative method of western analysis (Fig. 3).

hTERT Fibroblasts

Infant Fibroblasts

A.

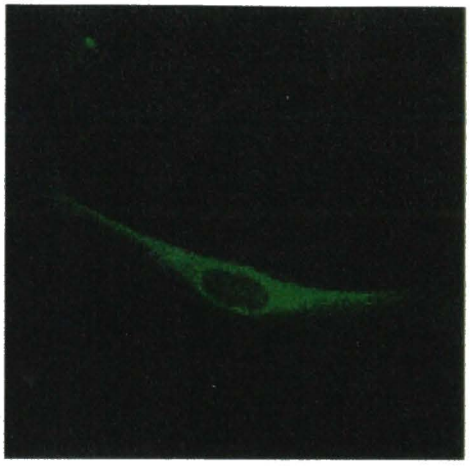

B.

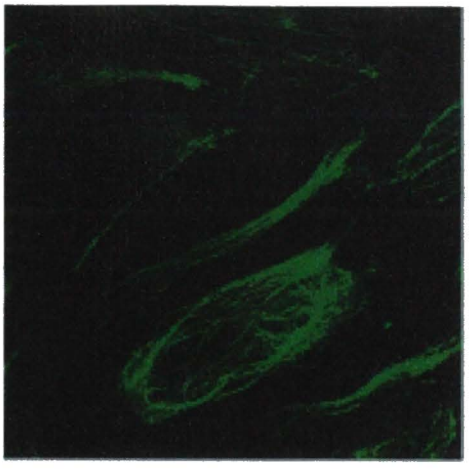

C.

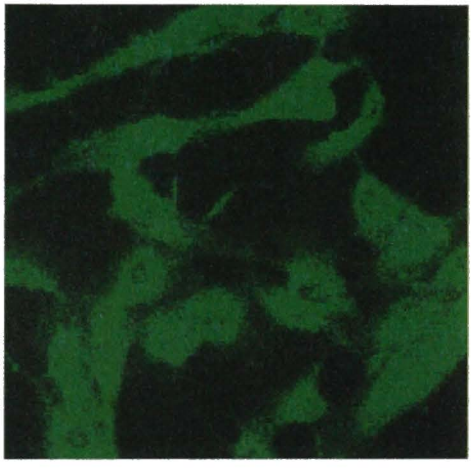

D.

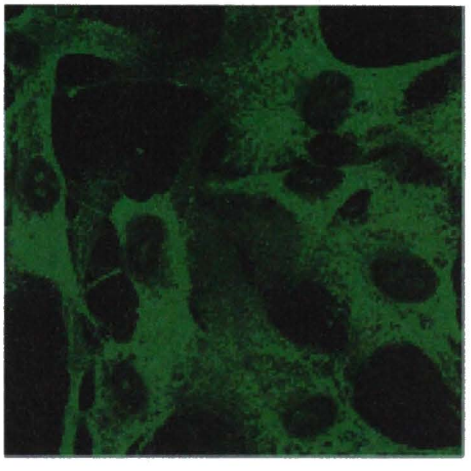

E.

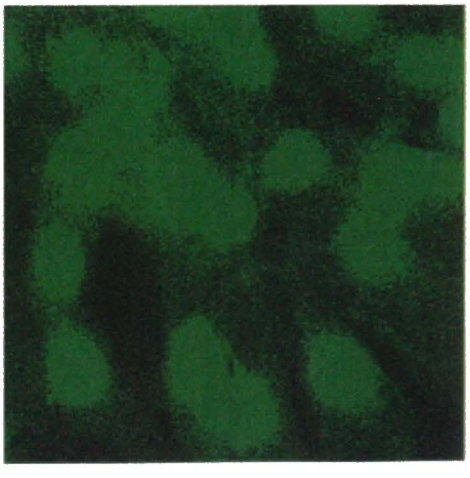

F.

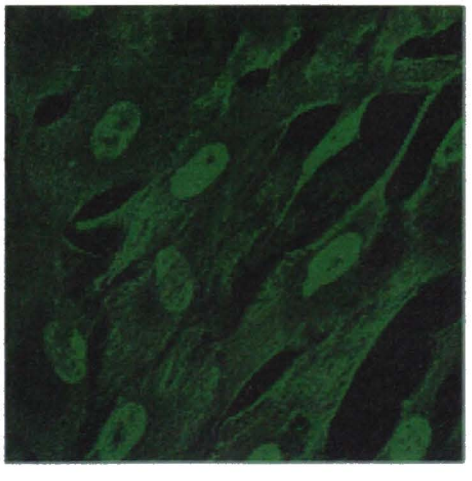

Figure 5. FGF2 stimulated proliferation of Infant and hTERT fibroblasts. Fibroblasts were stimulated with FGF2 (0 – 4nM) over 6 days in culture and the resulting proliferation was assayed using the sulfrhodamine B method. An unpaired t-test comparing the mean cell number of Infant and hTERT fibroblasts at each concentration of FGF2 was performed and no significant difference between the two cell types was found ($p>0.050$).

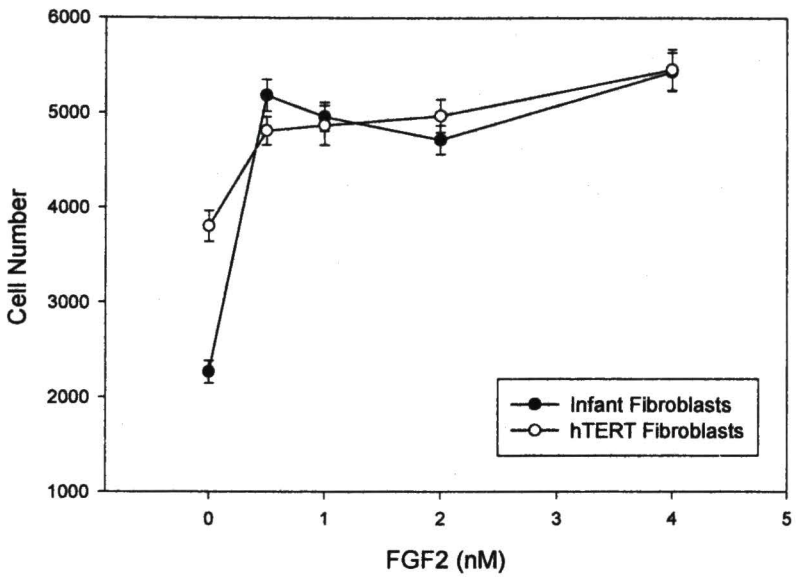
6000
5000
4000
3000
2000
1000
Cell Number
0
1
2
3
4
5
FGF2 (nM)
Infant Fibroblasts
hTERT Fibroblasts

Figure 6. Collagen synthesis by Infant and hTERT fibroblasts in response to ascorbate stimulation. Infant and hTERT fibroblasts were stimulated with ascorbate (50μg/mL) and assayed for collagen type I synthesis and secretion at 8 and 48 hours. Infant and hTERT fibroblasts mean total collagen +/- standard deviation was reported. The difference between Infant and hTERT fibroblasts mean total collagen at the two time points was analyzed by unpaired t-test and was not statistically significant ($p>0.050$).

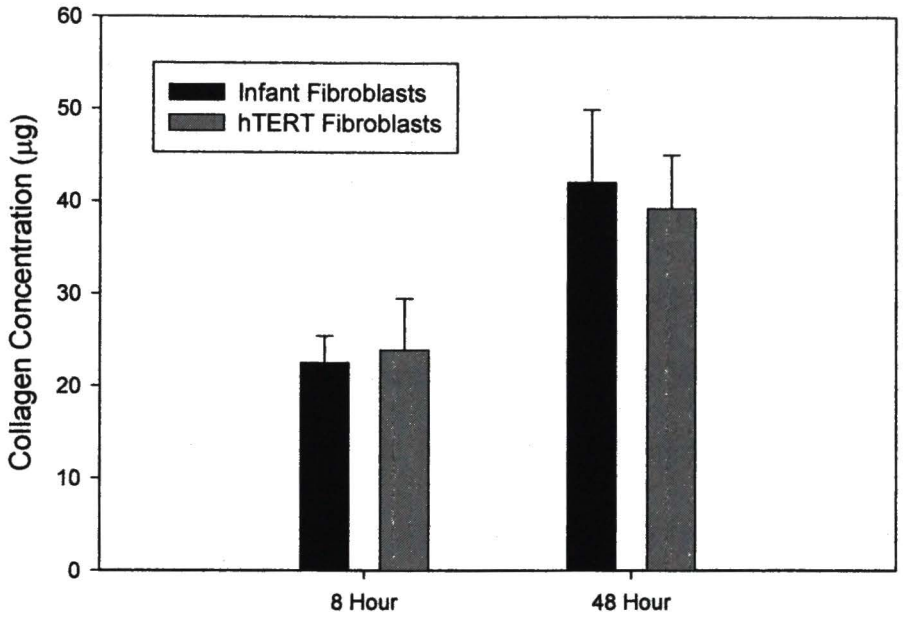
Collagen Concentration (µg)
60
50
40
30
20
10
0
Infant Fibroblasts
hTERT Fibroblasts
8 Hour
48 Hour

Figure 7. hTERT fibroblast contraction of a connective tissue equivalent. hTERT fibroblasts (250,000 cells/mL collagen) in 0.3% collagen were set up and allowed to polymerize and adapt for 6 hours. Addition of Ham's F-12 nutrient medium + 5% FBS (control) and 10 or 20% FBS (A) or 10ng/mL TGF-β (B) occurred at 6 hours. TE were weighed 18 hours, 3 days and 20 days after addition of medium in (A). An asterisk (*) denotes statistically significant difference from control TE treated with 5% FBS (ANOVA followed by Tukey Test, $p<0.050$). In (B), contraction took place for 20 days and then the TE were weighed. The difference between the control (5% FBS) and TGF-β mean wet weights was statistically significant (unpaired t-test, $p<0.001$).

A.

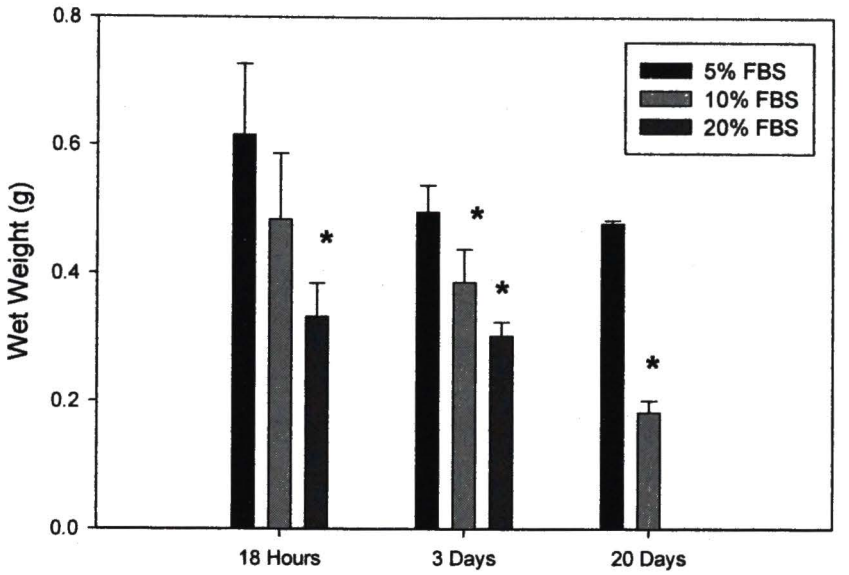
0.8
0.6
0.4
0.2
0.0
Wet Weight (g)
5% FBS
10% FBS
20% FBS
*
*
*
*
18 Hours
3 Days
20 Days

B.

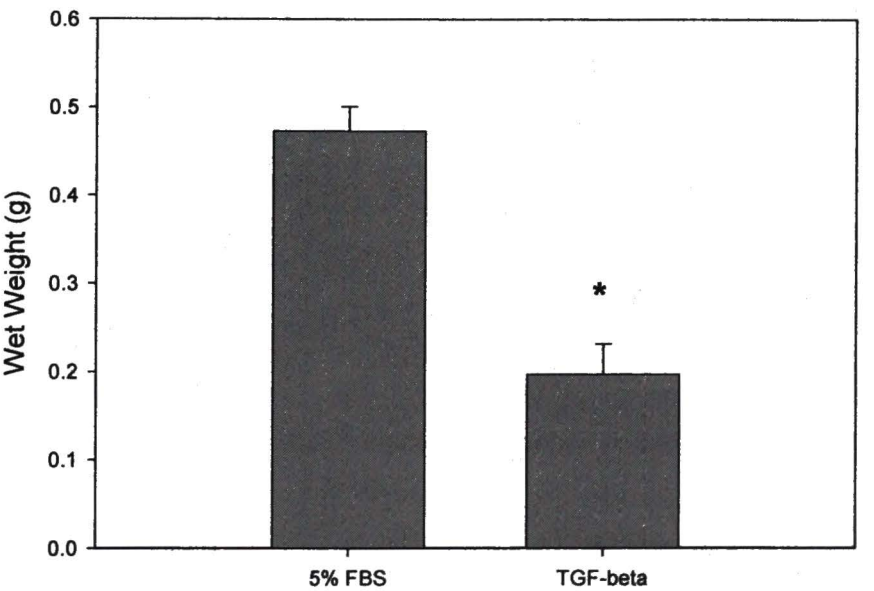
0.6
0.5
0.4
0.3
0.2
0.1
0.0
Wet Weight (g)
*
5% FBS
TGF-beta

Figure 8. hTERT + eGFP fibroblasts migrate into an acellular collagen matrix. Fibroblasts seeded on top of an acellular collagen gel migrated into it within two weeks. Optical sections (15μm) of the gel were taken using scanning laser confocal microscopy (A.1-12). The sections begin at the point farthest from the seeded cells and progress toward the cell monolayer. A graphic representation of the total fluorescence in each section is also reported (B). One major cell front is apparent and is followed by a small number of cells migrating behind it. These sections are representative of the data collected for three experiments.

A.

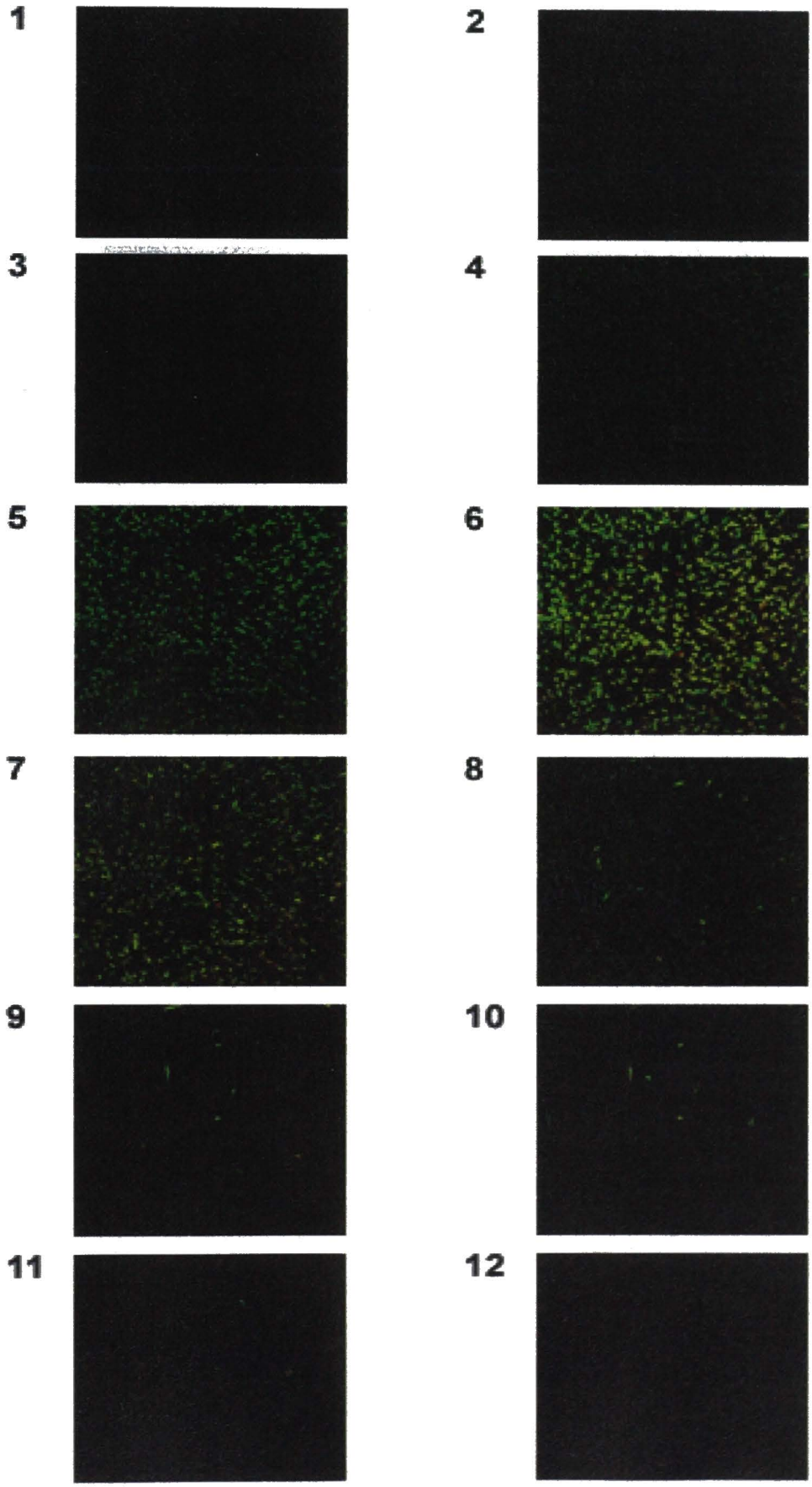

B.

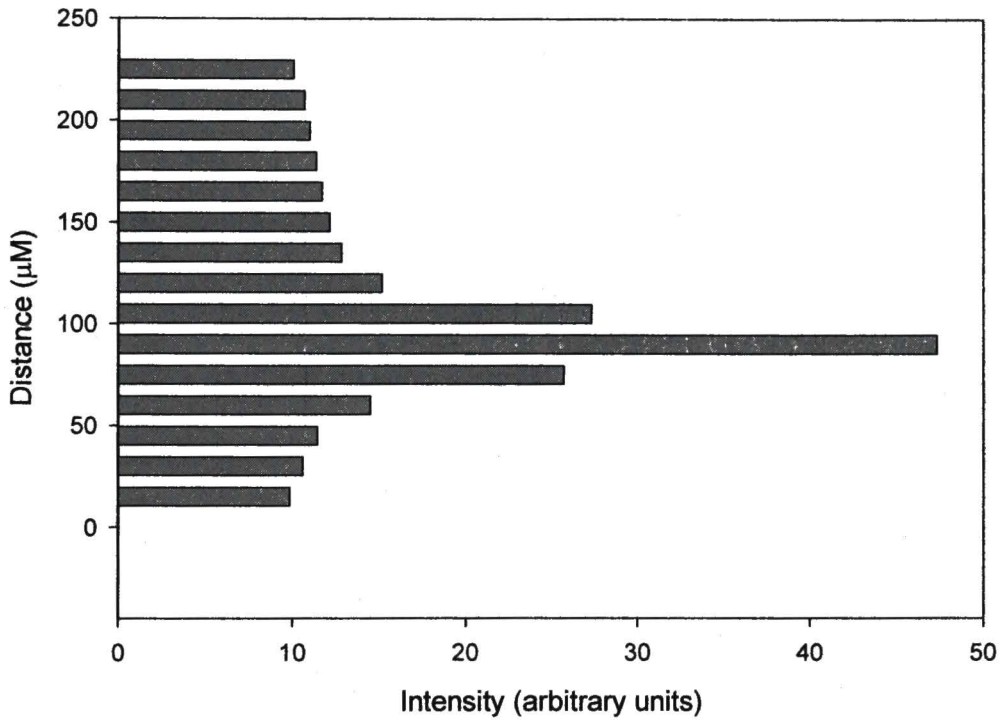
250
200
150
100
50
0
Distance (μM)
0
10
20
30
40
50
Intensity (arbitrary units)

Chapter III

Measurement of Contraction Initiation by Optical Fiber Interferometry

Introduction

Measurement of matrix contraction, particularly in the initial stages when it cannot be detected by light microscopy, has been a difficult task common to all studies that utilize various *in vitro* models. Common methods used to quantify gross contraction include determination of wet weight and change in diameter or thickness [9, 17, 35, 38, 40, 42, 45, 93]. Weight loss remains an obvious indicator of contraction, because as the resident cells contract the matrix, water is forced out of the equivalent matrix, thus reducing its wet weight. Along the same lines, measuring the diameter of the contracted model has frequently been used as the simplest method for measuring the extent of contraction. However, neither method is sensitive enough to determine the initiation of contraction or small but significant contraction caused by minor contractile ligands.

In order to determine when the initiation of contraction occurs, we are studying a method originally described for measuring the out-of-plane displacement of microelectromechanical structures. With a few minor adjustments, this optical fiber interferometer system can detect the initiation of contraction with sensitivity in the tens of nanometers. It also has a wide dynamic range of measurement, up to 2 mm. In addition, computer-assisted data

acquisition allows measurement of the contracting tissue equivalent over several hours continuously or as a series of sampling periods.

Materials and Methods

Cell Culture.

General. Cells were passaged before they reached confluency using trypsin/EDTA (Gibco) and were cultured in tissue culture flasks (Corning) at 37°C in 5% CO_2 incubators. They were cultured in DMEM + 10% FBS, unless otherwise indicated.

Infant Fibroblasts. Dermal fibroblasts were obtained from infant human foreskin explants as previously described [87]. Briefly, human infant foreskins were incubated at 4°C in a solution of 20 U/ml dispase (Collaborative Research) in DMEM for 48 hours. The epidermis was separated from the dermis and processed further for epidermal cells. Infant fibroblasts were obtained as out growths from explanted dermal tissue, following incubation at 37°C in DMEM + 10% FBS. All experiments were performed with Infant fibroblasts between passages 3 and 9, population doubling 9.13 to 27.67.

hTERT Fibroblasts. The catalytic subunit of human telomerase was retrovirally transfected into normal human fibroblasts [50]. This transfection was stable, and hTERT fibroblasts at population doubling 232.8 or higher were used in the experiments.

Tissue Equivalent Construction. The collagen solution was mixed thoroughly at 4°C as 8 parts collagen (0.3%, Vitogen-100, Celtrix Pharmaceuticals), 1 part 10X Ham's F-12 medium, and 1 part Reconstitution Buffer (0.05N NaOH, $NaHCO_3$, Hepes) and the pH was adjusted to 7.4. The appropriate number of cells was suspended in this collagen mixture which was allowed to polymerize at 37°C, 5% CO_2. Tissue equivalents (TE) were cast into multiwell plate inserts (Costar) that had been glued into a 6 well plate to insure stability during the measurement. Medium and/or contractile stimuli (TGF-β, 10ng/ml or FBS, 20%) were added to the bottom of the insert only. A single piece of glitter or glass coverslip (12 mm diameter) was positioned in the center of the TE to provide a reflective surface for the measurement.

Interferometer system configuration (Figure 1). Polarized light with a wavelength of 0.6328μm is coupled into a single mode optical fiber and then split with a 3-dB fused fiber coupler. One of the coupler's output pigtails is attached to a piezoelectric transducer stack, which moves the tip of the fiber in a direction along its axis. This pigtail serves as the probe of the interferometer. The other pigtail is unused, immersed in index matching fluid to minimize back reflections.

The tip of the probe is cleaved such that the normal to the cleaved fiber facet is collinear with the fiber axis. The cleaved facet serves as both the interferometer's beam splitter and beam combiner. The air/fiber interface at the cleaved facet of the fiber probe provides a 4% power reflection back into the single mode fiber. This reflected field is the interferometer's reference beam.

The light transmitted through the fiber probe's facet reflects off the glitter on the TE to be measured and is coupled back into the fiber. Consequently, the cleaved facet now acts as a beam combiner.

The distance traveled from the end of the fiber, to the glitter, and back into the fiber forms the signal path of the interferometer. The reference and signal fields co-propagate back through the fiber until they reach the fused fiber coupler, where an additional 3-dB power reduction is encountered. Finally, the interference signal is detected with a photodetector. The common signal and reference paths in this optical configuration eliminate signal fading due to non-signal induced polarization drift and optical path length drift in the fiber. Also, the common paths obviate the need for high-cost polarization-preserving single mode fiber.

Demodulation of the optical signal is implemented by sampling the photodetected signal and performing digital signal processing on it. Digital demodulation was performed using the commercially available OPD-200 Digital Demodulator (Optiphase, Inc.). The contraction, or movement of the glitter/TE away from the probe is reported as displacement in microns. Discontinuities in the displacement data result from the finite voltage range in the digital signal-to-analog converter (DAC). When the DAC reached its maximum output voltage, known as the rail voltage, the output cycles to its most negative voltage.

Results

High serum causes contraction. Initiation of fibroblasts contracting the tissue equivalent was detectable within the first ten minutes following stimulation with 20% FBS (**Figure 2B**). Nearly 300 microns of displacement was measured over the duration of the experiment, 2 hours. The baseline measurements were taken using a TE with fibroblasts which were not stimulated with 20% FBS in DMEM, but instead tap water was introduced to simulate the effects of adding the contractile stimulus to the well. A reasonably constant baseline was observed (**Figure 2A**). The slight drift toward the probe may be due to hydration of the TE. After approximately 12 min. the TE came into contact with the fiber probe and the measurement was discontinued (**Figure 2A**). In the future, medium (DMEM) lacking the contractile agent will be added instead of tap water to simulate the effects of adding the contractile stimulus without introducing additional variables.

Transforming Growth Factor–β stimulated contraction is also detected at an early stage. Since TGF-β has become a well-documented contractile agent found at the wound site, we also examined contraction due to TGF-β in TE using the interferometer setup. Again, slow, constant contraction was observed following TGF-β stimulation (**Figure 3**). Contraction was measured for five hours, and during that time a displacement of nearly 600 microns was recorded.

Discussion

The interferometer system greatly improves upon previous methods of matrix contraction measurement, particularly enabling the identification of contraction initiation. This process allows observation of contraction within five minutes of stimulus addition. Other methods are much less sensitive and rely on gross contraction, which is not detectable for hours [17, 38, 41]. The optic interferometry system also enables continuous data capture over a period of several hours and can be left unattended. In contrast, the measurements taken using other proposed methods occur at absolute time points and thus give no information with respect to the course of the contraction process taking place between measurements. This fact may be of particular importance, as we have observed a unique pattern of rapid contraction followed by longer periods of slow contraction in response to serum using the interferometer method (data not shown). Unfortunately, these results have not been replicated, possibly due to the fact that the experiments have been conducted at different room temperatures. It has been shown that an increase in temperature influences contraction, thus the low room temperature probably affected the contraction of the collagen matrix [40]. In order to address this concern, we are preparing to adjust the system to accommodate an environmental chamber that will allow maintenance of constant temperature during the measurement.

The greatest strength of this system is its sensitivity, since the optic interferometer allows measurement of displacement (contraction) to the tens of

nanometers. Contraction of fibrin gels has been measured using an Olympus inverted microscope equipped with a Mitutoyo digital indicator with a range of 0.01 – 10 mm [17]. Free-floating collagen gel contraction has been determined by measuring the diameter of the gel to the nearest 0.25 mm with a Nikon SMZ-1 stereoscope [38]. These methods utilizing light microscopy and optical methods to measure matrix contraction are the most sensitive proposed to date and yet, at best they are still 1000 – fold less sensitive than our interferometry system. This will be particularly important when studying a multi-component contractile system and may enable the differentiation between additive and synergistic effects.

The optic interferometer system proposed measures displacement (contraction) in one direction. One concern when developing a new technique to measure matrix contraction is how to take into consideration the entire contraction occurring, in every direction. While contraction generally takes place in all planes since the cells are randomly organized in the collagen matrix, in these experiments, the collagen matrix is polymerized in the insert and thus is attached on the sides of the well. This restricts the initial contraction to one direction [17, 41]. Therefore our system is appropriate to measure contraction in its initial stages, prior to gross contraction when the cells generate enough force to detach the matrix from the walls of the insert.

As these are preliminary studies directed towards the development of a novel method to measure collagen matrix contraction, further characterization of the system is certainly necessary. Incorporation of an environmental chamber will

undoubtedly produce more reproducible results and allow examination of the effect of temperature on the contraction process. In the future, studies of contraction over time in response to various known contractile agents should take place.

Figure 1. Fiber Optic Interferometry System. This system is introduced to measure the surface displacement of a collagen gel due to contraction following stimulation of the fibroblast cells within the matrix. The interferometric system is non-intrusive and offers a large dynamic range of measurement. Computer-controlled data acquisition allows continuous measurement of the contracting gel over a period of several hours.

Interferometric System

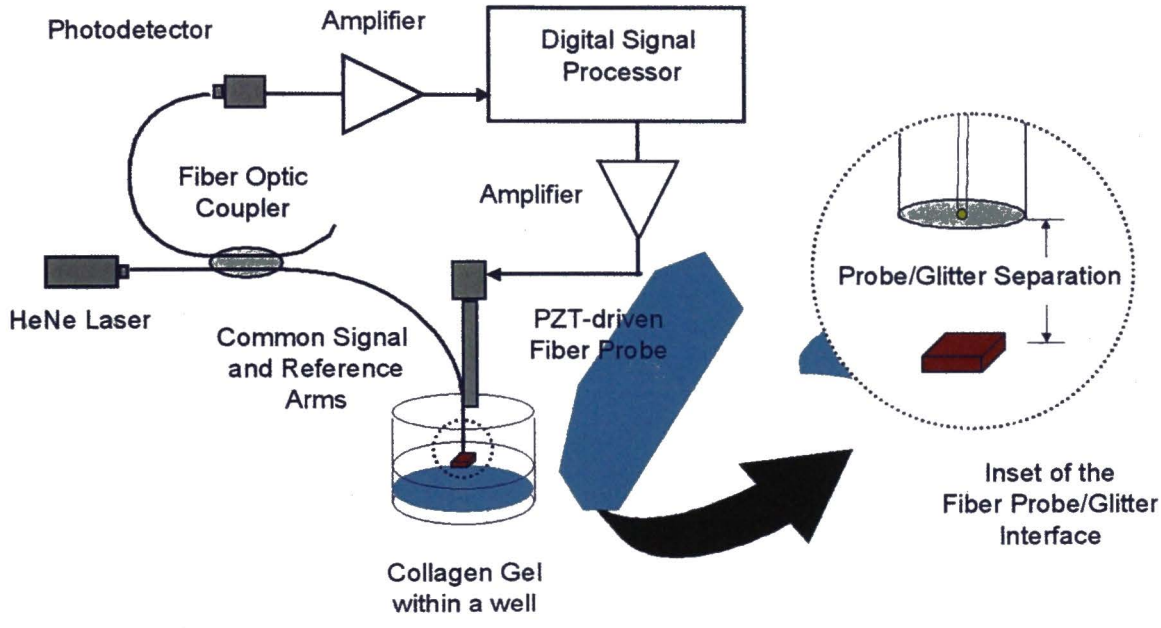

Figure 2. Serum stimulates slow, constant contraction. The fiber optic interferometry system was used to measure the onset of contraction stimulated by 20% FBS. Either 2.0 ml tap water (A) or 2.0 ml DMEM + 20% FBS (B) was added to TE (250,000 hTERT fibroblasts/ml Vitrogen-100 collagen) and contraction was measured as microns of displacement. Serum stimulated contraction was performed for two wells in this experiment, a representative graph is shown in (B).

A.

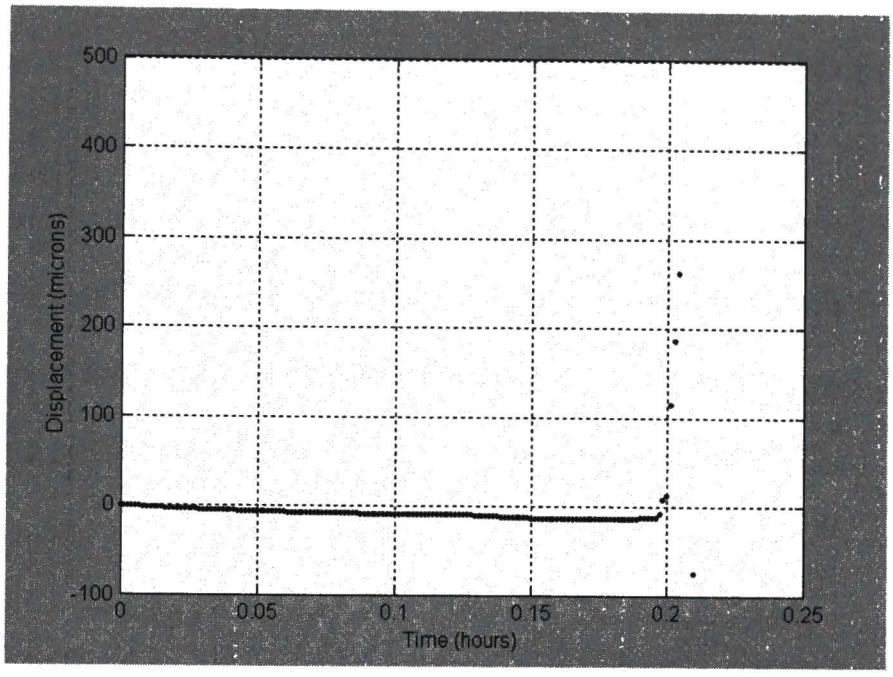
500
400
300
200
100
0
-100
Displacement (microns)
0
0.05
0.1
0.15
0.2
0.25
Time (hours)

B.

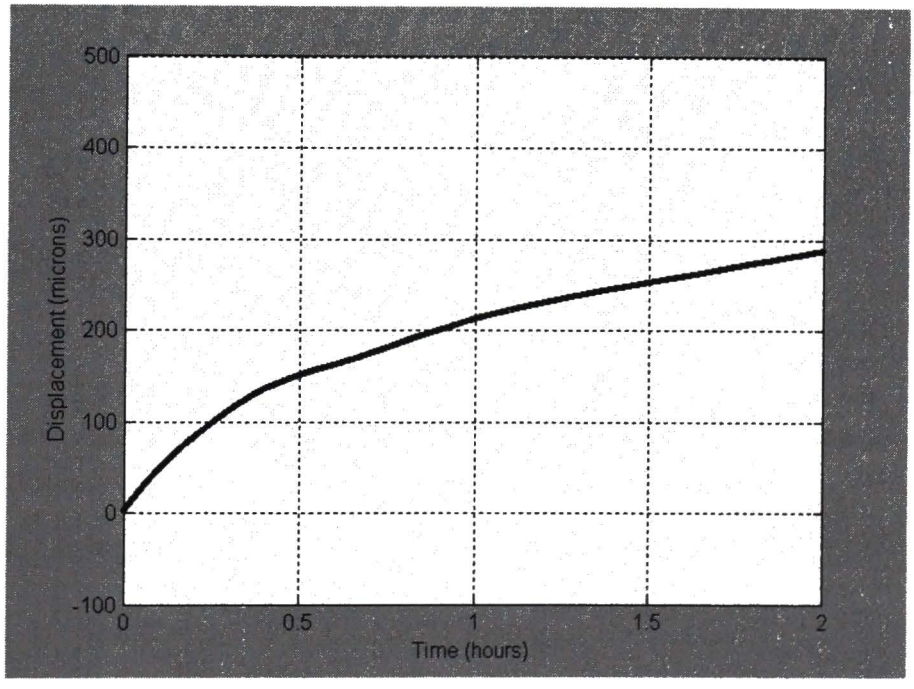
500
400
300
200
100
0
-100
Displacement (microns)
0
0.5
1
1.5
2
Time (hours)

Figure 3. Transforming Growth Factor – β stimulates slow, constant contraction. TE (250,000 hTERT fibroblasts/ml Vitrogen-100 collagen) displacement (microns) was collected over a 5 hour time period using the fiber optic interferometry system. TGF – β (20ng/ml) in Ham's F-12 + 5% FBS was added to the well 15 minutes after data collection began to stimulate contraction of the matrix. The graphs represent data from one experiment over the entire 5 hours of data collection (A) and the first hour of data collection (B).

A. Full data set (approximately 5 hrs.)

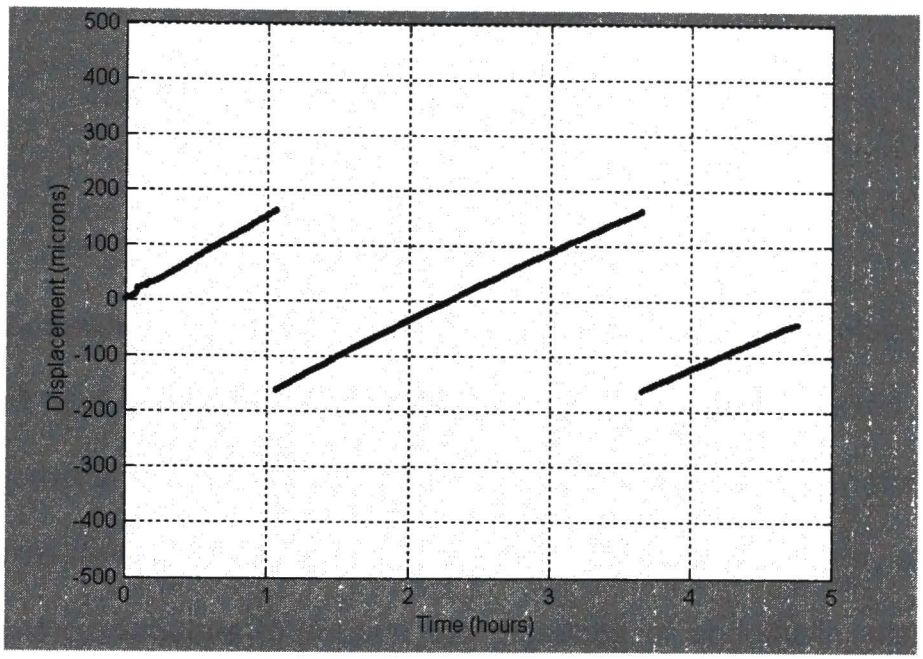

B. Same data set (plot of the first hour only)

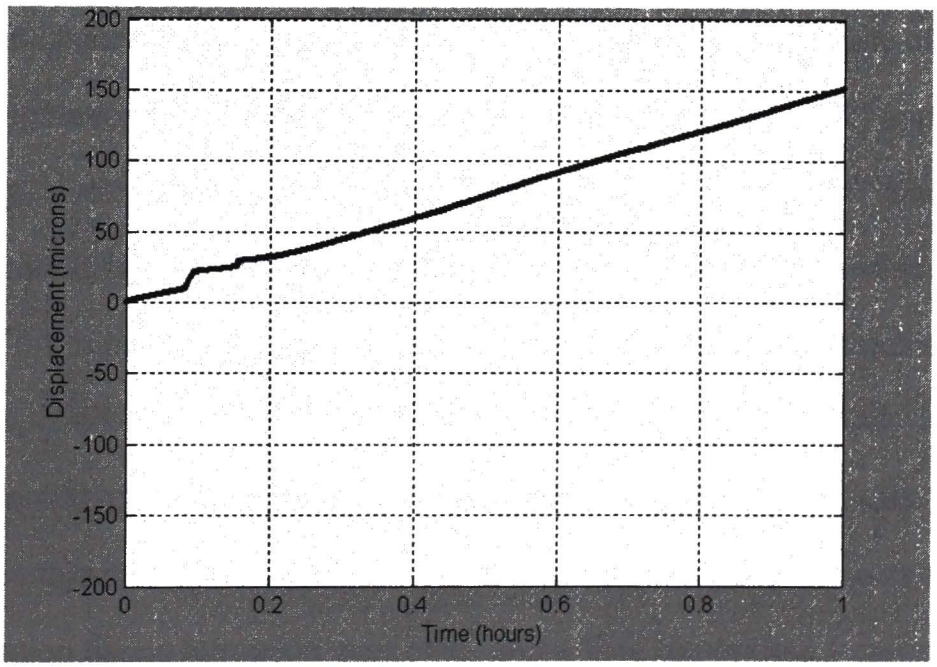

Chapter IV

The Role of Endothelin – 1 in Tissue Contraction

Introduction

Endothelin-1 (ET-1) is a potent vasoconstrictor originally isolated, purified, sequenced, and cloned by Yanagisawa et al from the culture media of porcine aortic endothelial cells in 1988 [69]. Since then, it has been widely studied for its potential role in vasculature and cardiovascular diseases. However, evidence is beginning to accumulate to support the presence of endothelin after injury in various systems. Using experimental animal models, changes in ET-1 levels (mRNA and protein), endothelin receptor kinetics and receptor activity (EC_{50}) have been observed, thus implicating ET-1 in the etiology of a variety of diseases [70]. Upregulation of ET-1 has been shown during renal injury [82] and elevated circulating levels of ET-1 have been reported in a variety of vascular and inflammatory diseases, and in the connective tissue disease scleroderma [84]. A role for ET-1 in the chronic inflammation associated with atherosclerosis has also been proposed. Myofibroblasts exhibited ET-1 immunoreactivity in human atherosclerotic coronary tissue [86]. In addition, male Wistar rats wounded dorsally by injection of croton oil showed an increase in myofibroblasts at the site of granulation tissue formation over time, and a time dependent increase in ET-1 expression in endothelial cells at the same sites was observed [83]. Therefore,

recent studies have implicated ET-1 in processes of wound healing and injury, and have suggested possible sources of ET-1 at the wound site. These include endothelial cells, fibroblasts, and various immune cells recruited to the site of injury during early stages of inflammation.

The wound healing process involves the activated fibroblast phenotype, the myofibroblast. Normal wound healing requires that the activated fibroblasts have the ability to (1) migrate within the provisional matrix of the wound, (2) proliferate to repopulate the wound site, (3) synthesize collagen to rebuild the extracellular matrix and (4) contract the matrix to close the wound. All phases of wound healing have been shown to be stimulated by ET-1 in a variety of injury models, involving Swiss 3T3 fibroblasts, sclerodermal fibroblasts and *in vivo* rat studies [32, 73, 79, 83, 84]. However, a clear role remains to be established for ET-1 as an important player in scar formation, especially with respect to the temporal aspects of wound healing and the activation of fibroblasts.

The signaling that occurs to produce contraction by non-muscle cells, such as fibroblasts, has been shown to involve the phosphorylation of key cytoskeletal and associated proteins. These activated proteins lead to the assembly of focal adhesion plaques and prepare the cell for interaction with the matrix. Furthermore, redistribution and activation of contractile proteins, such as alpha-smooth muscle actin (α-SMA) and myosin are required for cell contraction [27, 94]. Studies involving treatment with ET-1 in various cell types have shown phosphorylation of a number of proteins involved in the contraction process,

including the focal adhesion associated-protein, paxillin and myosin light chain [70, 73]. An important signaling cascade associated with cytoskeletal reorganization and cell activation is the Rho-associated kinase pathway. The stimulation of focal adhesion plaque formation by Rho and Rho-associated kinase in non-muscle cells has been well established [74-77]. However, the link between ET-1 and Rho signaling in normal fibroblasts has not been fully examined. Therefore, we propose that ET-1, acting through its receptor, activates Rho and Rho-associated kinase. Subsequent phosphorylation by Rho-kinase of key proteins activates fibroblasts and prepares the cytoskeleton for tissue contraction. Furthermore, it is also proposed that ET-1 acts through transforming growth factor-beta (TGF-β) to amplify and sustain the initial signal (**Fig. 1**).

In this study, the role of ET–1 as an activator of human fibroblasts to their contractile phenotype, and thus a mediator of tissue contraction, was established. In addition, the method of ET-1 stimulation of fibroblasts was examined. Both its direct action and its stimulation of TGF-β release in the tissue contraction process were studied.

Materials and Methods

Cell Culture.

General. Cells were passaged before they reached confluence, using trypsin/EDTA (Gibco), and were cultured in tissue culture flasks (Corning) at

37°C in 5% CO_2 incubators. They were cultured in DMEM + 10% FBS, unless otherwise indicated.

Infant Fibroblasts. Dermal fibroblasts were obtained from infant human foreskin explants as previously described [87]. Briefly, human infant foreskins were incubated at 4°C in a solution of 20 U/ml dispase (Collaborative Research) in DMEM for 48 hours. The epidermis was separated from the dermis and processed further for epidermal cells. Infant fibroblasts were obtained as out growths from explanted dermal tissue, following incubation at 37°C in DMEM + 10% FBS. All experiments were performed with Infant fibroblasts between passages 3 and 9, population doubling 9.13 to 27.67.

hTERT Fibroblasts. The catalytic subunit of human telomerase was transfected into normal human fibroblasts using the pBabe retroviral vector [50]. This transfection was stable, and hTERT fibroblasts at population doubling 232.8 or higher were used in the experiments.

Tissue Equivalent (TE) Construction. The collagen matrix was prepared by mixing 8 parts collagen (0.3%, Vitogen-100 (Celtrix Pharmaceuticals); 0.5%, ICN (ICN Biomedicals); or a combination of the two), 1 part 10X Ham's F-12 medium, and 1 part reconstitution buffer (0.05N NaOH, $NaHCO_3$, Hepes). The appropriate number of cells was suspended within the collagen mixture and the TE was allowed to polymerize at 37°C, 5% CO_2. TE were supplied with Ham's F-12 Nutrient Medium + 5% FBS (Gibco) every other day unless otherwise indicated.

Western Analysis. Infant or hTERT fibroblasts were stimulated with 10nM endothelin-1 in serum free DMEM for 24 hours and lysed using lysis buffer (1.0M Tris, pH 7; 0.5% SDS; 5% sucrose). The amount of total protein was determined using the BCA protein assay (Pierce). Briefly, it combines the reduction of Cu^{2+} to Cu^{1+} by protein in an alkaline medium (the biuret reaction) with the highly selective and sensitive colorimetric detection of the cuprous cation using a reagent containing bicinchoninic acid (BCA). Approximately 10 □g total protein was loaded in each well of a 4-15% gradient Tris-Glycine gel and SDS-PAGE was completed using the BioRad vertical electrophoresis system. The gels were transferred to a nitrocellulose membrane at 20 mAmps overnight using the BioRad transfer system. The membranes were then blocked with 1% Bovine Serum Albumin (BSA, Sigma) and 5% milk in 1X PBS, and then incubated with primary antibody diluted in 1X PBS + 0.1% Tween 20 at 4° C overnight (α – Smooth Muscle Actin, 1:400; Myosin Light Chains, 1:200; Myosin Heavy Chain, 1:1000). Membranes were washed with 1X PBS + 0.1% Tween 20, and the appropriate secondary antibody was incubated with the membrane for 30 min. to 1 hour at RT (1:1000 dilution in 1X PBS + 1% BSA). Once the membranes were washed again, the bands were detected using the ECL chemiluminescence method (Amersham).

Indirect Immunofluorescence. Normal infant fibroblasts and hTERT fibroblasts were cultured in chamber slides or on glass coverslips and stimulated with ET-1 (100nM) or transforming growth factor-beta (TGF-β, 10ng/ml) for 24

hours. Fibroblasts were pretreated for 30 minutes with an $ET_{A/B}$ mixed antagonist (PD-142893, Sigma) and fresh antagonist was added to the nutrient medium containing ET-1. In another set of experiments, fibroblasts were pretreated for 30 minutes with a rho-kinase inhibitor, Y-27632 (CalBiochem). After fixing with methanol: acetone (1:1) at 4°C for 10 min., the cells were blocked with 1% BSA in 1X PBS overnight at 4°C. The cells were incubated with primary antibodies diluted in 1% BSA in 1X PBS (ET_A, 1:200; α-Smooth Muscle Actin, 1:200; Myosin Light Chain, 1:200; or Myosin Heavy Chain, 1:50) overnight at 4°C. Following multiple washes with 0.1% Tween 20 in 1X PBS, the cells were incubated with secondary antibody (AlexaFluor, Molecular Probes, diluted 1:1000 in 1% BSA in 1X PBS) for 1 hr. at 37°C. The slides were washed again, mounted using FluorSave (CalBiochem) and examined by fluorescence microscopy.

Matrix Biosynthesis. hTERT fibroblasts were plated at 40,000 cells/well and cultured in 96 well plates. They were serum starved overnight and stimulated with ascorbate (50μg/ml) or ET-1 (0.1 and 1μM) in phenol red free DMEM + 0.1% BSA over 48 hours. Ascorbate has been shown to stimulate collagen synthesis through the induction of lipid peroxidation leading to increased collagen gene transcription [95]. Collagen synthesis was determined using a picrosirius dye, as described by Walsh et al [90]. Briefly, the medium was transferred from the wells at 8 and 48 hours into fresh 96 well plates, and was then allowed to evaporate. The plates were rinsed three times in distilled water and assayed immediately. Additionally, the collagen produced but still associated with the cells was

measured; cells were lysed with rapid freeze thawing and were allowed to dry on the plates. Once rinsed, the wells were filled with 100μl of 0.1% Sirius Red F3BA (Direct Red, Sigma) in saturated picric acid and stained for one hour at room temperature. The plates were washed five times with 200μl of 10mM HCl. The collagen bound stain was then eluted with 200μl of 0.1M NaOH for 5 min. The eluted stain was dispensed into a fresh 96 well plate and the absorbance read at 450nm. The dye is specific for collagen type I and the collagen concentration was derived form a standard curve of known collagen concentrations.

Tissue Contraction Assay. hTERT TE (1ml/well) were constructed in BSA (2% in 1X PBS) coated 24-well plates and then stimulated with ET-1 (0.01 – 10μM), TGF-β (10ng/ml), or a combination of the two to induce collagen gel contraction. To some TE, an $ET_{A/B}$ mixed antagonist, PD-142893 (Sigma) was added at the time of collagen polymerization and fresh antagonist was added with the nutrient medium. In a separate set of experiments, a rho-kinase inhibitor, Y-27632 (CalBiochem), was added to the collagen matrix of select TE prior to polymerization. Contraction was quantitated by weighing the contracted TE and compared to non-treated controls.

TGF-β Secretion. hTERT fibroblasts (400,000 cells/well) were cultured in a six-well plate for 24 hours. The cells were serum starved overnight and stimulated with ET-1 (1 – 100nm) for 24 hours. Quantitative determination of secreted human TGF-β following ET-1 stimulation was accomplished using a commercially available ELISA kit (R&D Systems).

Intracellular Calcium ($[Ca^{2+}]_i$) Measurement. Measurements of intracellular calcium were recorded as previously described [96]. Briefly, Infant and hTERT fibroblasts were cultured on coverslips (3000 cells/coverslip) and serum starved 1 hour prior to the experiment. The cells were incubated with 3 μM Fura-2 dye (Molecular Probes) in a modified Krebs-Ringers Buffer solution (KRB: 115 mM NaCl, 2.5 mM $CaCl_2$, 1.2 mM $MgCl_2$, 24 mM $NaHCO_3$, 5 mM KCl, 5 mM glucose, and 25 mM HEPES, pH 7.4) for 30 minutes at 37°C. Fura-2 fluorescence of these cells was monitored at 37°C by the ratio technique (excitation at 340 nm and 380 nm, emission at 500 nm) under a Nikon Diaphot microscope using Metafluor software (Universal Imaging, West Chester, PA). Conditions of high $[Ca^{2+}]_i$ were achieved by adding the Ca^{2+} ionophore, 4-Bromo-A23187 (1-3 μM) (Calbiochem), whereas conditions of low $[Ca^{2+}]_i$ were obtained by adding EGTA (4-5 mM). $[Ca^{2+}]_i$ for each treatment was measured in at least two coverslips, such that approximately 5 cells were monitored each time. Representative tracings are reported.

Results

Infant and hTERT fibroblasts express the endothelin receptor. Endothelin receptors (ET_A and ET_B) have been identified on several cell types [44, 69, 71, 97, 98]. To show that the endothelin receptor A (ET_A) is expressed in human fibroblasts, a monoclonal antibody against ET_A was used in indirect immunofluorescence studies of Infant and hTERT fibroblasts. Both cell types

expressed the receptor, and that expression was uniformly distributed along the cell membrane (**Fig. 2**). Expression of ET_B on fibroblasts was also examined, but no expression was detected. This may be a function of culture conditions or a cell type specific feature.

ET-1 stimulates collagen synthesis by hTERT fibroblasts. Since one function of the activated fibroblast is to synthesize and secrete collagen to rebuild the extracellular matrix, the ability of ET-1 to mediate collagen synthesis was examined. Untreated hTERT fibroblast collagen synthesis was compared to that of fibroblasts treated with ET-1 (0.1μM and 1μM) or ascorbate (50μg/ml) over 48 hours (**Fig. 3**). While at the 8-hour time point, there was no statistically significant difference between the 4 groups (unpaired t-test with Bonferroni correction, $p<0.017$), collagen synthesis by treated fibroblasts at 48 hours was statistically significantly higher than the control cells (unpaired t-test with Bonferroni correction, $p<0.017$). In addition, the ET-1 treated fibroblasts synthesized significantly less collagen than the fibroblasts treated with ascorbate (unpaired t-test with Bonferroni correction, $p<0.025$). Therefore, ET-1 increased collagen synthesis by fibroblasts, but not to the extent of ascorbate.

Cytoskeletal changes occur following ET-1 treatment. Western analysis was performed on 10nM ET-1 treated Infant and hTERT fibroblast cell lysates to examine expression of α-SMA and myosin light and heavy chains. It has been established that the culture density of fibroblasts in monolayer has a direct effect on the cytoskeletal expression of certain marker proteins, including

α-SMA [99, 100]. Typically, fibroblasts cultured at low density have the cytoskeletal profile of activated fibroblasts, while those plated at high density decrease their expression of these cytoskeletal proteins [100].

α-SMA. Since α-SMA expression is the accepted marker for fibroblast activation, changes in α-SMA expression in fibroblasts cultured at high and low densities and treated with ET-1 were examined [2, 30]. α-SMA expression was higher in the cells cultured at low density, for both Infant and hTERT fibroblasts (**Fig. 4A**). Also, the fibroblasts treated with ET-1 showed a slight increase in α-SMA.

Myosin Heavy Chain. Increased myosin heavy chain expression has been used as a secondary marker for fibroblast phenotypic change [25]. Again, myosin heavy chain expression was greater for the cells cultured at low density (**Fig. 4B**). However, a substantial difference was not observed between the control and the ET-1 treated cells.

Myosin Light Chain. Previously, we have shown that a better cytoskeletal marker for fibroblast activation may be expression of myosin light chain [101]. Thus, we examined changes in the expression of myosin light chain in Infant and hTERT fibroblasts following ET-1 treatment (**Fig. 4C**). Treatment of hTERT fibroblasts with ET-1 did not appear to increase myosin light chain expression. However, a third band appeared, particularly in the hTERT fibroblast lane, suggesting a possible shift from its unphosphorylated form to an active, phosphorylated protein.

ET-1 stimulates myosin light chain redistribution. To further elucidate the connection between ET-1 and myosin light chain in fibroblasts, myosin light chain localization was examined. hTERT fibroblasts plated sparsely on glass coverslips were analyzed for myosin light chain expression using indirect immunofluorescence. While basal expression of myosin light chain was highly localized in the perinuclear region with faint expression along the cell periphery (**Fig. 5A**), in ET-1 treated fibroblasts myosin light chain was redistributed throughout the cytoplasm (**Fig. 5B**). To determine if the ET-1 response was receptor mediated, fibroblasts were pretreated with $ET_{A/B}$ receptor mixed antagonist, PD-142893 (1μM) for 30 minutes prior to ET-1 stimulation. The highly localized and perinuclear myosin light chain localization in untreated controls was restored in fibroblasts treated with PD142893 before ET-1 treatment (**Fig. 5C**). Furthermore, ET-1 – mediated myosin light chain redistribution was blocked by Y-27632, a rho-kinase inhibitor (**Fig. 5D**).

Endothelin-1 stimulates contraction of TE populated with hTERT fibroblasts. The *in vitro* model of connective tissue utilized for this set of experiments has been characterized previously (US patent #6471958)[101]. TE is a three-dimensional model in which fibroblasts dispersed in a hydrated collagen matrix do not contract spontaneously, and is therefore the ideal *in vitro* model to study tissue contraction. Since any contraction initiators must diffuse through the collagen matrix, μM range of ET-1 was chosen. This is in contrast to the nM concentrations used for monolayer studies. The mean wet weights +/-

standard deviation of each treatment group is reported as a measure of matrix contraction [35, 93]. Weight loss is commonly used as an indicator of contraction, because as the resident cells contract the matrix, water is forced out of the equivalent, thus reducing its wet weight. ET-1 caused a significant reduction in TE wet weight (**Fig. 6A**). This decrease in wet weight was approximately 34% with 1 and 10μM ET-1. TE treated with 0.01μM ET-1 did not contract and thus represents the limiting concentration for this model. The difference between the control group and the TE treated with 1 and 10μM ET-1 was statistically significant (unpaired t-test with Bonferroni correction, $p<0.0125$). Moreover, the ET-mediated contraction of TE was blocked by PD-142893. The Rho-kinase inhibitor, Y-27632, also blocked the effect of ET-1. The mean wet weights of TE treated with ET-1 (0.01μM) and Y-27632 (10μM) or PD-142893 (1μM) were not significantly different from control TE (unpaired t-test with Bonferroni correction, $p<0.0125$). Therefore, it appeared that ET-1 stimulated TE contraction through its receptors and the rho-kinase pathway. TE were also treated with ET-1 (1μM), TGF-β (10ng/ml), or a combination of the two (**Fig. 6B**). TGF-β, a potent cytokine implicated in several stages of wound healing including tissue contraction, caused contraction of TE by approximately the same degree as ET-1 (i.e., 35%). Mean wet weight of TE treated with ET-1 or TGF-β alone was significantly different than control TE (*) and TE treated with both ET-1 and TGF-β (**) (unpaired t-test with Bonferroni correction, $p<0.001$). TGF-β and ET-1 produced additive effects on TE, reducing the wet weight by about 70%.

ET-1 does not increase intracellular calcium. To determine if fibroblast contraction by ET-1 is mediated by an increase in intracellular calcium, Fura-2 calcium imaging was performed on Infant (Fig. 7A) and hTERT (Fig. 7B) fibroblasts treated with ET-1 (1, 10, 100nM). No increase in intracellular calcium upon ET-1 addition was observed.

ET-1 stimulates TGF-β secretion from hTERT fibroblasts. Since ET-1 is hypothesized to be an initiator of contraction, we determined if ET-mediated contraction could also be sustained by TGF-β production. Serum starved hTERT fibroblasts were treated with ET-1 (1, 10, or 100nM) for 24 hours. The culture medium was assayed for secreted TGF-β by ELISA. Mean concentration of fibroblast secreted TGF-β +/- standard deviation is reported (**Fig. 8**). ET-1 caused nearly a 2-fold increase in TGF-β levels over a period of 24 hours. The difference in mean secreted TGF-β between control and ET-1 stimulated fibroblasts was statistically significant for the 10 and 100nM doses (unpaired t-test with Bonferroni correction, $p<0.017$).

Discussion

Crucial experiments in this study included the functional analysis of ET-1 as a contractile ligand and its capacity to initiate TGF-β secretion. hTERT fibroblasts dispersed in TE contracted the collagen matrix by 35% of control TE following ET-1 treatment. This ET-1 mediated contraction occurred through ET_R and the Rho-associated kinase pathway. The Rho-associated kinase signaling

pathway has been implicated in the assembly of focal adhesion plaques and stress fibers which are essential components of the contractile system in non-muscle cells [24, 74]. In Swiss 3T3 fibroblasts, active Rho was vital for the coordinated assembly of stress fibers and focal adhesions induced by various growth factors, including serum, epidermal growth factor, thrombin and TGF-β [102]. In addition, several studies have shown Rho-associated kinase phosphorylation of myosin light chain and myosin phophatase [103-105]. ET-1 induced myosin light chain redistribution and possible phosphorylation in hTERT fibroblasts was observed in the present study. Rho-associated kinase directly induced smooth muscle cell contraction through myosin light chain phosphorylation and independently of the calcium-calmodulin dependent signaling pathway [106]. Accordingly, an ET-1 mediated increase in intracellular calcium was not seen in hTERT fibroblasts, suggesting that a calcium-independent contraction pathway may be involved.

A link between ET-1 and the Rho-associated kinase pathway has recently been proposed. Contraction of hepatic stellate cells in culture by ET-1 (5nM) was attenuated in a dose-dependent manner by Y-27632, and Y-27632 also reduced ET-1 mediated F-actin stress fiber formation and phosphorylation of myosin light chain [78]. C3 transferase (which inactivates Rho through ADP-ribosylation) and Y-27632 inhibited serum (20%) and ET-1 (8nM) mediated myosin light chain phosphorylation and contractile force generation in chicken embryo fibroblasts dispersed in a collagen matrix [104]. We have presently demonstrated that TE

populated with hTERT fibroblasts contracted upon ET-1 treatment, which is blocked by Y-27632. Altogether, these studies identify the Rho-associated kinase pathway as a principal mediator of myosin light chain phosphorylation and consequent contraction of non-muscle cells by ET-1.

In addition to the direct roles proposed above, ET-1 may also act indirectly through TGF-β production and secretion. ET-1 has been shown to regulate gene expression to produce long-term responses [71]. Functional Rho and the Rho-associated kinase pathway have also been implicated in gene transcription [104, 107-109]. Specifically, the *c-fos* serum response element has been shown to effect gene transcription through the serum response factor induced by serum and Rho [107, 108]. Thus, the serum response factor has been established as a nuclear target of a novel, Rho-mediated signaling pathway and functional Rho is required for the regulated activity of the *c-fos* promoter [107, 108]. In addition, the expression of constitutively active Rho-associated kinase stimulated the transcriptional activity of *c-fos*, demonstrating a distinct role, downstream of Rho, in gene expression [109]. ET-1 treatment of hTERT fibroblasts over 24 hours resulted in a significant increase of TGF-β secretion. Since ET-1 and the Rho-associated kinase pathway have been implicated in gene transcription, it is reasonable to propose that ET-1 stimulates TGF-β production and secretion in hTERT fibroblasts. Future studies should focus on delineating the role of Rho and the Rho-associated kinase pathway in ET-1 mediated TGF-β secretion by hTERT fibroblasts. In addition, treatment of hTERT populated TE with ET-1 and

TGF-β together resulted in a significant increase in contraction as compared with TE treated with ET-1 or TGF-β alone. Therefore, the actions of ET-1 and TGF-β appear to be additive. It is possible that the production and secretion of TGF-β potentiates the ET-1 effects, sustaining the long-term effects on TE contraction and on the wound healing process.

Thus, these studies have identified ET-1 as a potential early initiator in wound healing and suggest a novel pathway through which it functions. This proposed mechanism includes both direct effects of ET-1 and indirect effects potentiated by TGF-β. In the future, studies should address whether TGF-β converges on the Rho-associated kinase pathway or acts independently through other signaling mechanisms. Furthermore, we are in the process of developing a promoter-reporter system to visualize α-SMA expression changes of fibroblasts populating TE, in real time. This approach will allow, for the first time, observation of changes in cytoskeletal protein expression and functional events (i.e. contraction) simultaneously. The discovery of tissue contraction early initiators is essential in the identification of potential therapeutic targets in the quest to reduce severe tissue contracture and scarring.

Figure 1. Schematic representation of proposed signaling by endothelin – 1 in wound healing fibroblasts.

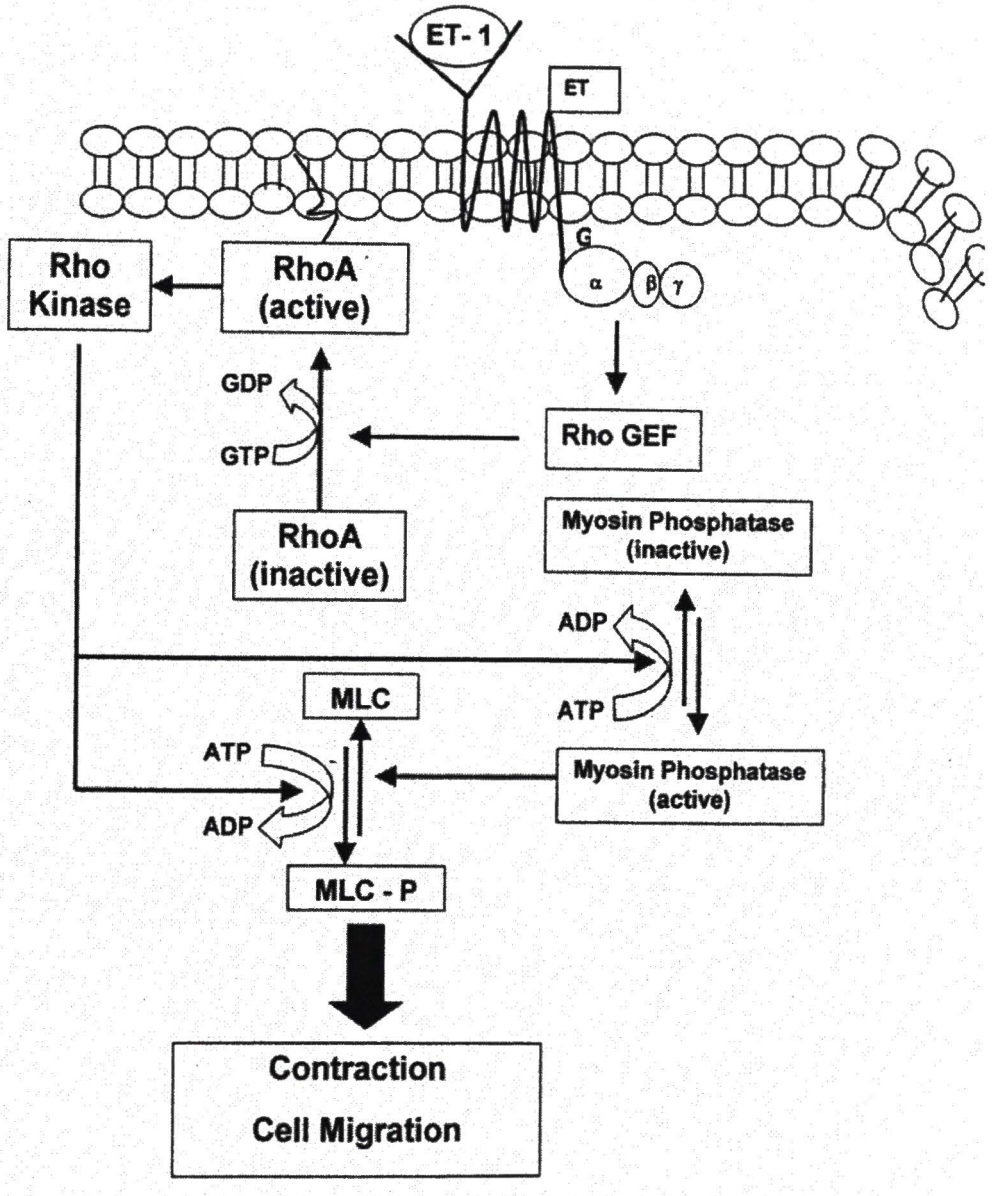
ET-1
ET
G
α
β
γ
Rho Kinase
RhoA (active)
GDP
GTP
Rho GEF
RhoA (inactive)
Myosin Phosphatase (inactive)
ADP
ATP
MLC
ATP
ADP
Myosin Phosphatase (active)
MLC - P
Contraction
Cell Migration

Figure 2. Endothelin Receptor (ET_A) is present in Infant and hTERT Fibroblasts. Indirect immunofluorescence using a monoclonal antibody to ET_A showed the presence of the endothelin receptor on both Infant (A) and hTERT (B) fibroblasts.

A.

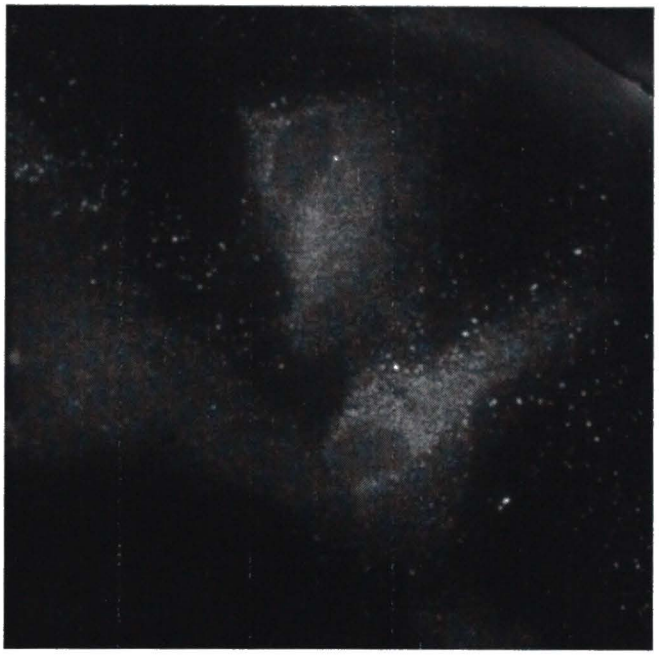

B.

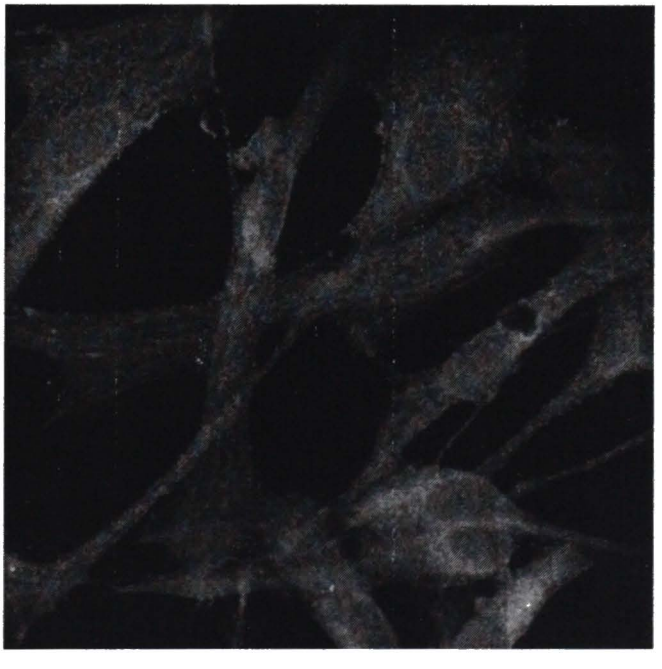

Figure 3. Endothelin-1 Stimulates Collagen Synthesis. Untreated (Ham's F-12 nutrient medium + 5% FBS) hTERT fibroblasts and fibroblasts stimulated with ascorbate (50μg/mL) or ET-1 (0.1μM or 1μM) were assayed for collagen type I synthesis and secretion at 8 and 48 hours. hTERT fibroblasts mean collagen synthesized +/- standard deviation was reported. There was no statistically significant difference between untreated and treated hTERT fibroblast collagen synthesis at 8 hours. However, at 48 hours all treated groups synthesized significantly more collagen than the untreated control cells (*, unpaired t-test with Bonferroni correction, $p<0.017$). ET-1 (0.1μM and 1μM doses) treated fibroblast collagen synthesis was significantly different from ascorbate stimulated collagen synthesis (**, unpaired t-test with Bonferroni correction, $p<0.025$).

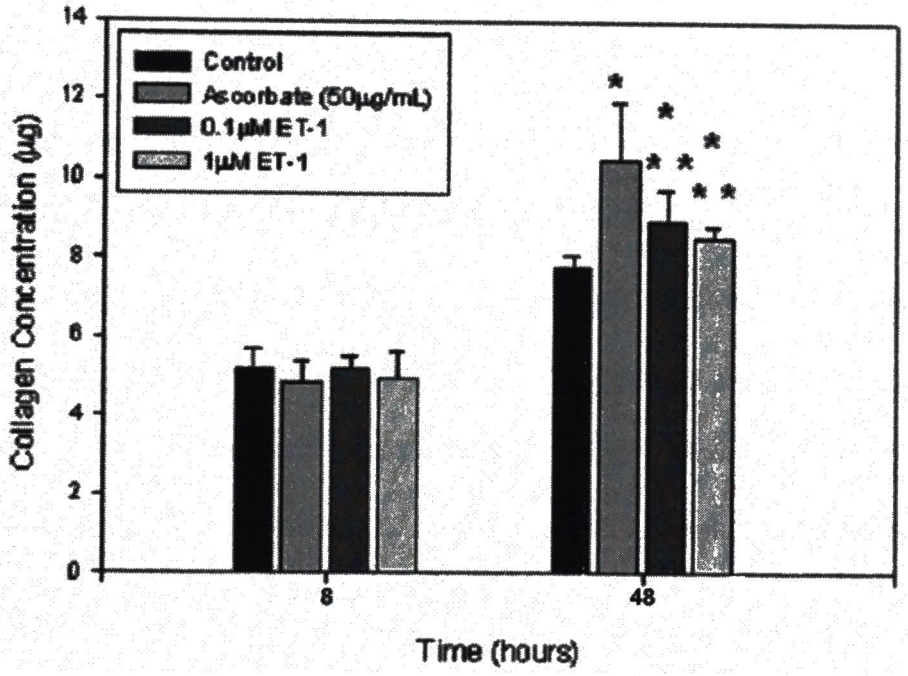
Control
Ascorbate (50µg/mL)
0.1µM ET-1
1µM ET-1
Collagen Concentration (µg)
0
2
4
6
8
10
12
14
8
48
Time (hours)

Figure 4. Cytoskeletal Changes Following Endothelin-1 Treatment. hTERT fibroblasts cultured at low density (LD) and high density (HD) were serum starved overnight and treated with 10nM endothelin-1 for 24 hours. Representative western blots are shown. Alpha-smooth muscle actin (α-SMA) expression of LD Infant and hTERT fibroblasts was higher than HD fibroblasts (A). LD fibroblasts treated with endothelin responded with a slight increase of α-SMA expression. Expression of myosin heavy chain in LD fibroblasts was somewhat higher than that of HD fibroblasts, both Infant and hTERT (B). However, there did not appear to be any change in myosin heavy chain expression due to endothelin-1 treatment. Finally, myosin light chain expression, in both its phosphoryated and unphosphorylated forms, increased marginally in response to endothelin-1 stimulation (C). The myosin light chain antibody appeared to recognize phosphorylated and unphosphorylated forms (two bands detected). All blots are representative of at least two separate experiments.

A.

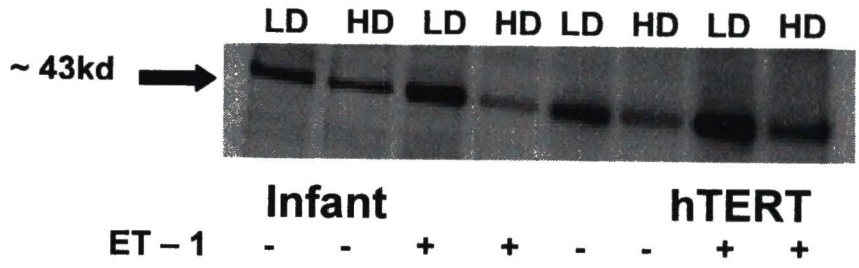
LD HD LD HD LD HD LD HD
~ 43kd
Infant
hTERT
ET – 1 - - + + - - + +

B.

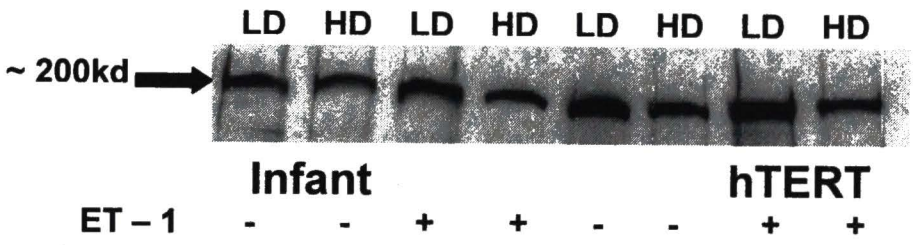
LD HD LD HD LD HD LD HD
~ 200kd
Infant
hTERT
ET – 1 - - + + - - + +

C.

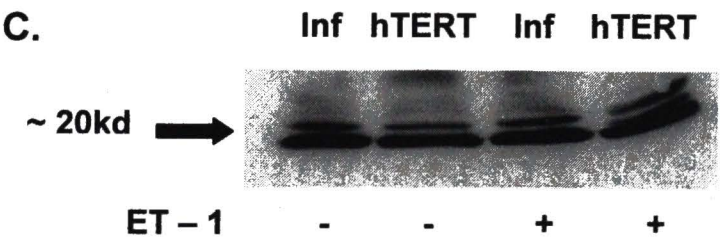
Inf hTERT Inf hTERT
~ 20kd
ET – 1 - - + +

Figure 5. Endothelin – 1 Alters Myosin Light Chain Localization. Indirect immunofluorescence of hTERT fibroblasts revealed perinuclear localization of myosin light chain (A). 10nM endothelin-1 treatment of hTERT fibroblasts for 24 hours resulted in the movement of myosin light chain into the cytoplasm (B), seen by indirect immunofluorescence. Pretreatment of fibroblasts with 10μM Y-27632 (C) or 1μM PD-142893 (D) prevented the endothelin-1 stimulated redistribution of myosin light chains. Light microscopy images of cells from A (E) and B (F) are also shown.

A.

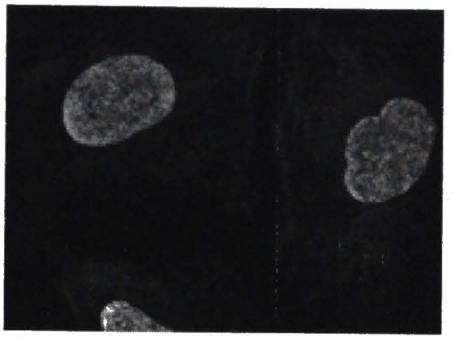

B.

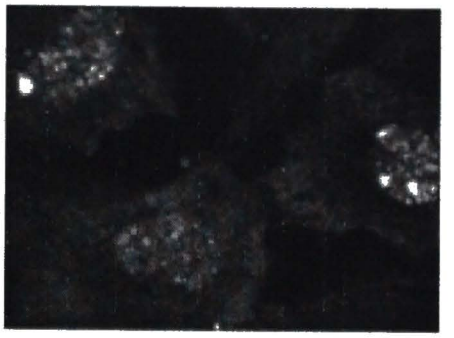

C.

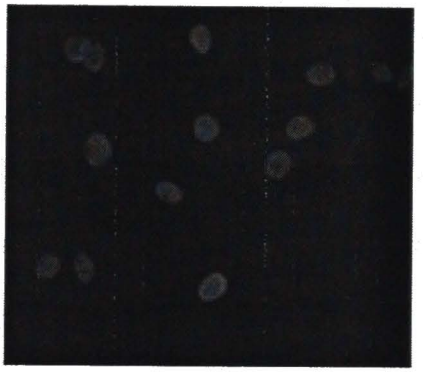

D.

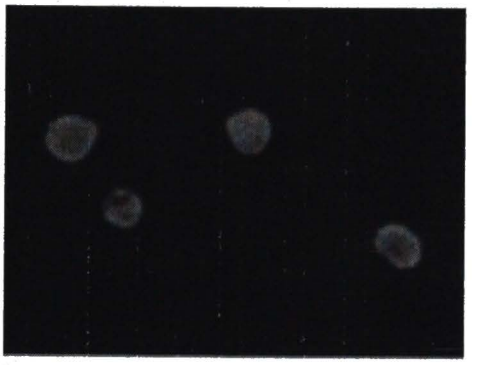

E.

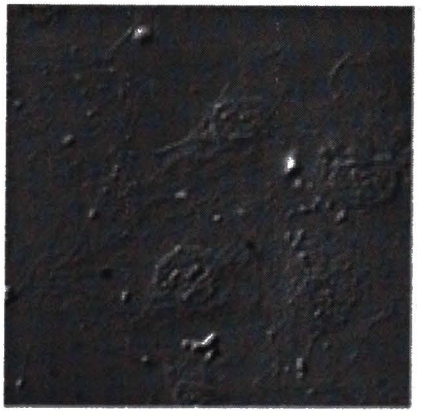

F.

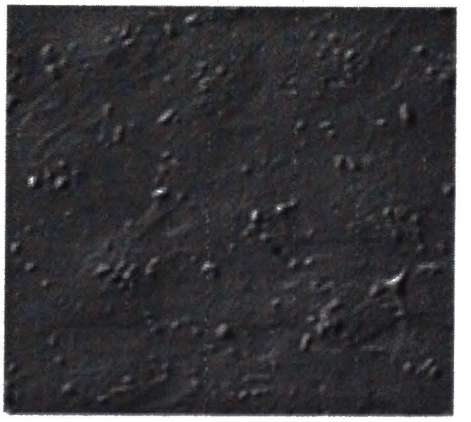

Figure 6. Endothelin – 1 Stimulates TE Contraction. hTERT fibroblasts in TE were allowed to polymerize and adapt for at least 6 hours. Ham's F-12 nutrient medium +/- endothelin – 1 (0.01μM, 1μM, 10μM) was added to each TE, and fresh medium + endothelin was added every two days for 15 days (A). Y-27632 (10μM) or PD-142893 (1μM) was incorporated into the TE prior to polymerization and added with medium and 1μM endothelin every two days. The mean wet weights of TE treated with 1 and 10μM endothelin were significantly different from the control TE and TE treated with Y-27632 and endothelin or PD-142893 and endothelin (unpaired t-test with Bonferroni correction, $p<0.0125$). In addition, TE were treated with 1μM endothelin-1, 10ng/ml TGF-β, or both endothelin (1μM) and TGF-β (10ng/ml) every 2 days for 15 days in culture (B). Mean wet weights of the endothelin and TGF-β treated TE were significantly different from control TE (*) and from TE treated with endothelin + TGF-β (**) (unpaired t-test with Bonferroni correction, $p<0.001$).

A.

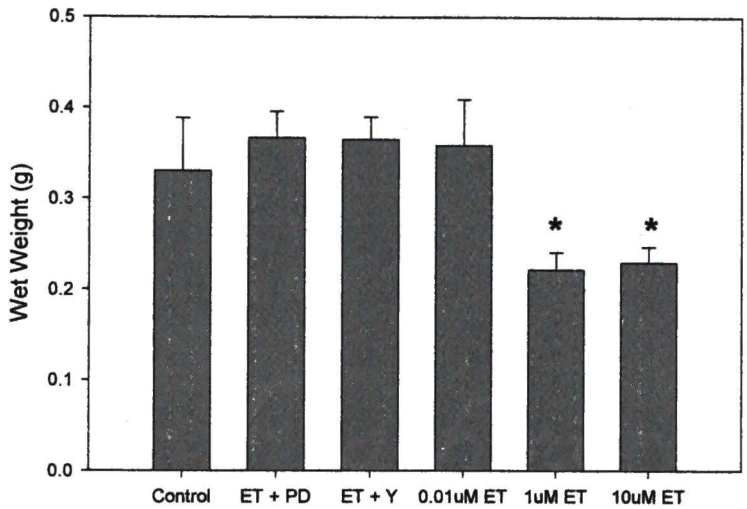
0.5
0.4
0.3
0.2
0.1
0.0
Wet Weight (g)
*
*
Control
ET + PD
ET + Y
0.01uM ET
1uM ET
10uM ET

B.

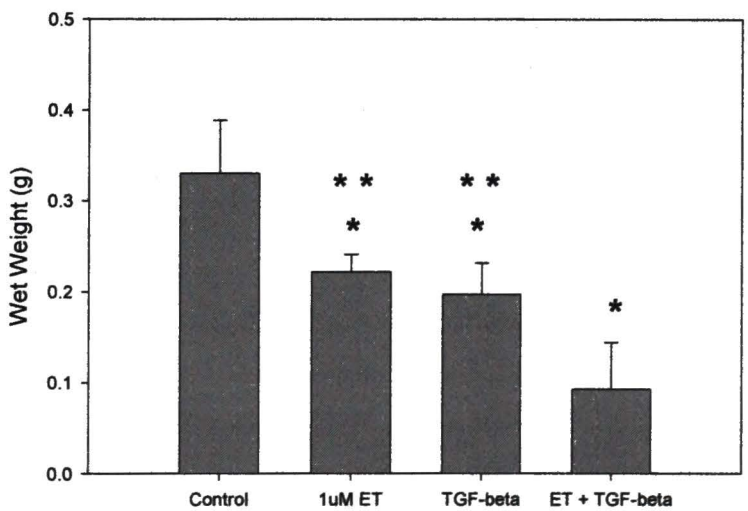
0.5
0.4
0.3
0.2
0.1
0.0
Wet Weight (g)
* *
*
* *
*
*
Control
1uM ET
TGF-beta
ET + TGF-beta

Figure 7. Intracellular Calcium ($[Ca^{2+}]_i$) Measurement of hTERT Fibroblasts Stimulated with Endothelin-1. Infant (A) and hTERT (B) fibroblasts were cultured glass coverslips and stimulated with endothelin-1. Fura-2 calcium imaging was utilized to show changes in intracellular calcium following addition of endothelin-1 (1nM at ~2.5 min., 10nM at ~6 min., 100nM at ~10 min., ionophore at 15-20 min.). No increase in intracellular calcium due to endothelin treatment was observed. Each graph is representative of at least two separate experiments and two coverslips per experiment.

A.

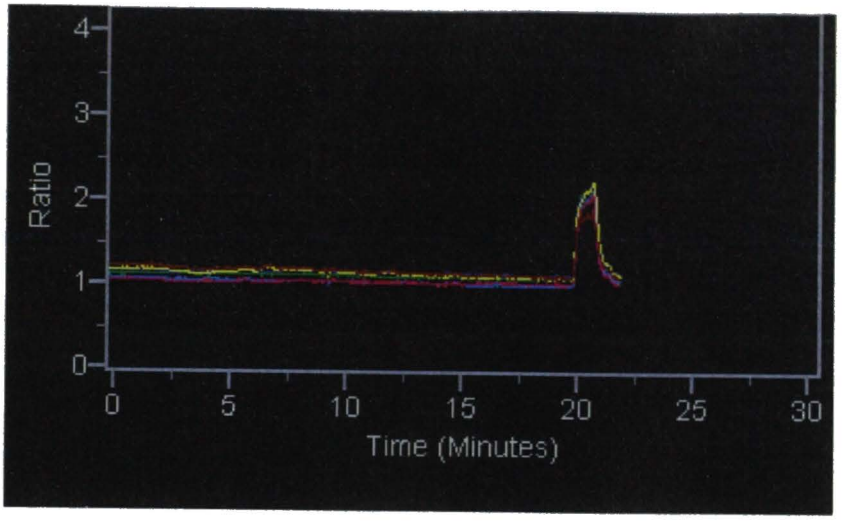
Ratio
0
1
2
3
4
0
5
10
15
20
25
30
Time (Minutes)

B.

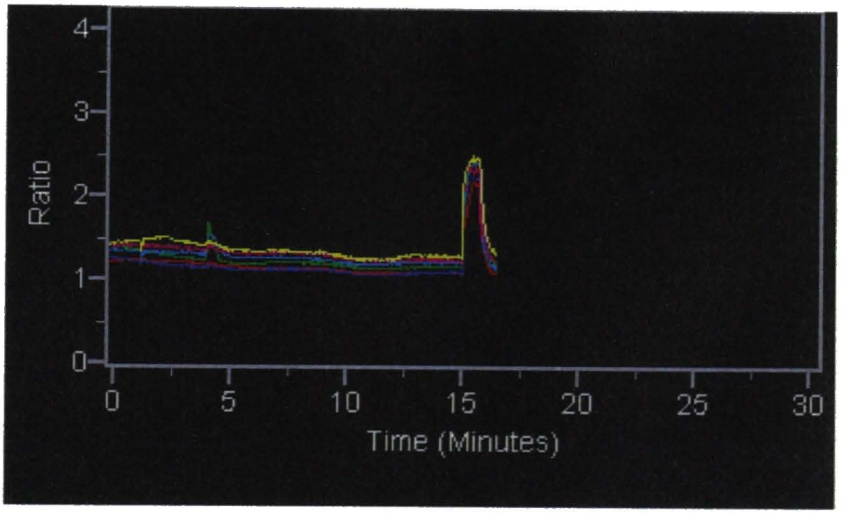
Ratio
0
1
2
3
4
0
5
10
15
20
25
30
Time (Minutes)

Figure 8. Stimulation of Transforming Growth Factor-β (TGF-β) Secretion by Endothelin – 1. hTERT fibroblasts were serum starved overnight and then treated with endothelin-1 (1, 10, or 100nM) in serum free DMEM for 24 hours. The supernatant was removed and assayed for TGF-β by ELISA. Mean concentration of TGF-β secreted by fibroblasts stimulated with 10 or 100nM endothelin-1 was significantly different from untreated control fibroblasts (n=4, unpaired t-test with Bonferroni correction, $p<0.017$).

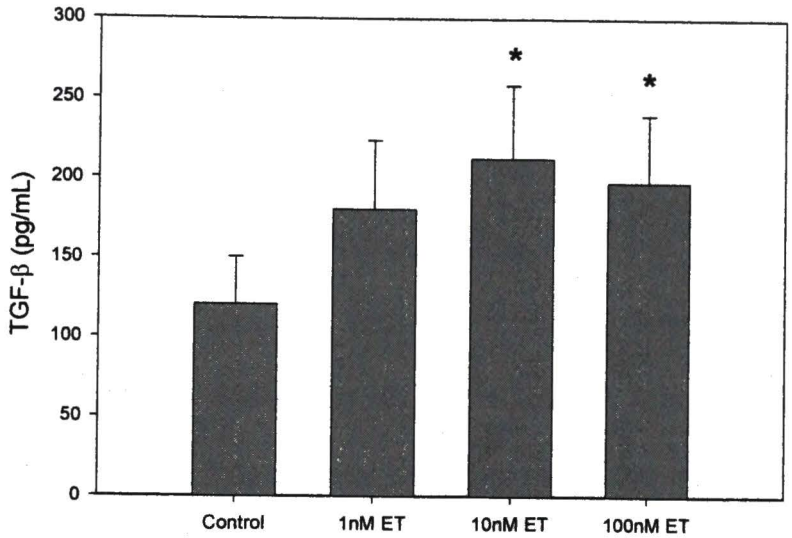
300
250
200
150
100
50
0
TGF-β (pg/mL)
*
*
Control
1nM ET
10nM ET
100nM ET

Chapter V

Development of an Alpha-Smooth Muscle Actin Promoter-Reporter System

Introduction

In the previous chapter, results from the western analysis of cell monolayer responses to endothelin were discussed. It is evident that there are difficulties in determining cytoskeletal changes using the monolayer culture as an approximation of cell behavior in tissue. These complexities have also been well documented in the literature describing TGF-β mediated responses. There is a clear need for a more direct and tissue relevant indicator of gene activation in response to contractile signals, so that the responses may be observed *in situ* and in real time.

To this end, studies were initiated to construct a promoter-reporter system that would be used to evaluate changes in relevant cytoskeletal proteins. Since α-Smooth Muscle Actin (α-SMA) plays a key role in tissue contraction and its expression is characteristic of the activated myofibroblast phenotype, its expression was chosen as a target for a promoter-reporter strategy in which α-SMA gene activation would be visualized through the expression of green fluorescent protein (GFP). This promoter-reporter system, in combination with our connective tissue equivalent model, is designed to allow non-intrusive, real-time observation of cell behavior in a three-dimensional matrix, using laser

scanning confocal microscopy. The development of this novel promoter-reporter system is essential for the study of fibroblast cytoskeletal changes in a three-dimensional tissue context during tissue contraction and cell migration, the events most heavily dependent on the functions of cytoskeletal proteins.

Materials and Methods

Materials. Miller's LB Broth Base (Gibco BRL), Agarose (Gibco-BRL), Agar (Fisher), Max Efficiency DH5α Competent Cells (Invitrogen), Platinum pfx polymerase (Invitrogen), Maxi- and Mini-Prep Kits (Qiagen), Gel Purification Kit (Qiagen), DNA Polymerase I Large Fragment (Klenow, New England Biolabs), Not I (Promega), Sal I (Promega), Sac II (Promega), Sma I (Promega), pd2EGFP (Clontech), ACC65 I (New England Biolabs).

DNA Gel Electrophoresis. The gels were made with 0.6% agarose in 1X Tris Acetate EDTA (TAE) + ethidium bromide and cast into the minigel apparatus. The samples and molecular weight standard (1kb, BioRad) were mixed with nucleic acid sample loading buffer (BioRad) and loaded into the wells of the gel. The gel was run at 90V until the dye front had progressed through approximately 2/3 of the gel. Each gel was examined under UV lamp.

Transformation. DNA (15 – 20ng) was added to Max Efficiency Competent Cells (50μl/reaction, Invitrogen) and incubated on ice for 30 min. Competent cells were then heat shocked in a 42°C water bath for 90 seconds and immediately returned to ice. Tubes containing 1ml Luria Broth (LB) + glucose

were inoculated with the competent cells and resulting cultures were shaken at 225 rpm for 1hour at 37°C. Dilutions of the LB culture were streaked on LB/Agar plates containing the appropriate antibiotic and were incubated upside-down overnight at 37°C. Single colonies were picked and cultured in 2ml or 250ml LB + antibiotic overnight at 37°C with shaking (225rpm). Freeze-downs of each culture were made in 15% glycerol and mini or maxi-prep of the culture was performed using the Qiagen MiniPrep Kit or the Qiagen Plasmid Maxi kit. DNA purification kit protocols are based on a modified alkaline lysis procedure followed by binding of plasmid DNA to Qiagen Anion-Exchange Resin under appropriate low-salt and pH conditions. RNA, proteins, dyes, and low molecular weight impurities are removed by a medium salt wash. Plasmid DNA is eluted in a high-salt buffer and then concentrated and desalted by isopropanol precipitation.

Polymerase Chain Reaction (PCR). The basic PCR reaction included 10X pfx polymerase buffer, 10mM dTNP mix, 50mM MgSo4, 0.2μM each primer, DNA template (10ng/μl), and Platinum pfx polymerase. Thirty cycles of 95°C denaturing (30 seconds), 60°C annealing (30 seconds) and 68°C elongation (5 minutes, 30 seconds) proceeded, and the resulting product was evaluated by DNA electrophoresis.

DNA Digestion and Gel Purification. DNA was digested according to the reaction specifications of each restriction enzyme in a thermocycler. The resulting DNA fragments were analyzed by gel electrophoresis and the band containing the fragment of interest was cut out of the gel and purified via the

Qiaex II method (Qiagen). With this kit, the extraction and purification of DNA fragments are based on the solubilization of agarose, followed by adsorption of the nucleic acids to the Qiaex II silica-gel particles in high salt. DNA elution is accomplished with a low-salt solution such as water.

Strategy and Results

The strategy contemplated was based on the cloning of the α-SMA promoter into the commercially available pd2EGFP plasmid and then stably transfecting into hTERT fibroblasts. The use of a cell line compensates for possible low efficiency of transfection. The full-length human α-SMA promoter cloned into pUC19 was a kind gift from Dr. Gary Owens [110]. Unfortunately, the pUC19 plasmid only contains two restriction sites, one on either end of the promoter region, which were recognized by restriction enzymes without also cutting within the promoter fragment sequence itself. Thus, the pUC19 plasmid was digested with Not I and Sal I to remove the intact promoter region and analyzed via DNA gel electrophoresis to confirm the size of the resulting fragment (**Fig. 1**). The resultant 3' and 5' ends of the promoter were not compatible with the multiple cloning sites available in the pd2EGFP plasmid. Therefore, following digestion to remove the promoter from the pUC19 plasmid, several attempts were made to amplify and generate compatible ends using polymerase chain reaction (PCR) and primers developed for that purpose. However, presumably due to the large size of the promoter (~5.5 kb), even using

a high fidelity polymerase approach did not produce desirable PCR results (**Fig. 2**). As an alternative approach, the promoter region was cloned into pBluescriptSK phagemid (**Fig. 3**). This allowed access to restriction sites that were somewhat compatible with the multiple cloning sites in the pd2EGFP plasmid (**Fig. 4**). The promoter therefore had to be cut out of pBluescriptSK with the isoschizomer ACC65 I and the 5' protruder was converted to a blunt end using Klenow. Then the 3' end of the promoter was cleaved with the restriction enzyme Sac II, and the promoter fragment was gel purified. pd2EGFP was digested with Sma I and Sac II and purified. Directional cloning of the promoter fragment into pd2EGFP was carried out in the laboratory of Dr. Daniel McMillan (University of Texas Southwestern).

Discussion and Future Directions

While the development of the promoter-reporter system is a complex process, we feel it is the most relevant and useful way to approach studies of cytoskeletal protein expression in tissue. Some of the difficulties encountered include issues related to working with a large, full-length promoter (~5.5kb), the need to generate appropriate ends for sub-cloning, and the necessity for stable transfection in the target cells. However, the advantages far out weigh the difficulties encountered.

First, it is essential to have real-time, three-dimensional measurement of cytoskeletal protein expression so that the cell-matrix interactions occurring at

various stages of the wound healing process can be studied. For example, this approach will, for the first time, show a direct link between upregulation of α-SMA expression and tissue contraction. While α-SMA has long been accepted as the key cytoskeletal marker for fibroblast activation in preparation for wound contraction, a direct connection between protein expression and contraction has not been made [93, 111]. Furthermore, the fate of the myofibroblast following tissue contraction has not been determined. A hypothesis has been proposed that myofibroblasts are eliminated through apoptosis [23]. However, this theory does not address the remodeling that occurs well after tissue contraction and which cells may be responsible for that process. This promoter-reporter approach is ideal for the observation of the activated fibroblast following tissue contraction and the determination of its fate.

Secondly, stable transfection of the promoter-reporter system is the only approach that allows experimental design that includes the use of a three-dimensional collagen matrix model and also will permit long-term experiments. Since it takes several days to generate a stable tissue equivalent with cultured cells and several more to visualize effects of an added ligand, which has to diffuse into the matrix, transient transfection (typically lasting only 2-3 days) is not appropriate.

The destabilized enhanced green fluorescent reporter protein, d2EGFP, was also carefully chosen. The fluorescence of the protein has been optimized for brighter fluorescence, which will enhance observation in a three-dimensional

collagen matrix. Also, the enhanced green fluorescent protein has been destabilized with the addition of a PEST amino acid sequence that targets the protein for degradation. Since the d2EGFP has a half-life of approximately two hours, it allows for repeated perturbations and real-time observations of changes in cytoskeletal protein expression. Luciferase is a common reporter used in similar systems, but is not appropriate for a three-dimensional model, particularly one that focuses studies on cell-matrix interactions. Since the detection of luciferase requires lysis of the cells, to use it in our collagen matrix system would require dissolution of the matrix, followed by cell lysis. By the time the collagen matrix had been dissolved, changes in the cytoskeletal protein expression will have taken place, negating this experimental approach. Also, by using d2EGFP, we obviate the need for an absolute end point, thus allowing observations and measurements of a single sample to be made as often throughout the course of the experiment as desired. Moreover, the d2EGFP reporter enables the employment of scanning laser confocal microscopy to optically section TE.

Therefore, this novel system allows, for the first time, a method to detect changes in cytoskeletal protein levels in cells within a three-dimensional matrix non-intrusively and in real time, as well as being applicable to monolayer studies. Once completed and stably transfected into hTERT fibroblasts, the promoter-reporter system will be used to study the real-time activation of these cells to their myofibroblast phenotype in a three-dimensional tissue equivalent. In addition, experiments performed following systematic truncation of the α-SMA

promoter region will facilitate the elucidation of the role that various promoter response elements play in its regulation. It has recently been shown that there is a conserved role for CArG boxes and a TGF-β control element involved in the upregulation of α-SMA expression in smooth muscle cells and non-muscle cells that is modified by a complex interplay of positive- and negative-acting cis elements in a cell-specific manner [112]. ET-1 mediated responses at the gene expression level also need to be described. Therefore, although it was problematic, it was necessary to initially use the full-length promoter. It is expected that it will be advantageous for future experiments focused on the delineation of the role that various response elements play. Finally, the system can be adapted to examine other target genes that participate in contraction, for example, myosin light chain. Further experiments along these lines could study focal adhesion plaque assembly and cell-matrix interactions.

Figure 1. DNA gel electrophoresis of pUC19 digest. Maxi-prep of pUC19 containing the α-SMA promoter was digested with Not I and Sal I and the resulting fragments were run on a 0.6% agarose in 1X TAE gel at 90V. The band at 6kb was cut out and gel purified.

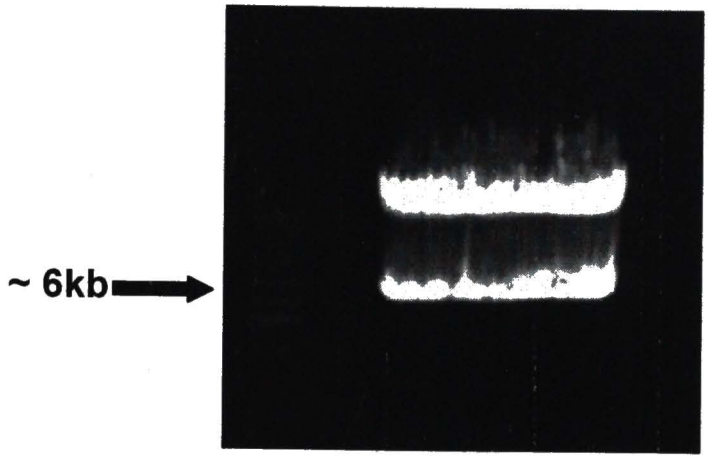
~ 6kb

Figure 2. DNA gel electrophoresis of PCR products. Using the DNA purified from Fig. 1, no PCR products of the correct size were obtained through multiple attempts. DNA gel (0.6% agarose in 1X TAE) was run at 90V.

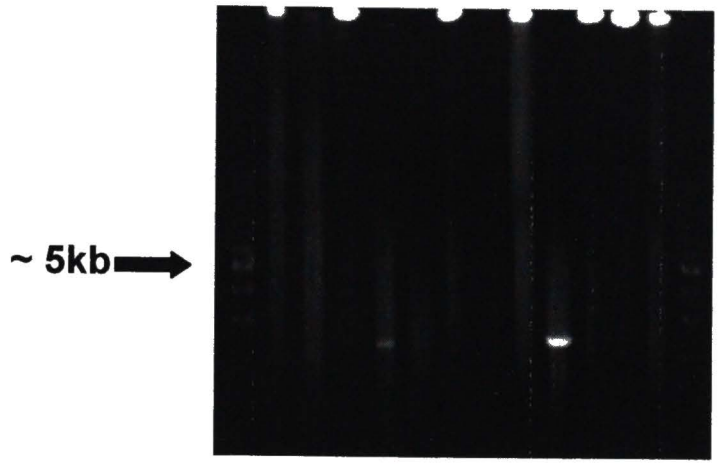
~ 5kb

Figure 3. pBluescript phagemid map.

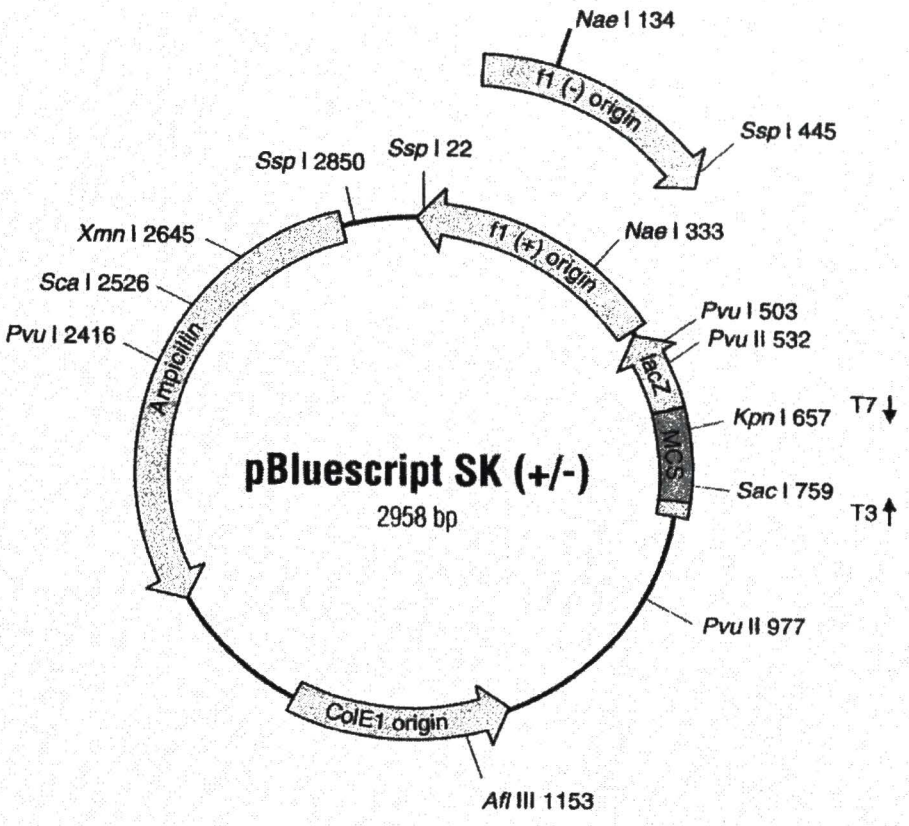
Nae I 134
f1 (-) origin
Ssp I 445
Ssp I 2850
Ssp I 22
Xmn I 2645
f1 (+) origin
Nae I 333
Sca I 2526
Pvu I 503
Pvu I 2416
Pvu II 532
Ampicillin
lacZ
Kpn I 657
T7
MCS
pBluescript SK (+/-)
2958 bp
Sac I 759
T3
Pvu II 977
ColE1 origin
Afl III 1153

Figure 4. pd2EGFP plasmid map.

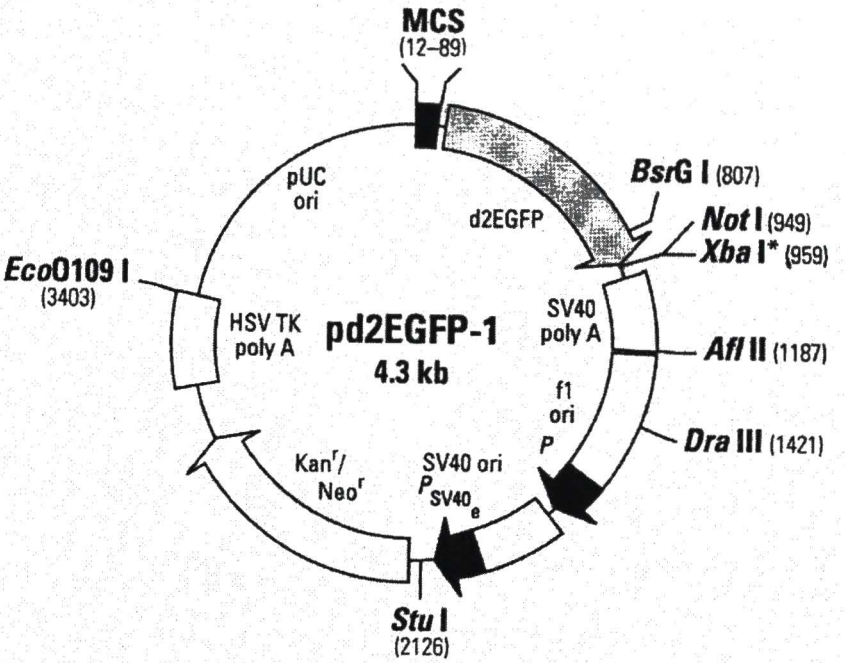
MCS
(12–89)
BsrG I (807)
Not I (949)
Xba I* (959)
Afl II (1187)
Dra III (1421)
Stu I
(2126)
Eco0109 I
(3403)
pUC
ori
d2EGFP
SV40
poly A
f1
ori
P
SV40 ori
P_{SV40_e}
Kan^r/
Neo^r
HSV TK
poly A
pd2EGFP-1
4.3 kb

Chapter VI

Conclusions

The focus of these studies was to characterize a novel connective tissue model for use in experiments examining possible contraction initiators in the wound healing process, i.e. endothelin-1 (ET-1). A variety of tissue models have been proposed, ranging from a simple monolayer of fibroblasts cultured on a collagen coating to fibroblasts dispersed into a three-dimensional matrix composed of various extracellular matrix macromolecules [3, 5, 8, 9, 23, 32, 33]. Unfortunately, every TE proposed to date contracts spontaneously. This contraction occurs within the first few hours of assembly and results in a dense, opaque tissue [5, 8]. Such models have been frequently used as research tools in studies examining the mechanisms of contraction and scar formation [31, 35-38], and have led to conclusions that do not clarify our understanding of the tissue contraction process. Since the fibroblasts have been activated to the contractile phenotype and the model is already in a state of contraction, the signaling cascade initiated by additional ligands is superimposed on an already activated pathway(s). These may act in an additive, synergistic, or opposing manner. Furthermore, once the model is dense and opaque, it is impossible to monitor the morphological status of the cells by simple non-intrusive methods (e.g. light, fluorescent, or scanning laser confocal microscopy).

The cellular components of the TE vary almost as much as the models do themselves. While human fibroblasts have become the benchmark for studies of wound healing in TE, they are not an optimal choice for ongoing studies requiring large numbers of cells. First, all normal human cells undergo a finite number of cell divisions when cultured *in vitro,* and ultimately enter a state of replicative senescence [49]. Secondly, *in vitro* behavior of primary fibroblasts varies significantly from donor to donor, with respect to donor age and gender, and from passage to passage [48]. Such variability produces data that is difficult to interpret and makes it formidable to demonstrate statistical significance of changes over the course of several experiments.

The human telomerase catalytic subunit (hTERT) when stably expressed has been shown to extend the life span of normal human cells [54]. Through these studies, it has been shown that use of a telomerized dermal fibroblast cell line addresses the concerns relating to variations due to heterogeneity of normal human cells cultured *in vitro*, without creating a cancerous cell line or interfering with normal phenotypic changes. This is particularly important since the wound healing process involves fibroblasts at various stages of phenotypic differentiation. In addition, the incorporation of telomerized cells into our TE, which does not spontaneously contract (US Patent #6471958), provides a unique model to study the contraction and scar formation process.

Using the TE populated with hTERT fibroblasts, an innovative technique was developed to identify the initiation of tissue contraction using an optical fiber

interferometry system. This system greatly improves upon previous methods of matrix contraction measurement, particularly enabling the identification of contraction initiation. The process allows observation of contraction within five minutes of stimulus addition. Other methods are much less sensitive and rely on gross contraction, which is not detectable for hours [17, 38, 41]. The optic interferometry system also enables continuous data capture over a period of several hours and can be left unattended. In contrast, the measurements taken using other proposed methods occur at absolute time points and thus give no information with respect to the course of the contraction process taking place between measurements. This fact may be of particular importance, as we have observed a unique pattern of rapid contraction followed by longer periods of slow contraction in response to serum using the interferometer method. The greatest strength of this system is its sensitivity, since the optic interferometer allows measurement of displacement (contraction) to the tens of nanometers. Contraction of fibrin gels has been measured using an Olympus inverted microscope equipped with a Mitutoyo digital indicator with a range of 0.01 – 10 mm [17]. Free-floating collagen gel contraction has been determined by measuring the diameter of the gel to the nearest 0.25 mm with a Nikon SMZ-1 stereoscope [38]. These techniques utilizing light microscopy and optical methods to measure matrix contraction are the most sensitive proposed to date and yet, at best they are still 1000 – fold less sensitive than the proposed interferometry system. This will be particularly important when studying a multi-

component contractile system and may enable the differentiation between additive and synergistic effects.

Along those lines, the current studies have identified ET-1 as a potential early initiator in wound healing and suggest a novel pathway through which it functions. This proposed mechanism includes both direct effects of ET-1 through the Rho-associated kinase pathway and indirect effects potentiated by TGF-β. Future studies addressing whether TGF-β converges on the Rho-associated kinase pathway or acts independently through other signaling mechanisms should be initiated. In addition, use of the optical fiber interferometry system to identify the beginning of contraction by ET-1 will further elucidate the role of ET-1 as an early initiator of tissue contraction and may enable differentiation of direct ET-1 and indirect, ET-1 mediated TGF-β contractile effects (i.e. the beginning of TGF-β involvement). The discovery of early initiators of tissue contraction is essential in the identification of potential therapeutic targets in the quest to reduce prolonged and severe tissue contracture and scaring.

Finally, studies have begun to develop a promoter-reporter system to visualize α-SMA expression changes in real time and in the three-dimensional TE model. This novel system allows, for the first time, a method to detect changes in protein levels in cells in a tissue-like environment, non-intrusively and in real time. Once completed and stably transfected into hTERT fibroblasts, the promoter-reporter system will be used to study the real-time activation of these cells to their myofibroblast phenotype in a three-dimensional TE, including in

response to ET-1 treatment. It has recently been shown that there is a conserved role for CArG boxes and a TGF-β control element involved in the upregulation of α-SMA expression in smooth muscle cells and non-muscle cells that is modified by a complex interplay of positive- and negative-acting cis elements in a cell-specific manner [112]. Therefore, experiments performed following systematic truncation of the α-SMA promoter region will facilitate the elucidation of the role that various promoter response elements play in its regulation. Lastly, the system can be adapted to examine other target genes that participate in contraction, such as, myosin light chain.

The characterization and use of these unique strategies, including the non-contracting TE populated with hTERT fibroblasts, the optical fiber interferometry system, and the promoter-reporter system, has led to a better understanding of tissue contraction and its mediators. Specifically, a role for ET-1 as an early initiator of contraction has been established. Future studies utilizing these techniques will further our understanding of these important tissue repair parameters.

References

1. Eckes, B., M. Aumailley, and T. Krieg, *Collagens and the Reestablishment of Dermal Integrity*, in *The Molecular and Cellular Biology of Wound Repair*, R.A.F. Clark, Editor. 1996, Plenum Press: New York. p. 493 - 512.
2. Clark, R.A.F., *Wound Repair: Overview and General Considerations*, in *The Molecular and Cellular Biology of Wound Repair*, R.A.F. Clark, Editor. 1996, Plenum Press: New York. p. 3 - 50.
3. Lamme, E.N., *et al.*, *Living Skin Substitutes: Survival and Function of Fibroblasts Seeded in a Dermal Substitute in Experimental Wounds.* Journal of Investigative Dermatology, 1998. **111**: p. 989-995.
4. Gallo, R.L. and M. Bernfield, *Proteoglycans and Their Role in Wound Repair*, in *The Molecular and Cellular Biology of Wound Repair*, R.A.F. Clark, Editor. 1996, Plenum Press: New York. p. 475 - 492.
5. Auger, F.A., *et al.*, *Tissue-engineered human skin substitutes developed from collagen- populated hydrated gels: clinical and fundamental applications.* Med Biol Eng Comput, 1998. **36**(6): p. 801-12.
6. Oyster, C.W., *The Human Eye: Structure and Function*. 1999, Sunderland: Sinauer Associates, Inc. 766.
7. Marieb, E.N., *Human Anatomy and Physiology*. 2nd ed. 1991, Redwood City: The Benjamin/Cummings Publishing Company, Inc. 1014.

8. Coulomb, B., *et al.*, *Advantage of the presence of living dermal fibroblasts within in vitro reconstructed skin for grafting in humans.* Plast Reconstr Surg, 1998. **101**(7): p. 1891-903.

9. Yang, E.K., *et al.*, *Tissue engineered artificial skin composed of dermis and epidermis.* Artif Organs, 2000. **24**(1): p. 7-17.

10. Silver, F.H., I. Horvath, and D.J. Foran, *Mechanical Implications of the Domain Structure of Fiber-Forming Collagens: Comparison of the Molecular and Fibrillar Flexibilities of the alpha1-Chains Found in Types I-III Collagen.* J Theor Biol, 2002. **216**(2): p. 243-254.

11. Rossert, J., C. Terraz, and S. Dupont, *Regulation of type I collagen genes expression.* Nephrol Dial Transplant, 2000. **15**(Suppl 6): p. 66-8.

12. Nuytinck, L., C. Coppin, and A. De Paepe, *A four base pair insertion polymorphism in the 3' untranslated region of the COL1A1 gene is highly informative for null-allele testing in patients with osteogenesis imperfecta type I.* Matrix Biol, 1998. **16**(6): p. 349-52.

13. Takahashi, S., *et al.*, *Cloning and characterization of the 5'-flanking region of the rat P4Halpha gene encoding the prolyl 4-hydroxylase alpha(I) subunit(1).* Biochim Biophys Acta, 2002. **1574**(3): p. 354-8.

14. Chen, M., *et al.*, *Development and characterization of a recombinant truncated type VII collagen "minigene". Implication for gene therapy of dystrophic epidermolysis bullosa.* J Biol Chem, 2000. **275**(32): p. 24429-35.

15. Mignatti, P., *et al.*, *Proteinases and Tissue Remodeling*, in *The Molecular and Cellular Biology of Wound Repair*, R.A.F. Clark, Editor. 1996, Plenum Press: New York. p. 427 - 474.

16. Stadelmann, W.K., A.G. Digenis, and G.R. Tobin, *Physiology and healing dynamics of chronic cutaneous wounds.* Am J Surg, 1998. **176**(2A Suppl): p. 26S-38S.

17. Tuan, T.L., *et al.*, *In vitro fibroplasia: matrix contraction, cell growth, and collagen production of fibroblasts cultured in fibrin gels.* Exp Cell Res, 1996. **223**(1): p. 127-34.

18. Myllyharju, J. and K.I. Kivirikko, *Collagens and collagen-related diseases.* Ann Med, 2001. **33**(1): p. 7-21.

19. Yamada, K.M., J. Gailit, and R.A.F. Clark, *Integrins in Wound Repair*, in *The Molecular and Cellular Biology of Wound Repair*, R.A.F. Clark, Editor. 1996, Plenum Press: New York. p. 311 - 338.

20. Calderwood, D.A., S.J. Shattil, and M.H. Ginsberg, *Integrins and actin filaments: reciprocal regulation of cell adhesion and signaling.* J Biol Chem, 2000. **275**(30): p. 22607-10.

21. Dogic, D., B. Eckes, and M. Aumailley, *Extracellular Matrix, Integrins and Focal Adhesions*, in *Current Topics in Pathology*, A. Desmouliere and B. Tuchweber, Editors. 1999, Springer - Verlag: Berlin. p. 75 - 85.

22. Friedl, P. and E.B. Brocker, *The biology of cell locomotion within three-dimensional extracellular matrix.* Cell Mol Life Sci, 2000. **57**(1): p. 41-64.

23. Grinnell, F., *et al.*, *Release of Mechanical Tension Triggers Apoptosis of Human Fibroblasts in a Model of Regressing Granulation Tissue.* Experimental Cell Research, 1999. **248**: p. 608 - 619.

24. Amano, M., *et al.*, *Formation of actin stress fibers and focal adhesions enhanced by Rho- kinase.* Science, 1997. **275**(5304): p. 1308-11.

25. Desmouliere, A. and G. Gabbiani, *The Role of the Myofibroblast in Wound Healing and Fibrocontractive Diseases*, in *The Molecular and Cellular Biology of Wound Repair*, R.A.F. Clark, Editor. 1996, Plenum Press: New York. p. 391 - 423.

26. Schurch, W., *The myofibroblast in neoplasia.* Curr Top Pathol, 1999. **93**: p. 135-48.

27. Grinnell, F., *Signal transduction pathways activated during fibroblast contraction of collagen matrices.* Curr Top Pathol, 1999. **93**: p. 61-73.

28. Gabbiani, G., *Some Historical and Philosophical Reflections on the Myofibroblast Concept.* Current Topics in Pathology, 1999. **93**: p. 1-5.

29. Moulin, V., *et al.*, *What's New in Human Wound-Healing Myofibroblasts?* Current Topics in Pathology, 1999. **93**: p. 123-33.

30. Gabbiani, G., *The Biology of the Myofibroblast.* Kidney International, 1992. **41**: p. 530-2.

31. Bell, E., B. Ivarsson, and C. Merrill, *Production of a tissue-like structure by contraction of collagen lattices by human fibroblasts of different*

proliferative potential in vitro. Proc Natl Acad Sci U S A, 1979. **76**(3): p. 1274-8.

32. Guidry, C. and M. Hook, *Endothelins produced by endothelial cells promote collagen gel contraction by fibroblasts.* J Cell Biol, 1991. **115**(3): p. 873-80.

33. Eaglstein, W.H. and V. Falanga, *Tissue engineering and the development of Apligraf a human skin equivalent.* Adv Wound Care, 1998. **11**(4 Suppl): p. 1-8.

34. McCallion, R.L. and M.W.J. Ferguson, *Fetal Wound Healing and the Development of Antiscarring Therapies for Adult Wound Healing*, in *The Molecular and Cellular Biology of Wound Repair*, R.A.F. Clark, Editor. 1996, Plenum Press: New York. p. 561-600.

35. Anderson, S.N., Z. Ruben, and G.C. Fuller, *Cell-mediated contraction of collagen lattices in serum-free medium: effect of serum and nonserum factors.* In Vitro Cell Dev Biol, 1990. **26**(1): p. 61-6.

36. Delvoye, P., *et al.*, *Measurement of mechanical forces generated by skin fibroblasts embedded in a three-dimensional collagen gel.* J Invest Dermatol, 1991. **97**(5): p. 898-902.

37. Guidry, C., S. Hohn, and M. Hook, *Endothelial cells secrete a factor that promotes fibroblast contraction of hydrated collagen gels.* J Cell Biol, 1990. **110**(2): p. 519-28.

38. Tomasek, J.J. and S.K. Akiyama, *Fibroblast-mediated collagen gel contraction does not require fibronectin-alpha 5 beta 1 integrin interaction.* Anat Rec, 1992. **234**(2): p. 153-60.

39. *Green Fluorescent Protein: Properties, Applications, and Protocols.* first ed, ed. M. Chalfie and S. Kain. 1998, New York: Wiley - Liss. 383.

40. Nishiyama, T., *et al.*, *Quantitative evaluation of the factors affecting the process of fibroblast-mediated collagen gel contraction by separating the process into three phases.* Coll Relat Res, 1988. **8**(3): p. 259-73.

41. Guidry, C. and C. Hardwick, *Extracellular matrix contraction by choroidal fibroblasts: inhibition by staurosporine.* Invest Ophthalmol Vis Sci, 1994. **35**(2): p. 503-508.

42. Villaschi, S. and R.F. Nicosia, *Paracrine interactions between fibroblasts and endothelial cells in a serum-free coculture model. Modulation of angiogenesis and collagen gel contraction.* Lab Invest, 1994. **71**(2): p. 291-9.

43. Choudhury, P., W. Chen, and R.C. Hunt, *Production of platelet-derived growth factor by interleukin-1 beta and transforming growth factor-beta-stimulated retinal pigment epithelial cells leads to contraction of collagen gels.* Invest Ophthalmol Vis Sci, 1997. **38**(5): p. 824-33.

44. Lee, Y.R., *et al.*, *Combination of insulin-like growth factor (IGF)-I and IGF-binding protein-1 promotes fibroblast-embedded collagen gel contraction.* Endocrinology, 1996. **137**(12): p. 5278-83.

45. Clark, R.A., *et al.*, *Platelet isoforms of platelet-derived growth factor stimulate fibroblasts to contract collagen matrices.* J Clin Invest, 1989. **84**(3): p. 1036-40.

46. Harris, A.K., P. Wild, and D. Stopak, *Silicone rubber substrata: a new wrinkle in the study of cell locomotion.* Science, 1980. **208**(4440): p. 177-9.

47. Roy, P., *et al.*, *Exertion of tractional force requires the coordinated up-regulation of cell contractility and adhesion.* Cell Motil Cytoskeleton, 1999. **43**(1): p. 23-34.

48. Funk, W.D., *et al.*, *Telomerase expression restores dermal integrity to in vitro-aged fibroblasts in a reconstituted skin model.* Exp Cell Res, 2000. **258**(2): p. 270-8.

49. Moorhead, P.S., *et al.*, *Standards of karyology for human diploid cells.* J Biol Stand, 1974. **2**(2): p. 95-101.

50. Bodnar, A.G., *et al.*, *Extension of Life - Span by Introduction of Telomerase into Normal Human Cells.* Science, 1998. **279**: p. 349 - 52.

51. MacKenzie, K.L., *et al.*, *Mass Cultured Human Fibroblasts Overexpressing hTERT Encounter a Growth Crisis Following an Extended Period of Proliferation.* Experimental Cell Research, 2000. **259**: p. 336 - 350.

52. Weinberg, R.A., *Bumps on the road to immortality.* Nature, 1998.

53. Bickenbach, J.R., *et al.*, *Telomerase is Not an Epidermal Stem Cell Marker and is Downregulated by Calcium.* Journal of Investigative Dermatology, 1998. **111**: p. 1045-1052.

54. Steinert, S., J.W. Shay, and W.E. Wright, *Transient Expression of Human Telomerase Extends the Life Span of Normal Human Fibroblasts.* Biochemical and Biophysical Research Communications, 2000. **273**: p. 1095 - 98.

55. Morales, C.P., *et al.*, *Absence of cancer-associated changes in human fibroblasts immortalized with telomerase.* Nat Genet, 1999. **21**(1): p. 115-8.

56. Martin, P., *Wound Healing - Aiming for Perfect Skin Regeneration.* Science, 1997. **276**(April 4): p. 75 - 81.

57. Yamada, K.M. and R.A.F. Clark, *Provisional Matrix*, in *The Molecular and Cellular Biology of Wound Repair*, R.A.F. Clark, Editor. 1996, Plenum Press: New York. p. 51 - 93.

58. Haslett, C. and P. Henson, *Resolution of Inflammation*, in *The Molecular and Cellular Biology of Wound Repair*, R.A.F. Clark, Editor. 1996, Plenum Press: New York. p. 143 - 168.

59. Riches, D.W.H., *Macrophage Involvement in Wound Repair, Remodeling, and Fibrosis*, in *The Molecular and Cellular Biology of Wound Repair*, R.A.F. Clark, Editor. 1996, Plenum Press: New York. p. 95 - 141.

60. Woodley, D.T., *Reepithelialization*, in *The Molecular and Cellular Biology of Wound Repair*, R.A.F. Clark, Editor. 1996, Plenum Press: New York. p. 339 - 354.

61. Selman, M., T.E. King, and A. Pardo, *Idiopathic pulmonary fibrosis: prevailing and evolving hypotheses about its pathogenesis and implications for therapy.* Ann Intern Med, 2001. **134**(2): p. 136-51.

62. Wang, B., *et al.*, *Decreased Smad 7 expression contributes to cardiac fibrosis in the infarcted rat heart.* Am J Physiol Heart Circ Physiol, 2002. **282**(5): p. H1685-96.

63. Neubauer, K., B. Saile, and G. Ramadori, *Liver fibrosis and altered matrix synthesis.* Can J Gastroenterol, 2001. **15**(3): p. 187-93.

64. Goumenos, D.S., *et al.*, *Transforming growth factor-beta(1) and myofibroblasts: a potential pathway towards renal scarring in human glomerular disease.* Nephron, 2001. **87**(3): p. 240-8. EF&action=render&rendertype=fulltext&uid=NEF.nef87240.

65. Madri, J.A., S. Sankar, and A.M. Romanic, *Angiogenesis*, in *The Molecular and Cellular Biology of Wound Repair*, R.A.F. Clark, Editor. 1996, Plenum Press: New York. p. 355 - 371.

66. Buchman, V.L., M. Sporn, and A.M. Davies, *Role of transforming growth factor-beta isoforms in regulating the expression of nerve growth factor and neurotrophin-3 mRNA levels in embryonic cutaneous cells at different stages of development.* Development, 1994. **120**(6): p. 1621-9.

67. Lonaker, M.T., *et al.*, *Studies in Fetal Wound Healing: I. A Factor in Fetal Serum That Stimulates Deposition of Hyaluronic Acid.* Journal of Pediatric Surgery, 1989. **24**(8): p. 789-92.

68. Estes, J.M., *et al.*, *Hyaluronate Metabolism Undergoes an Ontogenic Transition During Fetal Development: Implications for Scar - Free Wound Healing.* Journal of Pediatric Surgery, 1993. **28**(10): p. 1227 - 31.

69. Rubanyi, G.M. and M.A. Polokoff, *Endothelins: molecular biology, biochemistry, pharmacology, physiology, and pathophysiology.* Pharmacol Rev, 1994. **46**(3): p. 325-415.

70. Douglas, S.A. and E.H. Ohlstein, *Signal TransductionMechanisms Mediating the Vascular Actions of Endothelin.* Journal of Vascular Research, 1997. **34**: p. 152 - 164.

71. Simonson, M.S. and M.J. Dunn, *Cellular signaling by peptides of the endothelin gene family.* FASEB, 1990. **4**: p. 2989 - 3000.

72. Muldoon, L.L., *et al.*, *Stimulation of phosphatidylinositol hydrolysis, diacylglycerol release, and gene expression in response to endothelin, a potent new agonist for fibroblasts and smooth muscle cells.* J Biol Chem, 1989. **264**(15): p. 8529-36.

73. Zachary, I., *et al.*, *Bombesin, vasopressin, and endothelin rapidly stimulate tyrosine phosphorylation of the focal adhesion-associated protein paxillin in Swiss 3T3 cells.* J Biol Chem, 1993. **268**(29): p. 22060-5.

74. Chrzanowska-Wodnicka, M. and K. Burridge, *Rho-stimulated contractility drives the formation of stress fibers and focal adhesions.* J Cell Biol, 1996. **133**(6): p. 1403-15.

75. Amano, M., Y. Fukata, and K. Kaibuchi, *Regulation and functions of Rho-associated kinase.* Exp Cell Res, 2000. **261**(1): p. 44-51.

76. Kaibuchi, K., S. Kuroda, and M. Amano, *Regulation of the cytoskeleton and cell adhesion by the Rho family GTPases in mammalian cells.* Annu Rev Biochem, 1999. **68**: p. 459-86.

77. Hall, A., *Rho GTPases and the actin cytoskeleton.* Science, 1998. **279**(5350): p. 509-14.

78. Kawada, N., *et al.*, *ROCK inhibitor Y-27632 attenuates stellate cell contraction and portal pressure increase induced by endothelin-1.* Biochem Biophys Res Commun, 1999. **266**(2): p. 296-300.

79. Takuwa, N., *et al.*, *A novel vasoactive peptide endothelin stimulates mitogenesis through inositol lipid turnover in Swiss 3T3 fibroblasts.* J Biol Chem, 1989. **264**(14): p. 7856-61.

80. Lahaye, D.H., *et al.*, *Phenotypic transformation of normal rat kidney fibroblasts by endothelin-1. Different mode of action from lysophosphatidic acid, bradykinin, and prostaglandin f2alpha.* Biochim Biophys Acta, 1999. **1449**(2): p. 107-18.

81. Dawes, K.E., *et al.*, *Changes in collagen metabolism in response to endothelin-1: evidence for fibroblast heterogeneity.* Int J Biochem Cell Biol, 1996. **28**(2): p. 229-38.

82. Mayer, D.C. and L.A. Leinwand, *Sarcomeric gene expression and contractility in myofibroblasts.* J Cell Biol, 1997. **139**(6): p. 1477-84.

83. Appleton, I., *et al.*, *Effect of endothelin-1 on croton oil-induced granulation tissue in the rat. A pharmacologic and immunohistochemical study.* Lab Invest, 1992. **67**(6): p. 703-10.

84. Shi-Wen, X., *et al.*, *Fibroblast matrix gene expression and connective tissue remodeling: role of endothelin-1.* J Invest Dermatol, 2001. **116**(3): p. 417-25.

85. Koyama, Y. and A. Baba, *Endothelins are extracellular signals modulating cytoskeletal actin organization in rat cultured astrocytes.* Neuroscience, 1994. **61**(4): p. 1007-16.

86. Ihling, C., *et al.*, *Endothelin-1-like immunoreactivity in human atherosclerotic coronary tissue: a detailed analysis of the cellular distribution of endothelin- 1.* J Pathol, 1996. **179**(3): p. 303-8.

87. Dimitrijevich, S.D., *et al.*, *Effect of hyperbaric oxygen on human skin cells in culture and in human dermal and skin equivalents.* Wound Repair Regen, 1999. **7**(1): p. 53-64.

88. Douglas, J., *et al.*, *Efficient transduction of human lymphocytes and CD34+ cells via human immunodeficiency virus-based gene transfer vectors.* Hum Gene Ther, 1999. **10**(6): p. 935-45.

89. Papazisis, K.T., *et al.*, *Optimization of the sulforhodamine B colorimetric assay.* J Immunol Methods, 1997. **208**(2): p. 151-8.

90. Walsh, B.J., *et al.*, *Microplate reader-based quantitation of collagens.* Anal Biochem, 1992. **203**(2): p. 187-90.

91. Steenfos, H.H., *Growth factors and wound healing.* Scand J Plast Reconstr Surg Hand Surg, 1994. **28**(2): p. 95-105.

92. Martin, P., J. Hopkinson-Woolley, and J. McCluskey, *Growth factors and cutaneous wound repair.* Prog Growth Factor Res, 1992. **4**(1): p. 25-44.

93. Guidry, C., *Extracellular matrix contraction by fibroblasts: peptide promoters and second messengers.* Cancer Metastasis Rev, 1992. **11**(1): p. 45-54.

94. Kolodney, M.S. and E.L. Elson, *Correlation of myosin light chain phosphorylation with isometric contraction of fibroblasts.* J Biol Chem, 1993. **268**(32): p. 23850-5.

95. Geesin, J.C., *et al.*, *Modulation of collagen synthesis by growth factors: the role of ascorbate-stimulated lipid peroxidation.* Arch Biochem Biophys, 1991. **289**(1): p. 6-11.

96. Tao, W., *et al.*, *Endothelin receptor A is expressed and mediates the [Ca2+]i mobilization of cells in human ciliary smooth muscle, ciliary*

nonpigmented epithelium, and trabecular meshwork. Curr Eye Res, 1998. **17**(1): p. 31-8.

97. Devesly, P., *et al.*, *Receptor kinetics differ for endothelin-1 and endothelin-2 binding to Swiss 3T3 fibroblasts.* Biochem Biophys Res Commun, 1990. **172**(1): p. 126-34.

98. Schiffrin, E.L., *Endothelin: potential role in hypertension and vascular hypertrophy.* Hypertension, 1995. **25**(6): p. 1135-43.

99. Petridou, S., *et al.*, *TGF-beta receptor expression and smad2 localization are cell density dependent in fibroblasts.* Invest Ophthalmol Vis Sci, 2000. **41**(1): p. 89-95.

100. Masur, S.K., *et al.*, *Myofibroblasts differentiate from fibroblasts when plated at low density.* Proc Natl Acad Sci U S A, 1996. **93**(9): p. 4219-23.

101. Kern, J., J. Shay, and S. Dimitrijevich, *Telomerized Human Fibroblasts Respond Normally to a Wound Healing Environment.* In Preparation.

102. Ridley, A.J. and A. Hall, *The small GTP-binding protein rho regulates the assembly of focal adhesions and actin stress fibers in response to growth factors.* Cell, 1992. **70**(3): p. 389-99.

103. Kimura, K., *et al.*, *Regulation of myosin phosphatase by Rho and Rho-associated kinase (Rho- kinase).* Science, 1996. **273**(5272): p. 245-8.

104. Yee, H.F., Jr., A.C. Melton, and B.N. Tran, *RhoA/rho-associated kinase mediates fibroblast contractile force generation.* Biochem Biophys Res Commun, 2001. **280**(5): p. 1340-5.

105. Amano, M., *et al.*, *Phosphorylation and activation of myosin by Rho-associated kinase (Rho- kinase).* J Biol Chem, 1996. **271**(34): p. 20246-9.

106. Kureishi, Y., *et al.*, *Rho-associated kinase directly induces smooth muscle contraction through myosin light chain phosphorylation.* J Biol Chem, 1997. **272**(19): p. 12257-60.

107. Hill, C.S. and R. Treisman, *Transcriptional regulation by extracellular signals: mechanisms and specificity.* Cell, 1995. **80**(2): p. 199-211.

108. Hill, C.S., J. Wynne, and R. Treisman, *The Rho family GTPases RhoA, Rac1, and CDC42Hs regulate transcriptional activation by SRF.* Cell, 1995. **81**(7): p. 1159-70.

109. Chihara, K., *et al.*, *Cytoskeletal rearrangements and transcriptional activation of c-fos serum response element by Rho-kinase.* J Biol Chem, 1997. **272**(40): p. 25121-7.

110. Blank, R.S., *et al.*, *Elements of the smooth muscle alpha-actin promoter required in cis for transcriptional activation in smooth muscle. Evidence for cell type- specific regulation.* J Biol Chem, 1992. **267**(2): p. 984-9.

111. Arora, P.D. and C.A. McCulloch, *Dependence of collagen remodelling on alpha-smooth muscle actin expression by fibroblasts.* J Cell Physiol, 1994. **159**(1): p. 161-75.

112. Hautmann, M.B., P.J. Adam, and G.K. Owens, *Similarities and differences in smooth muscle alpha-actin induction by TGF-beta in smooth muscle*

versus non-smooth muscle cells. Arterioscler Thromb Vasc Biol, 1999. **19**(9): p. 2049-58.